STABILITY ANALYSIS OF AN ISLANDED MICROGRID WITH RING AND RADIAL DISTRIBUTION

Hitihamilage Dayan Buddhi Prabasara Herath

(188507A)

Degree of Master of Science

Department of Electrical Engineering

University of Moratuwa
Sri Lanka

January 2022

STABILITY ANALYSIS OF AN ISLANDED MICROGRID WITH RING AND RADIAL DISTRIBUTION

Hitihamilage Dayan Buddhi Prabasara Herath

(188507A)

Dissertation submitted in partial fulfillment of the requirements for the degree Master of Science

Department of Electrical Engineering

University of Moratuwa
Sri Lanka

January 2022

DECLARATION PAGE OF THE CANDIDATE & SUPERVISOR

I declare that this is my own work and this thesis does not incorporate without acknowledgement any material previously submitted for a Degree or Diploma in any other University or institute of higher learning and to the best of my knowledge and belief it does not contain any material previously published or written by another person except where the acknowledgement is made in the text.

Also, I hereby grant to University of Moratuwa the non-exclusive right to reproduce and distribute my dissertation, in whole or in part in print, electronic or other medium. I retain the right to use this content in whole or part in future works (such as articles or books).

Signature: Date:

The above candidate has carried out research for the Masters dissertation under my supervision.

Dr.Lidula N.Widanagama Arachchige Date

Dr.P.S. Narendra de Silva Date

ABSTRACT

Colombo being the commercial hub of Sri Lanka, maintaining high reliability of electricity supply is critical. Thus, the electricity distribution network of Colombo city comprises of six, 11 kV ring networks formed around five grid substations and five primary substations. However, the network is currently operated in open-ring topology.

In the present operation, under maintenance periods, at times of load shedding and "self-generation" schemes, diesel generators are connected to the network. The generators, which are connected under the self-generation schemes are synchronized with the network. The generators, which are connected during maintenance and times of load shedding, are not synchronized. Hence, it is required to split the satellite belts into several sub sections to match the capacity of the generator to the load, so that the generator would not be tripped due to over loading. With the government policies to encourage renewable generation, solar PV generation has also been increasingly connected to the distribution network, which are not dispatched. With increasing penetration of solar PV, proper planning is required to maintain system stability and reliability under grid failures.

The substations in Colombo city do not follow the conventional diurnal load pattern of Sri Lanka; instead, during day time, the load reaches a peak and during night time it drops. This load pattern follows a curve similar to the diurnal generation curve of solar PV. Thus, by introducing solar PV to such substations, the installed diesel generation capacity can be reduced and the rings can be operated as microgrids when the grid fails.

In this research a case study is carried for the ring network based on primary substation-B of the Colombo city network with the distributed generation of solar PV and diesel generators to evaluate the ability of forming ring-connected microgrids for a commercial city with peak, day-time loading. The ring is split into smaller rings to form microgrids with capacity below 10 MVA. The satellites are considered as open looped. Loads of the satellite loop and the generation (solar PV/ diesel generators) are lumped to the respective radial/ ring substation.

The results indicate that when the network has three, 2 MVA generators fixed to the highest loaded substations, the system is stable and when the network has 1 MVA generators fixed to all the substations, the system becomes unstable at N-1 emergency operation. Instability occurs due to small perturbations to diesel generators at some substations.

Research reveals that with increasing penetration of solar PV, the system can be planned to be operated in ring-connected microgrids in stable operation to maintain the system reliability under grid failures.

ACKNOWLEDGEMENT

I humbly express my gratitude to my internal supervisor Dr. (Ms.) Lidula N. Widanagama Arachchige for the guidance and encouragement throughout the research. I would like to appreciate the support given to me by my external supervisor Dr. P.S. Narendra De Silva.

I thank the academic staff of the department of Electrical Engineering, Faculty of Engineering, University of Moratuwa for their comments and support given to me during the presentations.

I am grateful to CEB management for allowing me to use the data of Colombo city. I would like to thank to Eng. Menaka Divaratne - EE (Planning), Eng. Sachinthala Fernando - EE (Planning), Eng. Neranjan Ratnayake - EE (Planning), Eng. Gihan Chamara – EE (Energy Management), Eng. Vindya Wickramarachchi - EE (Energy Management) and Eng. Thilina Rajapakshe – EE (High Tension Maintenance) for the support rendered by facilitating the field data and models. Further, I would like to mention all the engineers in Colombo City and my M.Sc. colleagues for the support they have provided.

Finally, I would like to thank my wife, Dr. Nadisha Ratnasekera, kids, Angelo, Nathan and out parents for easing me from my family commitments to do the research and for the continuous encouragement.

TABLE OF CONTENTS

LIST OF FIGURES

LIST OF TABLES

LIST OF APPENDICES

CHAPTER 01

BACKGROUND

1.1. Electricity Distribution Network of Colombo City

Colombo city distribution network is comprised of an underground (UG) network. The primary distribution voltage of the network is 11 kV. Both ring and radial topologies are used in the network.

There are five primary substations (PS) (33 / 11 kV) and five grid substations (GS) (132 kV / 11 kV) as initial feeding centers of the Colombo city. Six rings are constructed around the above ten substations as illustrated in Figure 1.1. From the ring and radial substations, satellites are formed where the substations in the satellites are used to step down the voltage at 11 kV to 400 V, and for secondary distribution. [1]

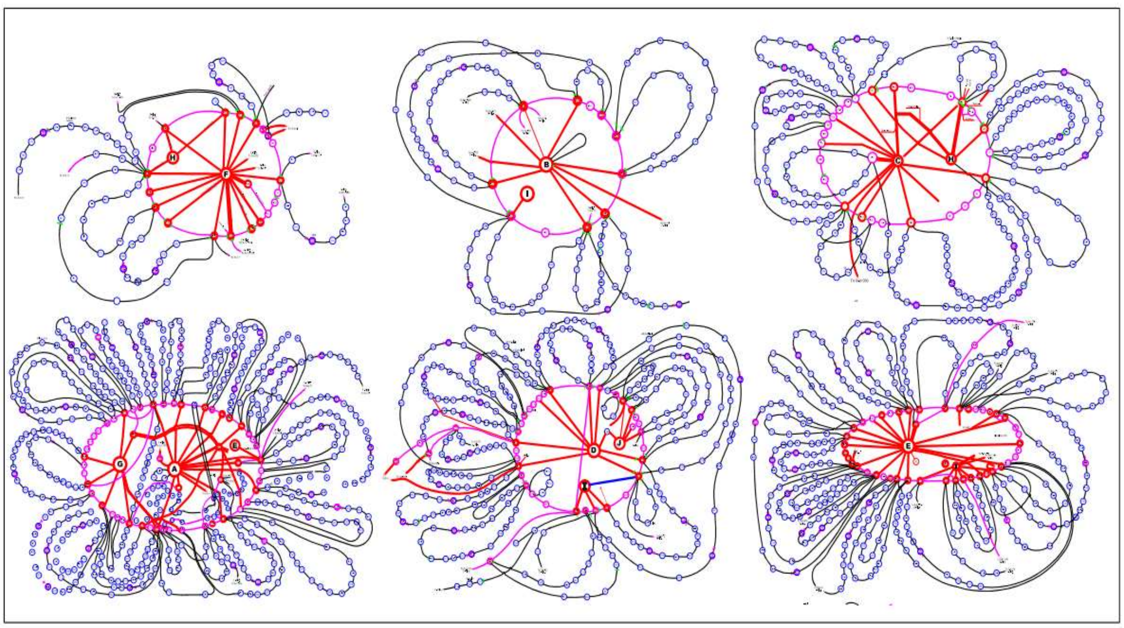

Figure 1.1 Ring distributions networks formed in Colombo city [1]

Low Voltage (LV) (400 V) distribution is also comprised of a UG network and a small amount of overhead (OH) lines where UG is not possible. Feeder pillars and mini feeder pillars are used in the LV network.

1.2. Emergency Generator Arrangement in Colombo City

Colombo city network is operated according to (N-1) operating criteria. Hence in case of a failure in a UG cable, it is possible to feed the loads from the backup feeding arrangement. However, if the backup arrangement is also faulted, it is not possible to feed the loads till the fault is repaired. The repair times of such faults (cable faults, equipment failures) are fairly high due to excavation permission issues and technical procedures. Hence in such situations, an emergency generator is coupled to the selected satellites to feed the network.

The generator is connected to the LV bus bar at the satellite substation and the MV network is fed through the transformer. As the load catering is limited by the generator capacity (1,250 kVA max) and transformer capacity (1,000 kVA max) only a few substations can be fed from this arrangement. Figure 1.2 depicts emergency generator connection diagram. These backup generators do not have synchronizing capacity. Hence, the satellite belt has to be isolated.

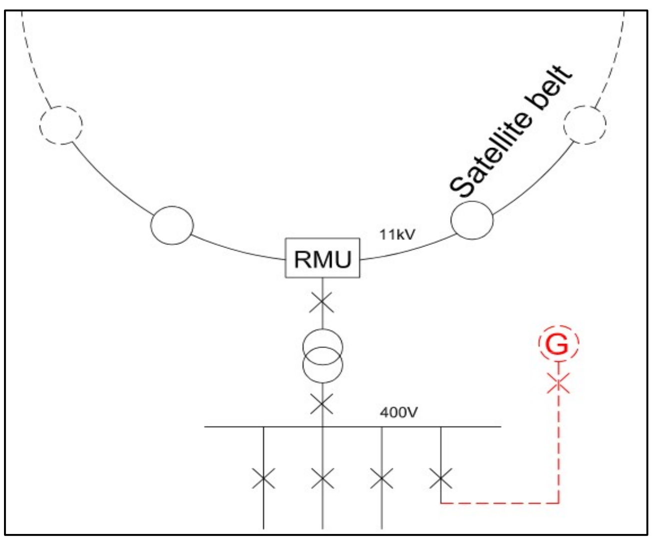

Figure 1.2 Emergency generator connection diagram

1.3. Load Curves of Substations in Colombo City

Unlike the conventional load pattern of Sri Lanka (Figure 1.3), the load pattern of Colombo city has a day peak and an elephant-shaped curve. The daily load pattern of all the 10 primary and grid substations are depicted in Figure 1.4.

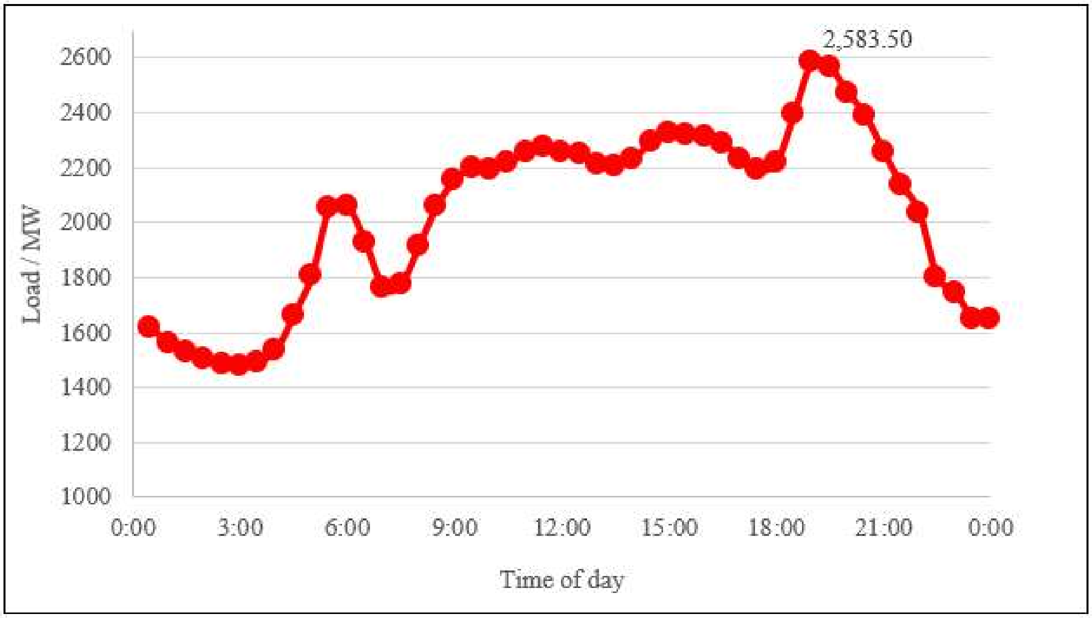

Figure 1.3 Load curve of Sri Lanka at 30/05/2019

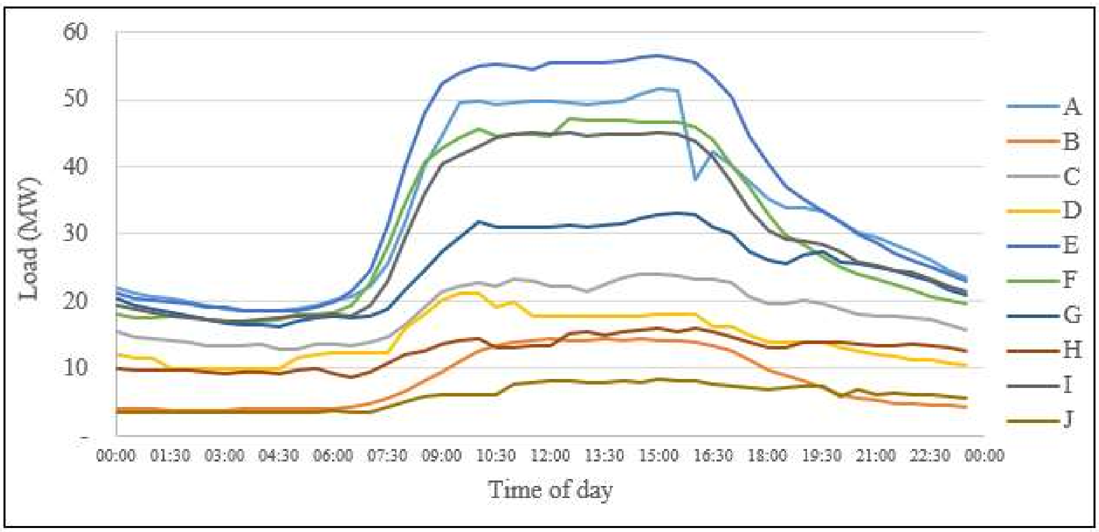

Figure 1.4 Daily load curve of all the substations at 21/05/2019 [2]

1.4. Problem Statement

As the peak demand of Colombo city occurs during day time, the required diesel generation capacity can be reduced by introducing solar PV to such substations.

Figure 1.5 depicts the normalized demand curves of primary substation B, and solar PV generation. The data recorded as the highest demand in Colombo city upto date on 21/05/2019 was used to plot the load curve. Average bi-hourly solar generation for two months (16/11/2019 – 14/01/202) was used to plot the average solar power generation in the selected system. Subtraction of above two gives the load seen by the grid.

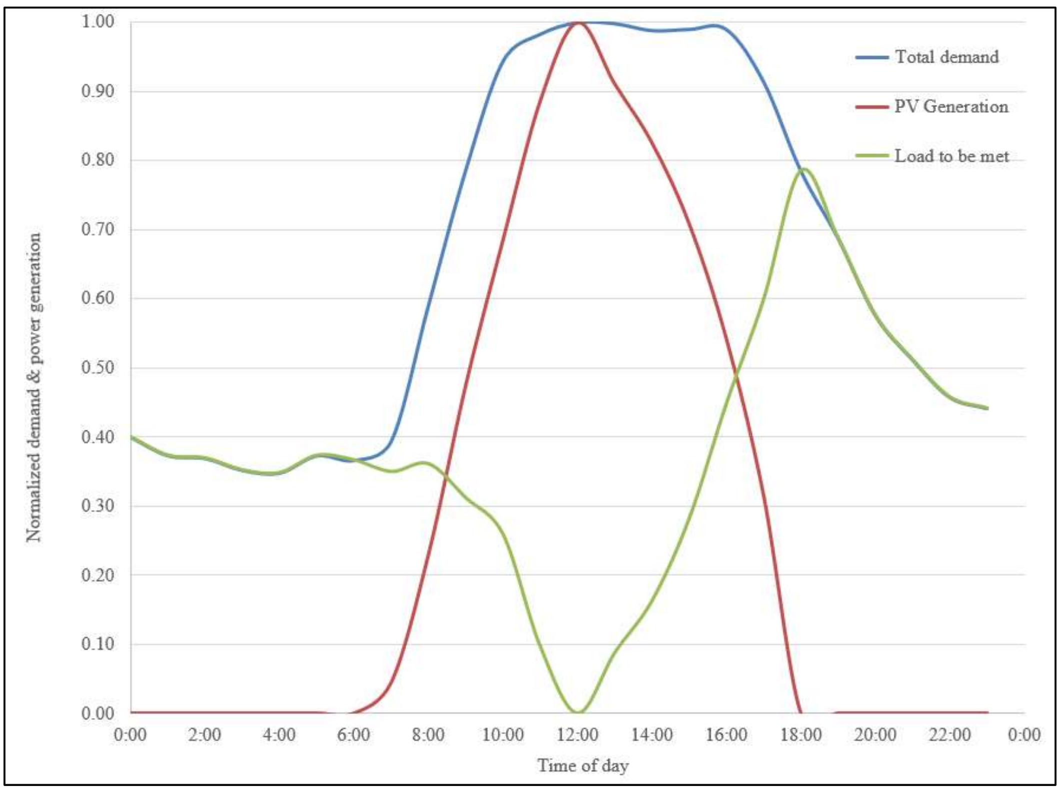

Figure 1.5 Demand of primary substation B and power generation of a solar PV normalized to their peak values.

Yet, no research has been done on analyzing the effect of high solar PV penetration to the distribution network in Colombo city or on evaluating the possibility of increasing solar PV penetration with planned microgrid operation in ring network with radial feeder arrangement of the Colombo city power distribution. Small signal stability analysis allows identifying critical parameters for maintaining stability in a system. Therefore, this research is focused on evaluating critical parameters for system stability in designing an islanded microgrid in a ring network with radial feeder arrangement for increased penetration of solar PV.

1.5. Scope

In order to verify the model an actual ring network in Colombo city was used. However, currently the ring is operated in open loop topology. Therefore, it was redesigned for closed loop topology. A portion of the ring network based on primary substation B was used.

Satellites were considered as open loop. Loads of the corresponding satellite loops were lumped to the corresponding ring/radial substation. Generators were also lumped to the corresponding ring/radial substation.

Figure 1.6 depicts the ring of PS-B. Figure 1.7 depicts the selected portion of the ring and the arrangement after lumping the loads. Figure 1.8 depicts the geographical area electrified by the selected portion of the PS-B ring.

As presented in Figure 1.9, microgrid has two operating topologies named grid connected mode and islanded (off grid) mode. Islanded mode also can be analyzed in two modes as hybrid mode and diesel generator only mode. Hybrid mode again can be analyzed in different levels of irradiance. Hybrid topology in off grid mode was considered in this study.

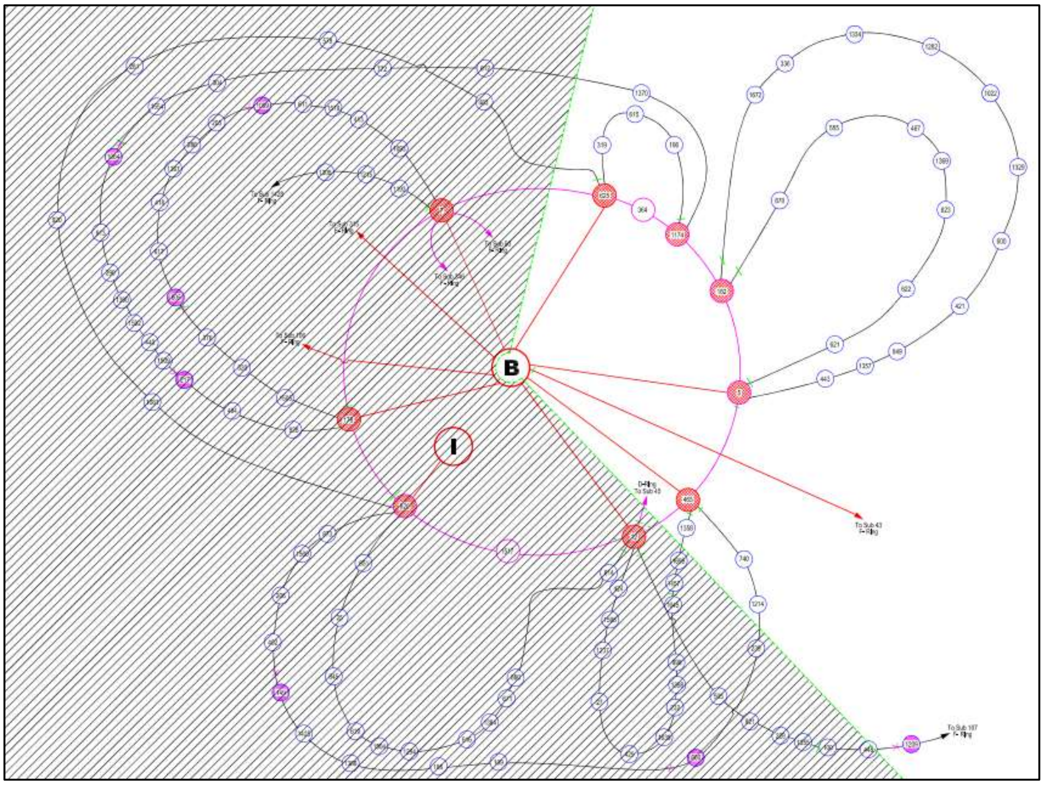

Figure 1.6 Primary substation B ring [1]

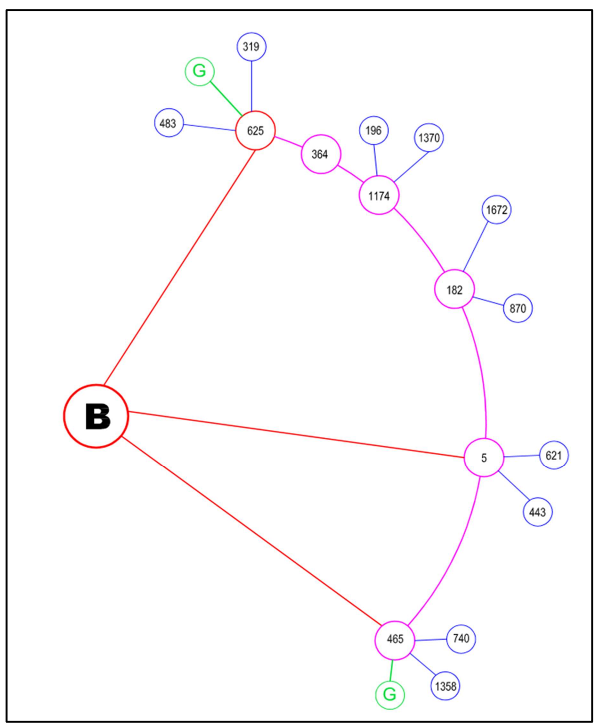

Figure 1.7 Selected portion of the primary substation B ring

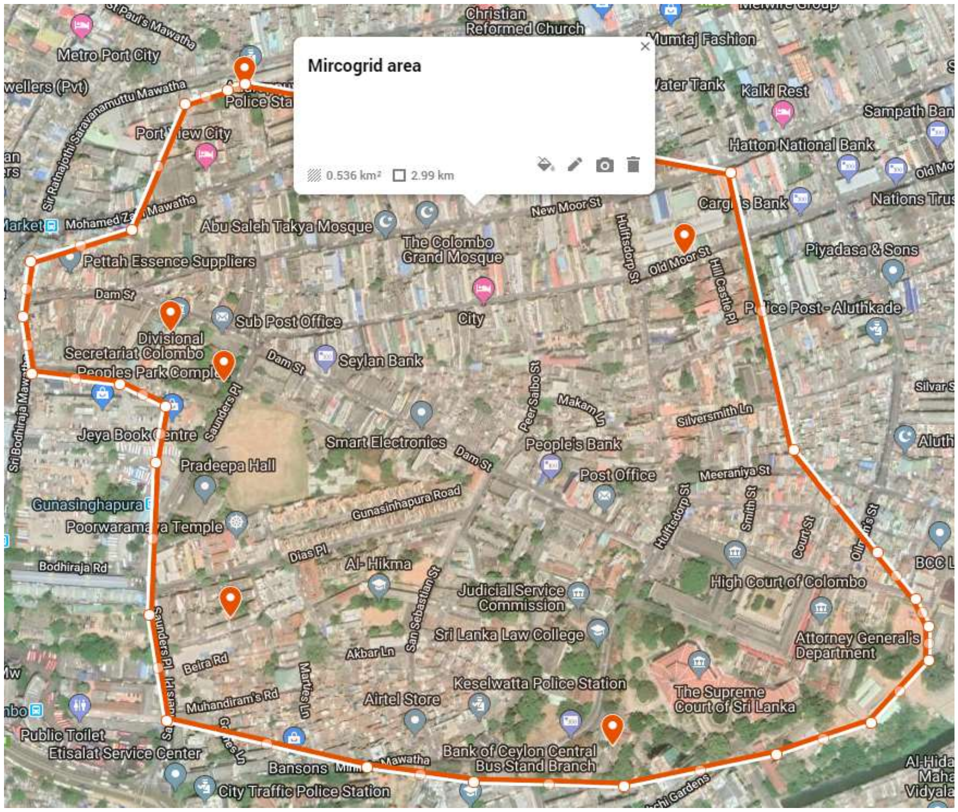

Figure 1.8 Geographical area electrified by the selected portion of the ring

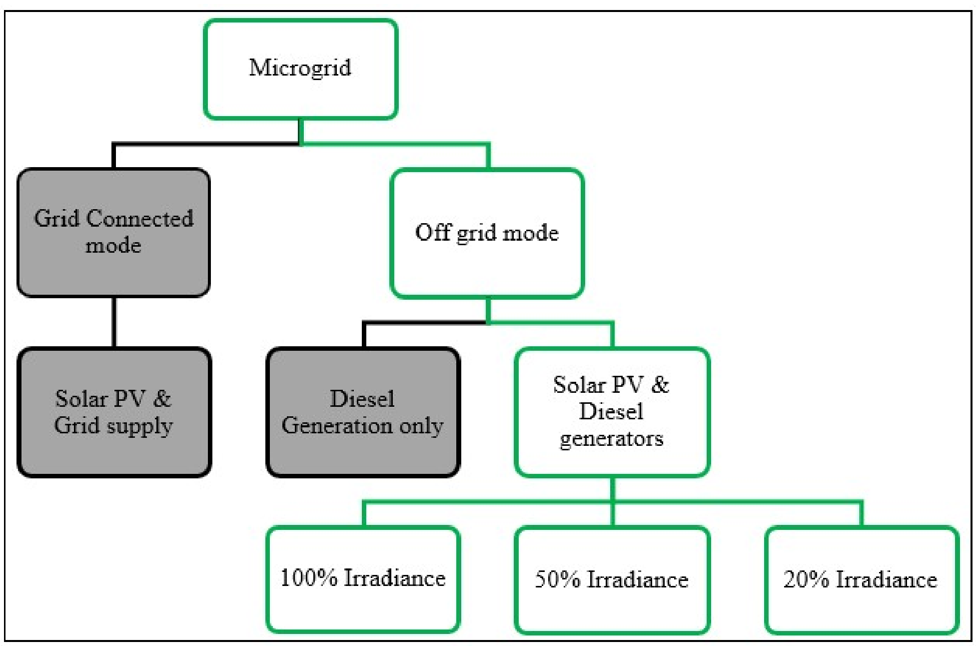

Figure 1.9 Operating modes of a microgrid

1.6. Objectives

The main objective of this research is to design an islanded microgrid in closed-loop ring architecture with radial distribution for increased penetration of solar PV for maintaining system stability under small disturbances.

1.7. Thesis Outline

This thesis contains a comprehensive study on developing a methodology to evaluate the steady-state stability of a microgrid with both ring and radial distribution topology in islanded mode.

Chapter 02 consists of the literature review done during the research. It contains the theory on power generation of solar PV, power flow analysis and small signal analysis. Further, it contains the extracts of publications of researches on the subjects of distribution network topologies, microgrids, power generation of solar PV, small signal analysis of parallel connected energy sources.

Chapter 03 elaborates the methodology used throughout the research. The methodology has three main steps. Hence the chapter contains three main sub chapters.

Chapter 04 presents the method and results of power flow analysis. This includes the modeling, data input to the software and the results of the software.

Chapter 05 presents the method and results of small signal analysis. It further includes the modeling, data input to the software, the results of the software and the conclusion based on the software.

Chapter 06 concludes the research outcomes.

CHAPTER 02

LITERATURE REVIEW

Chapter 2 consists of theoretical collection of related literature used for the research.

2.1. Distribution Network Topologies

Various kinds of network topologies are used in electricity distribution networks and they are discussed in the following sections [3].

2.1.1. Simple Radial System

A simple radial system is where the distribution transformer is directly connected to one medium voltage (MV) feeder. The secondary side of the transformer is connected to the low voltage (LV) bus bar and the LV distribution feeders are connected to the LV bus bar. Protective devices are used on both sides of the transformers and to all the outgoing feeders.

2.1.2. Expanded Radial System

This is a modified arrangement to the simple radial system. Instead of one large transformer in a simple radial system, in an expanded radial system one MV radial feeder is connected to several small transformers. The secondary sides of the transformers are connected to independent bus bars. Protective devices are used on both sides of the transformers and to all the outgoing feeders. In some systems, a common protective device is used for the primary side of the transformers.

2.1.3. Secondary Selective System

This is an improved arrangement to the expanded radial System. Pairs of substations are connected through a normally open secondary tie circuit breaker. In normal operation, the tie-breaker is open, and in fault operation, the tie-breaker is closed.

2.1.4. Primary Selective System

Two primary feeders are extended to each transformer. Interlocked selector switches are provided to each transformer to select the connected feeder.

2.1.5. Looped Primary

The primary sides of the transformers are connected to an MV loop.

2.1.6. Secondary Network System

This is an improved arrangement to the secondary selective system. Instead of two transformers, several transformers are connected through interlocked selector switches and each transformer is provided with "Network Protector" switches on the LV side to avoid reverse power flow.

2.1.7. Ring Distribution System

All the substations are connected in a loop, forming an MV ring topology. These ring distribution systems are operated in both closed and open-loop arrangements [4] [5] [6].

Advantages in closed-loop topology

- **Increases the reliability and supply security** [4]
  Since the feeding arrangement can be shifted to the backup mode in case of a failure, the repair time is less irrespective of failure and, it reduces the "Energy Not Served".

- **Achieves the availability of power on demand** [4]
  As there are multiple feeding arrangements supplying maximum power on demand is possible at any time.

- **The network losses and the voltage drop are low** [4]
  The current is fed through several feeding points sharing the maximum required load current. Hence, the voltage drop (current × resistance) and the losses (current^2 × resistance) are reduced.

- **Facilitates increased penetration of distributed generation** [4]
  As there are multiple feeding paths, the generation in lower levels can also flow through the same paths without a requirement of system re-designing.

Challenges in closed-loop topology

- **Complex power flow** [5]
  As there are multiple feeding paths, power flow analysis is difficult.

- **Complex protection schemes** [5] [6]
  It requires complex protection schemes as there can be several paths feeding the fault. Wrong selection and coordination could result in tripping off of several lines. Hence, bi-directional protection schemes with fast-acting protection relays with advanced processors and communication are required in order to ensure proper isolation and selectivity.

- **Increased current ratings**
  In case of a fault, the closed-loop distribution systems are designed to operate as an open-loop distribution network. Hence, the network has to be designed to operate in high current ratings, which would increase the cross-sections of bus bars, screens, and conductors in the infrastructure.

2.2. Microgrids

A microgrid at the distribution level, is a small-scale distribution network in the capacity of 1~10 MW containing a set of distributed energy resources such as wind, hydro, solar, thermal, and energy storage supplying a load in an identified area. A microgrid can operate in both modes: as grid connected or as a controllable power island. A microgrid maximizes the reliability, availability, efficiency, economic performance, and security. [7] [8]

In the grid-connected operation, the microgrid is connected to the grid and operates as a part of the grid. The controlling mode of the microgrid is based on master-slave technology, where the grid is the master, which handles the load frequency control (LFC) and the microgrid is the slave, which handles the voltage control (VC). In the islanded operation microgrid takes over both LFC and VC. [7]

Therefore, the stability analysis of the microgrid in islanded operation is a critical factor in designing a microgrid.

2.2.1. Operation mode of the inverters

Inverters are used to integrate renewable energy sources like solar panels, wind turbine driven generators and also, energy storages. Even though the main application of an inverter is to harness the maximum possible power from its source and deliver it to the load, in a microgrid they are expected to perform as controllers as well to maintain the reliable operation. The main control modes of inverters are grid forming mode, grid feeding mode, and grid following mode [9] [10].

Grid forming mode

In grid forming mode, the inverter is used to form the grid by maintaining the frequency and voltage constant within respective standard limits. This mode is used only in the islanded operation of the microgrid.

Grid feeding model

Grid feeding mode is the conventional and most common mode of inverter operation, in which the inverter extracts the maximum possible power from the connected source and supplies it to the grid in unit power factor. Thus, the maximum power from the distributed generator can be obtained in this mode.

Grid following mode

Grid following mode is called as the grid-supporting mode as well. In grid following mode, the inverter operates in droop control for both LFC and VC. Other than that, inverters are used to provide ancillary services such as negative-sequence compensation, harmonic compensation, and voltage support during low voltage ride through conditions to the grid as well.

2.3. Power Generation of Solar PV

Solar PV system comprises of two main components namely the PV array and the inverter. There are several parameters related to both these components that determines the power output of the solar PV system as discussed in the following sections.

2.3.1. Parameters related to the Photovoltaic (PV) array

Output power of a solar PV array can be given as in 2.3.1 [11].

$P_{PV} = \eta . S . \Phi . [1 - 0.005(T_a + 25)]$

(2.3.1)

where,

P_{PV} – Power generation by PV array

S - Area of the PV panel

Φ - Irradiance level

η - Efficiency of the PV panel

T_a - Ambient temperature

When considering installed PV arrays, ambient temperature, measured area and conversion efficiency do not change in very short periods that would be considered in small signal stability studies.

Hence, 2.3.1 can be simplified to 2.3.2.

$$P_{PV} = K_{PV} \Phi \quad (2.3.2)$$

Hence, power output of PV array can be considered as proportionate to the irradiance.

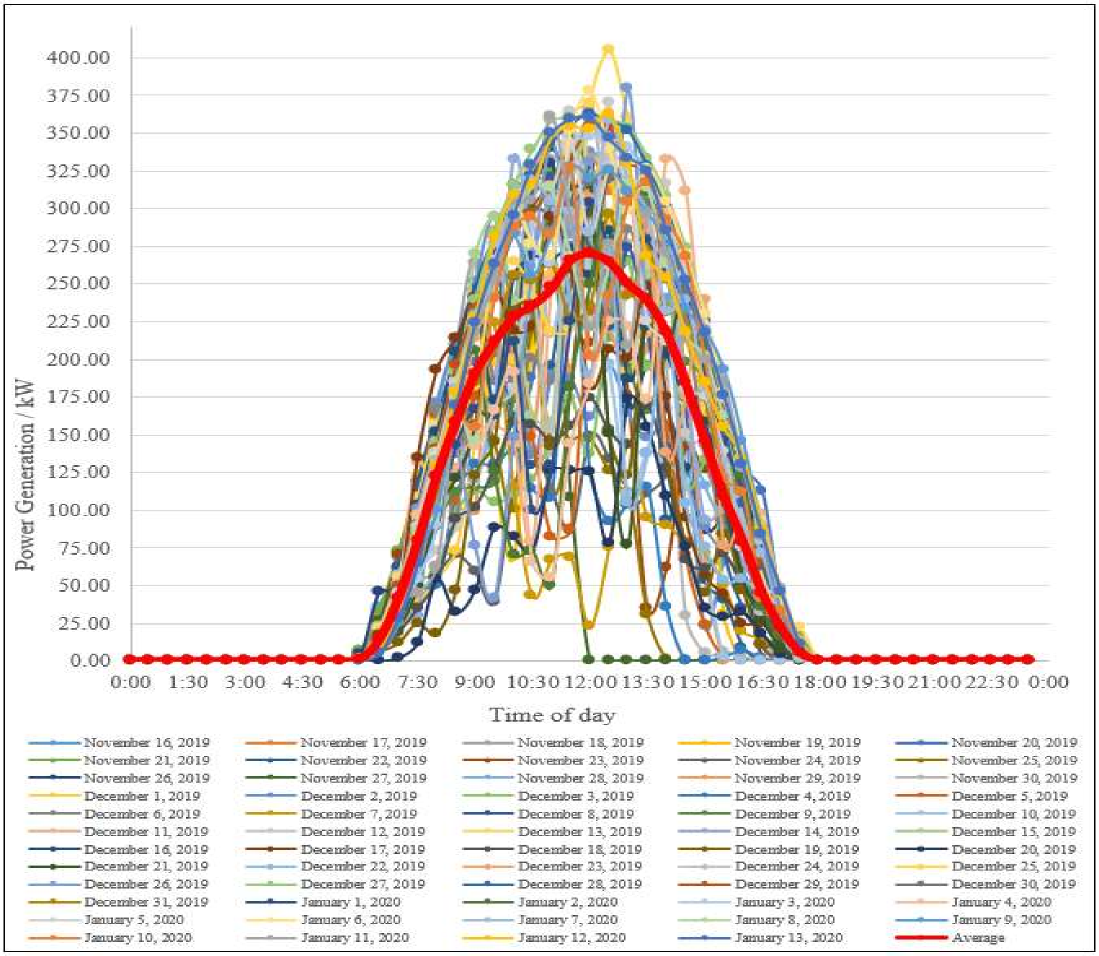

Figure 2.1 Daily power generation curves of solar for two months

Figure 2.1 depicts the daily power generation of a solar net metering connection, recorded at a particular customer for a period of two months. The bold line depicts the average power generation curve for the two-month period, where it indicates daily peak of nearly 275 kW at 12 noon.

2.4. Power Flow Analysis of Microgrids

The commonly used methods for power flow analysis are Newton-Raphson method, Gauss-Siedel method and Fast-Decoupled method. [5]

Power flow analysis of microgrids is quite complex compared to that of normal distribution networks due to the bi-directional (two way) power flow in microgrids with the integrated distributed generation [8]. Also, in considering ring networks with radial feeders, there are multiple branches, which makes power flow analysis a complex problem. For microgrids, power flow analysis has to be carried out for both islanded and grid connected operation modes, if full system analysis is considered [12]. Further, the behavior of the network for different levels of installed diesel generators and solar PV has to be evaluated too. Therefore, performing power flow analysis manually for a microgrid in ring configuration would be complicated. Software tools such as PSS/E designed for power flow analysis in balance complex networks, which use the prevailing power flow analysis methods can be used for microgrid applications as well.

Modeling the network for power flow analysis is also critical. Most of the distributed generators as well as loads are connected to low voltage network. Hence, each load bus and generator bus have to be connected via a transformer to the network.

2.5. Small Signal Analysis

Section 2.5 describes the theoretical background of the small signal analysis applied in the research. [13] [14]

When evaluating small-signal of a microgrid the islanded mode is more crucial than the grid connected mode. The contribution of distributed generation is influencive in the islanded mode compared to the grid connected mode as the distributed generation is connected at the low voltage lines furthest from the grid [5] [8]. In islanded mode, three types of inverter operation modes are to be evaluated as grid forming inverter for frequency control (either a diesel generator or an energy storage), grid following inverters and grid feeding inverters.

The state-space representation of the network has to be obtained to perform the small-signal analysis. Two methods were found to obtain the state-space representation of a closed-loop network with distributed solar PV and diesel generators. In both cases, the network has to be converted to a global d-q frame. [15] [16].

In the first method, small-signal models of individual inverter are found separately. Then multi-inverter model is obtained by Kirchhoff's current law. However, this method is quite cumbersome when there are more than two energy sources. [15]

In the second method, the multi-inverter model is obtained directly by writing the equations for time-average model. Bus admittance matrix is used in this method. [16]

2.5.1. State Space Representation

The behavior of the power system, which is an autonomous dynamic system can be characterized by a set of ***n*** number of first order differential equations given by 2.5.1.

$$\begin{aligned} \dot{x_1} &= f_1(x_1, x_2, .., x_n ; u_1, u_2, .., u_r ; t) \\ \dot{x_2} &= f_1(x_1, x_2, .., x_n ; u_1, u_2, .., u_r ; t) \\ \dot{x_n} &= f_1(x_1, x_2, .., \dot{x}_n ; u_1, u_2, .., u_r ; t) \end{aligned} \qquad (2.5.1)$$

Where

x_i - i[th] state variable

r - Number of inputs

n - Order of the system

This can be also represented by 2.5.2,

$$\dot{x} = f(x , u , t) \qquad (2.5.2)$$

where

$$x = \begin{bmatrix} x_1 \\ x_2 \\ . \\ x_n \end{bmatrix} \qquad \mathrm{u} = \begin{bmatrix} u_1 \\ u_2 \\ . \\ u_r \end{bmatrix} \qquad f = \begin{bmatrix} f_1 \\ f_2 \\ . \\ f_n \end{bmatrix}$$

x - State vector u - Input vector

Let the derivative of state variable with respect to time denoted by $\dot{x}$. As the system is autonomous (2.5.2) can be written as;

$$\dot{x} = f(x, u) \qquad (2.5.3)$$

The output of the system can be represented by 2.5.4.

$$y = g(x, u) \qquad (2.5.4)$$

$$\mathrm{y} = \begin{bmatrix} y_1 \\ y \\ . \\ y_m \end{bmatrix} \qquad g = \begin{bmatrix} g_1 \\ g_2 \\ . \\ g_m \end{bmatrix}$$

This is called the State Space Representation of the system.

2.5.2. Linearization of Non-linear Systems

The equations (2.5.3) and (2.5.4) are non-linear equations. In order to analyze the stability, it is required to make them linear. Therefore, small signal perturbation is used.

Consider an equilibrium point where state vector is $\boldsymbol{x_0}$ and input vector is $\boldsymbol{u_0}$.

$$\dot{x}_0 = f(x_0, u_0) = 0 \tag{2.5.5}$$

Consider a small perturbation;

When $(\boldsymbol{x} = \boldsymbol{x_0} + \Delta \boldsymbol{x})$ and $(u = u_0 + \Delta u)$, then $(\dot{\boldsymbol{x}} = \dot{\boldsymbol{x}}_{\boldsymbol{0}} + \Delta \dot{\boldsymbol{x}})$

From 2.5.3,

$$\dot{x} = f(x, u)$$

$$\dot{x}_0 + \Delta\dot{x} = f[(x_0 + \Delta x),\ (u_0 + \Delta u)] \tag{2.5.6}$$

As the perturbations are very small, ***f(x,u)*** can be represented in Taylor's series.

$$\dot{x}_i = \dot{x}_{i0} + \Delta\dot{x}_i = f_i[(x_0 + \Delta x),\ (u_0 + \Delta u)]$$

$$\dot{x}_i = \dot{x}_{i0} + \Delta\dot{x}_i = f_i(x_0, u_0) + \frac{\partial f_i}{\partial x_1}\Delta x_1 + .. + \frac{\partial f_i}{\partial x_n}\Delta x_n + \frac{\partial f_i}{\partial u_1}\Delta u_1 + .. + \frac{\partial f_i}{\partial u_r}\Delta u_r$$

As $\dot{x}_{i0} = f_i(x_0, u_0)$

$$\Delta\dot{x}_i = \frac{\partial f_i}{\partial x_1}\Delta x_1 + .. + \frac{\partial f_i}{\partial x_n}\Delta x_n + \frac{\partial f_i}{\partial u_1}\Delta u_1 + .. + \frac{\partial f_i}{\partial u_r}\Delta u_r \tag{2.5.7}$$

Similarly, from equation 2.5.4;

$$\Delta\dot{y}_j = \frac{\partial g_j}{\partial x_1}\Delta x_1 + .. + \frac{\partial g_j}{\partial x_n}\Delta x_n + \frac{\partial g_j}{\partial u_1}\Delta u_1 + .. + \frac{\partial g_j}{\partial u_r}\Delta u_r \tag{2.5.8}$$

By arranging the equations (2.5.7) and (2.5.8), the linearized equations for (2.5.9) and (2.5.10) can be obtained;

$$\Delta\dot{x} = A\,\Delta x + B\,\Delta u \tag{2.5.9}$$

$$\Delta y = C\,\Delta x + D\,\Delta u \tag{2.5.10}$$

$$A = \begin{bmatrix} \frac{\partial f_1}{\partial x_1} & \cdots & \frac{\partial f_1}{\partial x_n} \\ \cdots & \cdots & \cdots \\ \frac{\partial f_n}{\partial x_1} & \cdots & \frac{\partial f_n}{\partial x_n} \end{bmatrix}$$; State/plant matrix $B = \begin{bmatrix} \frac{\partial f_1}{\partial u_1} & \cdots & \frac{\partial f_1}{\partial u_r} \\ \cdots & \cdots & \cdots \\ \frac{\partial f_n}{\partial u_1} & \cdots & \frac{\partial f_n}{\partial u_r} \end{bmatrix}$; Control/input matrix

$$C = \begin{bmatrix} \frac{\partial g_1}{\partial x_1} & \cdots & \frac{\partial g_1}{\partial x_n} \\ \cdots & \cdots & \cdots \\ \frac{\partial g_m}{\partial x_1} & \cdots & \frac{\partial g_m}{\partial x_n} \end{bmatrix}$$; Output matrix $D = \begin{bmatrix} \frac{\partial g_1}{\partial u_1} & \cdots & \frac{\partial g_1}{\partial u_r} \\ \cdots & \cdots & \cdots \\ \frac{\partial g_m}{\partial u_1} & \cdots & \frac{\partial g_m}{\partial u_r} \end{bmatrix}$;Proportion of input in o/p

2.5.3. Local Stability of a Dynamic System

The system can be considered as "Locally Stable" around an equilibrium point, if the resultant movement due to the small perturbation, stays within a small region around the said equilibrium point.

By applying the Laplace transformation of (2.5.9) and (2.5.10);

$$s\Delta X(s) - \Delta X(0) = A\,\Delta X(s) + B\,\Delta U(s) \tag{2.5.11}$$

$$\Delta Y(s) = C\,\Delta X(s) + D\,\Delta U(s) \tag{2.5.12}$$

From (2.5.11);

$$(sI - A)\Delta X(s) = \Delta X(0) + B\,\Delta U(s)$$

$$\Delta X(s) = (sI - A)^{-1}[\Delta X(0) + B\,\Delta U(s)]$$

$$= \frac{adj(sI-A)}{det(sI-A)}[\Delta X(0) + B\,\Delta U(s)] \tag{2.5.13}$$

Similarly, from 2.5.12;

$$\Delta Y(s) = C\,\frac{adj(sI-A)}{det(sI-A)}[\Delta X(0) + B\,\Delta U(s)] + D\,\Delta U(s) \tag{2.5.14}$$

The poles of $\Delta X(s)$ and $\Delta Y(s)$ can be obtained at;

$$det(sI - A) = 0 \tag{2.5.15}$$

Equation (2.5.15) is called as the characteristic equation of matrix $A_{n\times n}$.

The values for the $\boldsymbol{s}$, which satisfy the above equation (roots of the characteristic equation) are called the Eigenvalues of the matrix $A_{n\times n}$.

Stability of the system can be predicted by examining the Eigenvalues.

i. If the real parts of all the Eigenvalues are negative, then the system is asymptotically stable, which means the system returns to its original state when **t** increases.
ii. If the real parts of the Eigenvalues are zero, behavior of the system is not possible based on first approximation.
iii. If the set of Eigenvalues have at least one positive real part, the original system is unstable.
iv. If the Eigenvalues are complex, the system response is oscillatory.

When observing the set of complex Eigenvalues, conjugate Eigenvalues can be found. It is required to find the oscillation frequency and the damping ratio as these Eigenvalues can move to the positive part of the real axis under a disturbance due to the behavior of the oscillation. These Eigenvalues are the ones, which can cause instabilities in the system. They are called "dominant Eigenvalues".

2.5.4. Analysis of Eigen matrix and modal matrices

For any state matrix ($A_{n\times n}$) Eigen matrix, left modal matrix and right modal matrix can be defined as follows:

Let,

λ_i - i^th^ Eigen value of A for which a non-trivial value is existing

$$A_{n\times n}\,\phi_{n\times 1} = \lambda_i\,\phi_{n\times 1} \qquad ;\ \phi_{n\times 1} \text{ - vector where } \phi_{n\times 1} \neq 0 \qquad (2.5.16)$$

Equation (2.5.16) can be arranged as,

$$(A - \lambda_i\, I)\phi = 0 \qquad (2.5.17)$$

For a non-trivial solution of (2.5.17):

$$det(A - \lambda_i\, I) = 0 \qquad (2.5.18)$$

Since there are n number of solutions for λ_i, $\boldsymbol{n}$ number of $\phi_{n\times 1}$ column matrix exists, which could be represented as (2.5.19).

$$\phi = \begin{bmatrix} \phi_{1i} \\ \phi_{2i} \\ . \\ . \\ \phi_{ni} \end{bmatrix} \tag{2.5.19}$$

Equation (2.5.19) can be expanded as in (2.5.20).

$$\phi = \begin{bmatrix} \phi_{11} & \phi_{12} & \cdots & \phi_{1i} & \cdots & \phi_{1n} \\ \phi_{21} & \phi_{22} & \cdots & \phi_{2i} & \cdots & \phi_{2n} \\ \vdots & \vdots & \vdots & \vdots & \ddots & \vdots \\ \phi_{i1} & \phi_{i2} & \cdots & \phi_{ii} & \cdots & \phi_{in} \\ \vdots & \vdots & \vdots & \vdots & \ddots & \vdots \\ \phi_{n1} & \phi_{n2} & \cdots & \phi_{ni} & \cdots & \phi_{nn} \end{bmatrix} \tag{2.5.20}$$

Equation (2.5.20) is called the right modal matrix.

Similarly,

$$\psi_{n\times 1} A_{n\times n} = \lambda_i \, \psi_{n\times 1} \tag{2.5.21}$$

$$\psi_i = [\psi_{i1} \;\; \psi_{i2} \;\; \psi_{i3} \dots \;\; \psi_{in}] \tag{2.5.22}$$

$$\psi = [\psi_1^T \;\; \psi_2^T \;\; \psi_3^T \dots \;\; \psi_n^T] \tag{2.5.23}$$

$$\psi = \begin{bmatrix} \psi_{11} & \psi_{12} & \cdots & \psi_{1i} & \cdots & \psi_{1n} \\ \psi_{21} & \psi_{22} & \cdots & \psi_{2i} & \cdots & \psi_{2n} \\ \vdots & \vdots & \vdots & \vdots & \ddots & \vdots \\ \psi_{i1} & \psi_{i2} & \cdots & \psi_{ii} & \cdots & \psi_{in} \\ \vdots & \vdots & \vdots & \vdots & \ddots & \vdots \\ \psi_{n1} & \psi_{n2} & \cdots & \psi_{ni} & \cdots & \psi_{nn} \end{bmatrix} \tag{2.5.24}$$

Equation (2.5.24) is called the left modal matrix.

Let the diagonal matrix of Eigenvalues as given by (2.5.25):

$$\Lambda = \begin{bmatrix} \lambda_1 & 0 & 0 & \cdots & 0 \\ 0 & \lambda_2 & 0 & \cdots & 0 \\ 0 & 0 & \lambda_i & \cdots & 0 \\ \vdots & \vdots & \vdots & \ddots & \vdots \\ 0 & 0 & 0 & \cdots & \lambda_n \end{bmatrix} \tag{2.5.25}$$

From (2.5.20), (2.5.24) and (2.5.25),

$$A\phi = \phi\Lambda \tag{2.5.26}$$

$$\psi\phi = I \tag{2.5.27}$$

$$\psi = \phi^{-1} \tag{2.5.28}$$

$$\psi A\phi = \Lambda \tag{2.5.29}$$

2.5.5. Participation Matrix

Equation (2.5.29) shows that the Eigenvalues (λ) of the ***A*** matrix are linked with the left and right Eigen matrices. Also, the Eigenvalues are dependent on the values of state variables. Hence, in order to find the relationship of state variables to Eigenvalues, **Participation Matrix (P)** can be used. Participation matrix combines both left and right Eigen matrices. Consider the participation matrix ***P*** with the elements P_{ik}, as shown in equation (2.5.30).

$$P = \begin{bmatrix} P_{11} & P_{12} & \cdots & P_{1k} & \cdots & P_{1n} \\ P_{21} & P_{22} & \cdots & P_{2k} & \cdots & P_{2n} \\ \vdots & \vdots & \ddots & \vdots & \vdots & \vdots \\ P_{i1} & P_{i2} & \cdots & P_{ik} & \cdots & P_{in} \\ \vdots & \vdots & \vdots & \vdots & \ddots & \cdots \\ P_{n1} & P_{n2} & \cdots & P_{nk} & \cdots & P_{nn} \end{bmatrix} \tag{2.5.30}$$

The elements of the participation matrix can be given as equation (2.5.31).

$$P = \begin{bmatrix} \phi_{11}\varphi_{11} & \phi_{12}\varphi_{21} & \cdots & \phi_{1k}\varphi_{k1} & \cdots & \phi_{1n}\varphi_{n1} \\ \phi_{21}\varphi_{12} & \phi_{22}\varphi_{22} & \cdots & \phi_{2k}\varphi_{k2} & \cdots & \phi_{2n}\varphi_{n2} \\ \vdots & \vdots & \ddots & \vdots & \vdots & \vdots \\ \phi_{i1}\varphi_{1i} & \phi_{i2}\varphi_{2i} & \cdots & \phi_{ik}\varphi_{ki} & \cdots & \phi_{in}\varphi_{ni} \\ \vdots & \vdots & \vdots & \vdots & \ddots & \cdots \\ \phi_{n1}\varphi_{1n} & \phi_{n2}\varphi_{2n} & \cdots & \phi_{nk}\varphi_{kn} & \cdots & \phi_{nn}\varphi_{nn} \end{bmatrix} \tag{2.5.31}$$

$P_{ik} = (\phi_{ik}\varphi_{ki})$; Participation factor of $\boldsymbol{k}^{th}$ state for $\boldsymbol{i}^{th}$ Eigen value (2.5.32)

As the Eigen matrix is normalized:

$$\left.\begin{aligned} \textstyle\sum_{i=1}^{n} P_{ik} = 1 \\ \textstyle\sum_{k=1}^{n} P_{ik} = 1 \end{aligned}\right\} \tag{2.5.33}$$

Equation (2.5.33) gives that addition of elements along any raw or a column in participation matrix is unity.

$P_{ik}\%$ can be considered as the contribution of k^{th} state for the stability of i^{th} Eigen value. Therefore, the states with highest participation factors contributes highest for the stability of the Eigen value. These states are called the "**effective states**".

Hence, by evaluating the effective states of the dominant Eigenvalues, the states which can cause instabilities in the system can be predicted.

CHAPTER 03

METHODOLOGY

3.1. Step 01 - Identifying and modeling the network

The following items were identified and modeled:

a. Models of generators, solar PV, cables and loads for power flow analysis and small signal stability analysis.
b. Substations, feeders and interconnectors of the selected network.
c. Loads connected to each substation.
d. Diesel generators and solar PV connected to each substation.

3.2. Step 02 - Power flow analysis

Power flow analysis was performed under the following conditions:

a. Different percentages in solar PV generation as per irradiance
b. Different loading conditions
e. Rapid dispatch and fast load removing scenarios

3.3. Step 03 - Stability analysis

Small signal stability model was initialized using the results of power flow analysis. Then the state matrix, right Eigen matrix and left Eigen matrix were derived.
Stability analysis was carried under the following conditions:

a. Different scenarios
b. Perturbations of different states

3.4. Identifying different operating scenarios

Depending on characteristics of the microgrid, several operating scenarios were proposed. Three main criteria were developed based on the following conditions:

a. Availability of diesel generators in the substations
b. Amount of solar PV connected to each substation
c. Operating mode of the network

3.4.1. Availability of diesel generators in the substations

Availability of diesel generators in the substation depends on many parameters like capacity of the substation, location, surrounding, accessibility, space of the substation, existing network arrangement, load of the substations and the capital expenditure incurring to introduce the diesel generator.

However, two modes of generator connections were considered in this thesis. Figure 3.1 depicts the two diesel generation connection modes.

- 2 MVA generators connected to primary substation B, substation 1174 and substation 5.

  Substation 1174 and substation 5 are the two highest loaded ring/radial substations in the selected network.

- 1 MVA generators connected to all substations

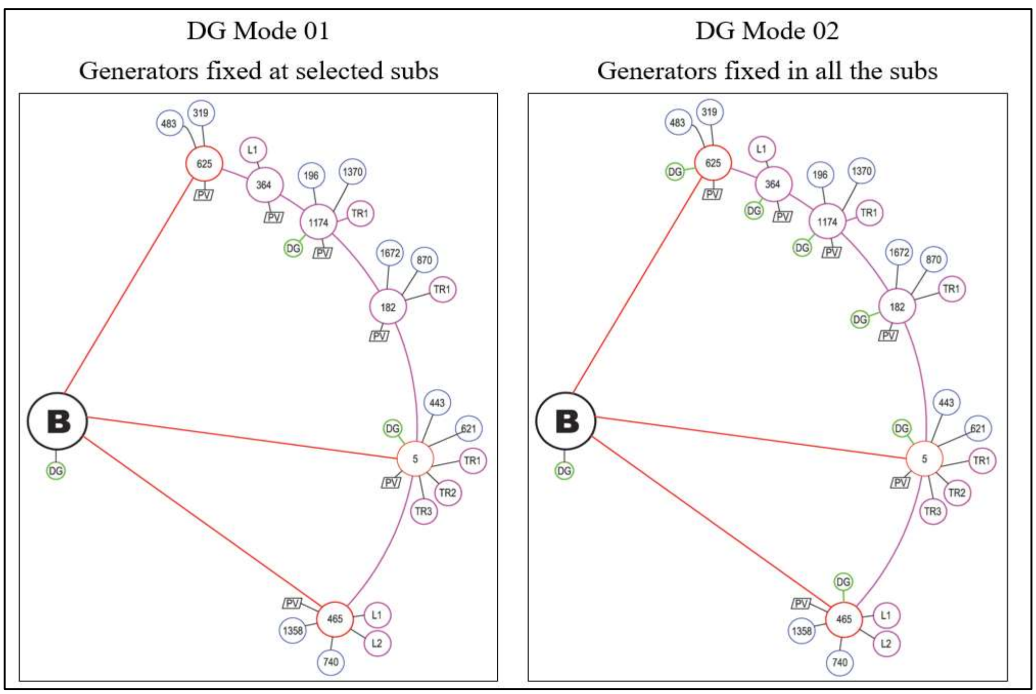

Figure 3.1 DG connection modes

3.4.2.Amount of solar PV connected to each substation

Amount of installed solar PV capacity was considered as a percentage, in three levels as 100%, 50% and 20% of maximum demand. Figure 3.2 depicts the load to be met by the grid or diesel generators for the different levels of installed solar PV capacity.

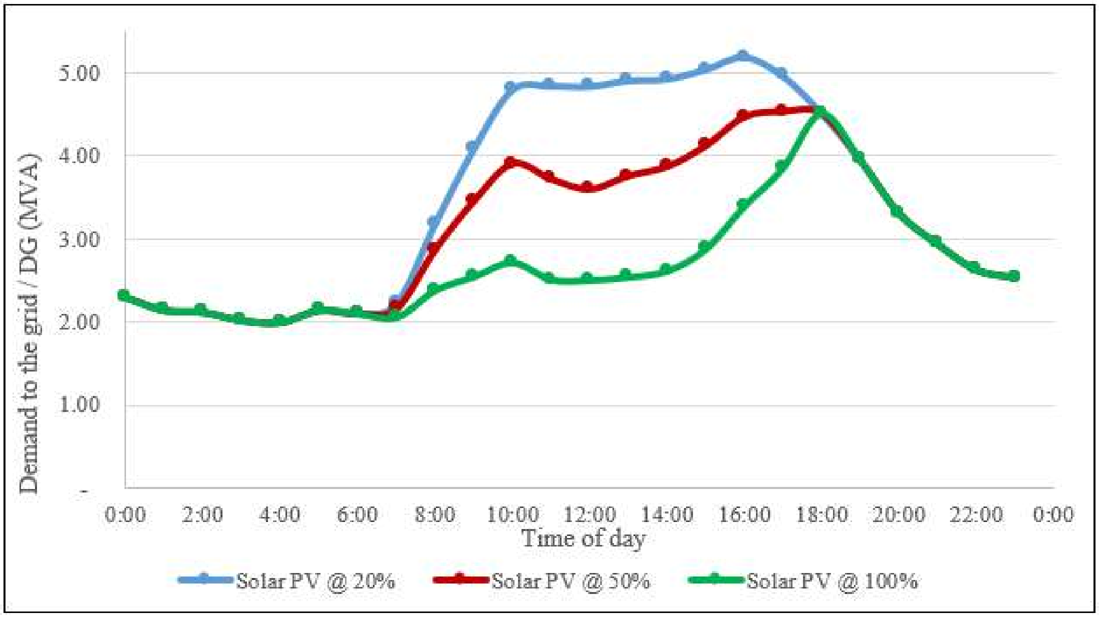

Figure 3.2 Demand to the grid/DG for different levels of solar PV

3.4.3.Operating mode of the network

Microgrid was operated in closed ring topology, which was labeled as the normal operating mode. All the circuit breakers in 11 kV network were considered as closed. To evaluate the stability under emergency state, N-1 operating mode was introduced. At the N-1 emergency operation state, the radial feeder B-5 is considered as out of operation. Radial B-5 is the highest loaded cable in the selected network. Hence, the worst-case scenario is considered in N-1 emergency operation. Figure 3.3 depicts the operating modes considered.

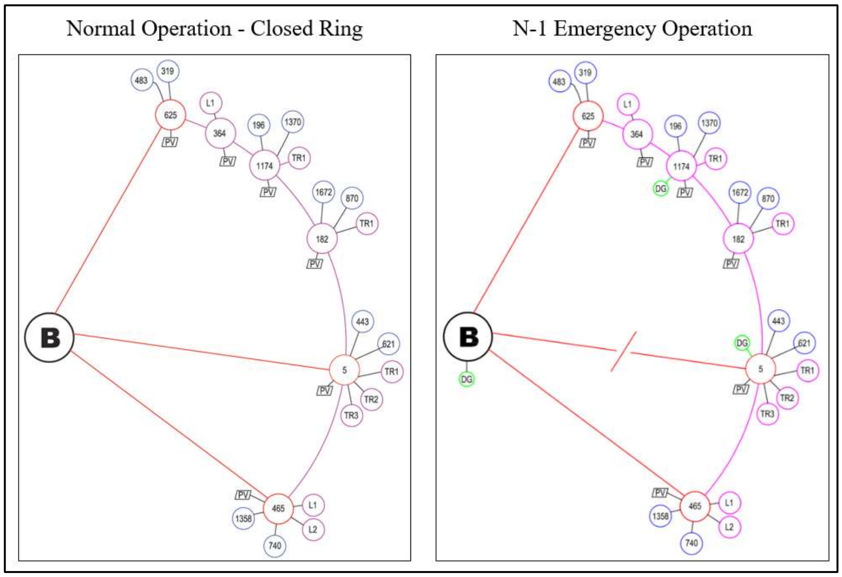

Figure 3.3 Operating modes

Based on the three criteria, 12 scenarios were derived. Each scenario has scenario has 24 operating points as one operating point for each hour. Figure 3.4 depicts all the 12 scenarios. Hence, to evaluate the network for all the scenarios, both power flow and small-signal analysis were performed for 288 operating points.

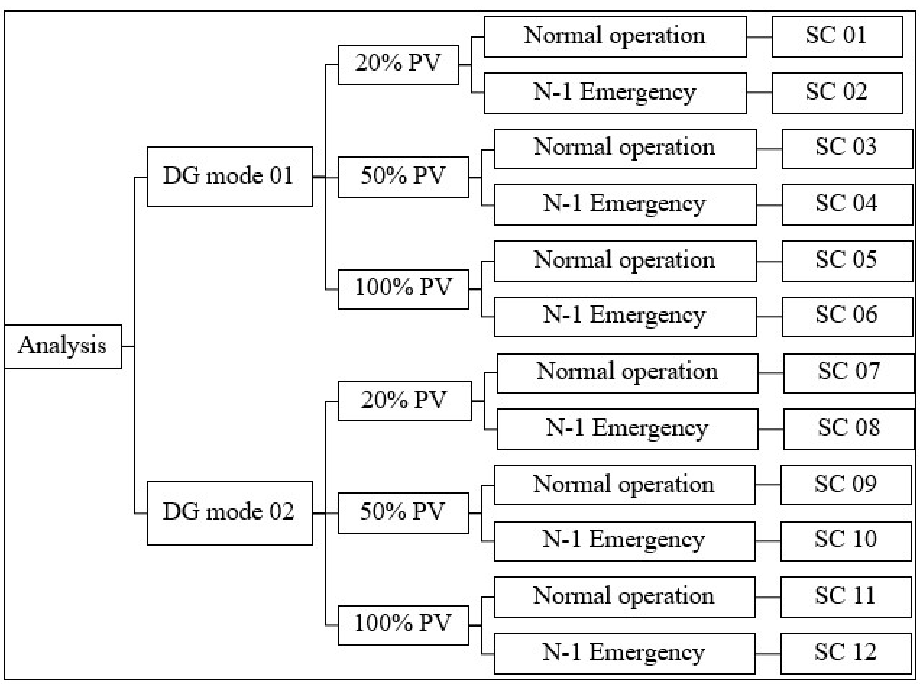

Figure 3.4 Derived scenarios

CHAPTER 04

POWER FLOW ANALYSIS OF THE SELECTED NETWORK

4.1. Modeling the selected network

Figure 4.1 depicts the selected portion from the ring network of Primary Substation B. The diagram consists of substations and the feeders in 11 kV network.

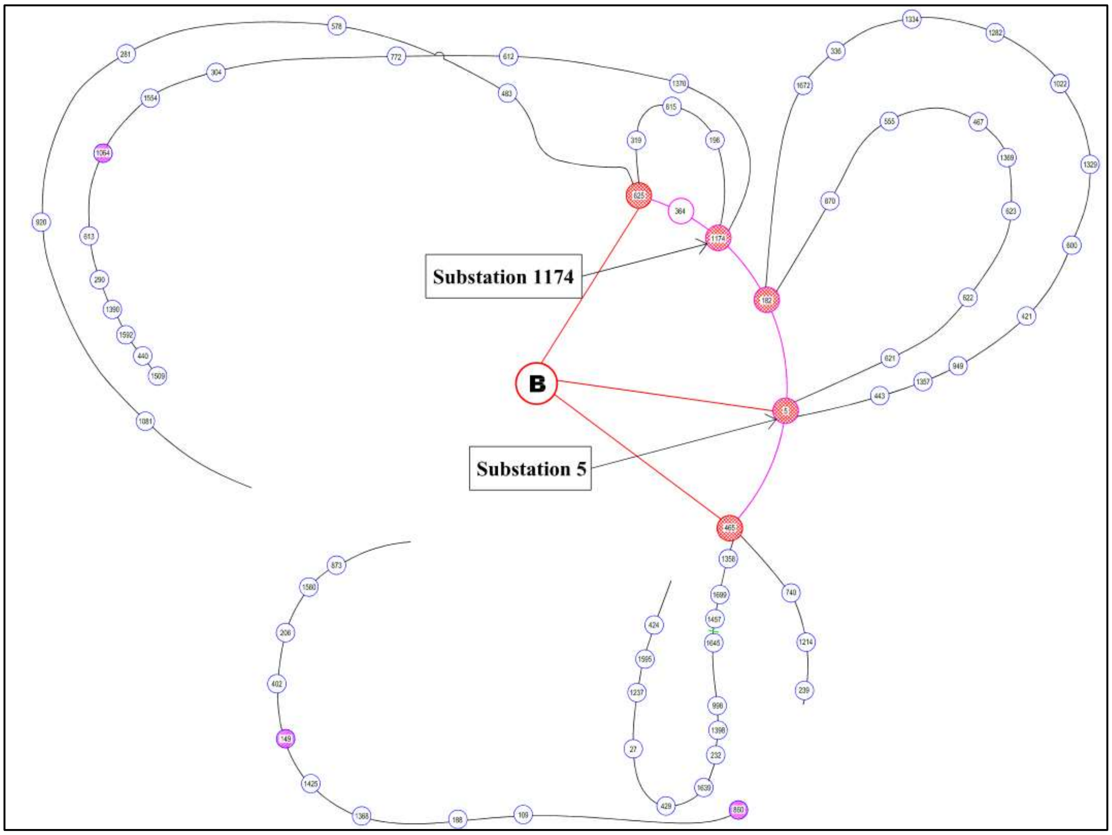

Figure 4.1 Selected ring portion of the primary substation B ring [1]

4.1.1. Substations

The system consists of three radial substations, three ring substations and 63 satellite substations in seven satellites. However, in this research, the system is modeled considering the satellites to be operated in open loop topology and the loop is denoted by the first satellite substation connected to the respective ring or radial substation.

4.1.2. Loads

Actual load data was considered in modeling. Data was obtained from the database at Colombo City SCADA system. As per the recorded data since 2012 to date, the highest load was recorded on 21/05/2019 [2]. Loads of all the satellite substations in a loop were lumped to the first substation of the loop. Load of each substation is shown in Table 4.1. Data in Table 1 shows that the total capacity of the selected network is 5.75 MVA, which can be configured to operate as a microgrid [7].

Table 4.1 Load of each substation at peak

Substation	Load / kW	Load / kVar
625	483.93	234.38
364	376.95	182.56
1174	1,354.61	656.07
182	240.80	116.62
5	2,205.47	1,068.16
465	514.32	249.10
Total	**5,176.08**	**2,506.89**

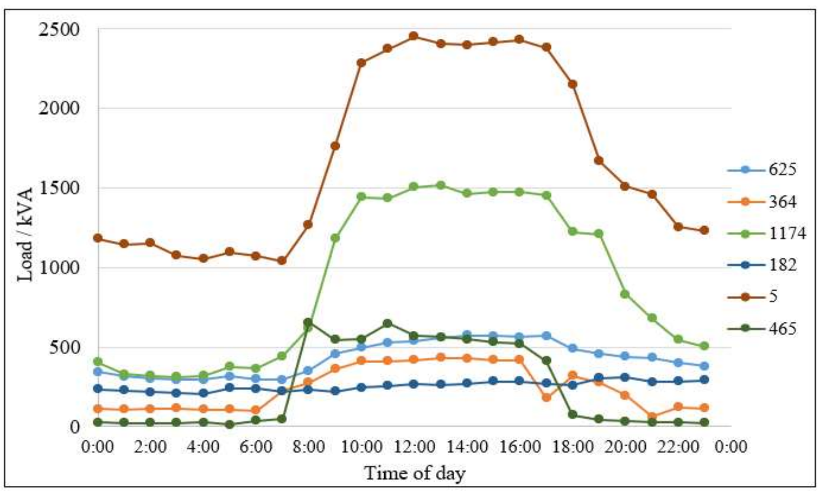

Figure 4.2 Daily load curve of each ring and radial substation on 21/05/2019 [2]

Figure 4.2 depicts the daily load curve on 21/05/2019 of each substation in the selected ring portion. All the six substations follow the typical load pattern on Colombo city described in 1.3. The highest load was recorded at the substation 5 and the second highest load was recorded at the substation 1174.

4.1.3. Cables

The selected system is utilizing two types of cables.

For the radial feeders 11kV/Cu/XLPE/240sqmm/3core/SWA cables are used. For the ring feeders 11kV/Cu/ XLPE/95sqmm/3core/SWA cables are used.

Cables were modeled using the actual cable parameters: length, resistance, impedance and capacitance of the Colombo city network. Table 4.2 depicts the per kilometer parameters of each cable type used in the selected network and, Table 4.3 depicts the length and actual parameters of each feeder.

Table 4.2 Parameters of different cable types used

Cable	R (Ω/km)	X (Ω/km)	B (S/km)
11kV/Cu/XLPE/240sqmm/3c	0.0984	0.0890	0.00015
11kV/Cu/XLPE/95sqmm/3c	0.2160	0.1020	0.000105

Table 4.3 Parameters of each cable

Branch	Type	Length / m	Ract (Ω)	Xact (Ω)	B (S)
B-625	11kV / Cu / 240sqmm / 3c	237.50	0.0234	0.0211	0.00004
B-5	11kV / Cu / 240sqmm / 3c	1,137.50	0.1119	0.1012	0.00017
B-465	11kV / Cu / 240sqmm / 3c	889.30	0.0875	0.0791	0.00013
625-364	11kV / Cu / 95sqmm / 3c	429.40	0.0928	0.0438	0.00005
364-1174	11kV / Cu / 95sqmm / 3c	277.70	0.0600	0.0283	0.00003
1174-182	11kV / Cu / 95sqmm / 3c	479.60	0.1036	0.0489	0.00005
182-5	11kV / Cu / 95sqmm / 3c	712.00	0.1538	0.0726	0.00007
5-465	11kV / Cu / 95sqmm / 3c	1,765.50	0.3813	0.1801	0.00019

4.1.4. Solar PV Generation

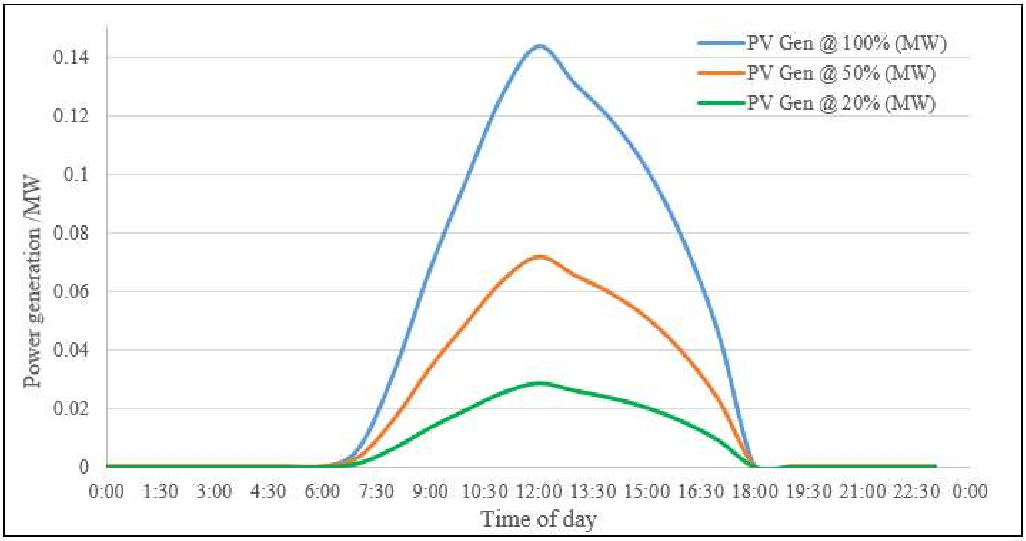

Figure 4.3 Average daily power generation of a solar PV

Figure 4.3 depicts the equally adjusted average daily solar PV generation curves for different percentages of installed solar PV capacities for one substation. It can be noted that the solar power generation starts after 6.00 AM and ends around 6.00 PM. It peaks at 12.00 noon. Solar generation was considered as negative loads to each ring and radial substation.

4.1.5. Diesel Generator

Two modes of generator connections were used as shown in Table 4.4. Primary substation B was used as the slack bus. The capacities and the number of generators were selected based on the peak load of the selected system.

Table 4.4 Generator modes

	Mode 01	Mode 02
Generator capacity	2 MVA	1 MVA
No. of generators	3	7
Substations with generators	Primary Substation B substation 1174 substation 5	All substations

4.2. Analysis

Power flow analysis was done for all the 288 operating points (discussed in section 3.4.3) using PSS/E University 33 software. Figure 4.4 depicts the PSSE model of the network for mode 01 operation of the diesel generator.

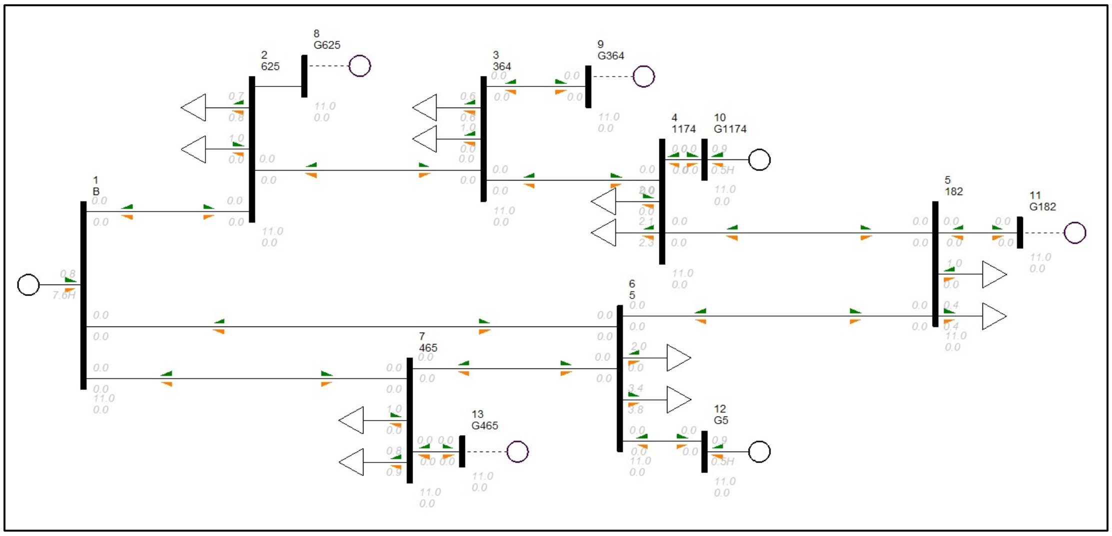

Figure 4.4 PSS/E model of the selected network

4.2.1. Bus bar data

Generator buses were introduced to each substation. Bus bar of primary substation B was used as the slack bus. Figure 4.5 depicts the network data of the buses used to configure the PSS/E model for mode 01 operation of the diesel generator.

Bus Number	Bus Name	Base kV	Area Num	Area Name	Zone Num	Zone Name	Owner	Owner Name	Code	Voltage (pu)	Angle (deg)	Normal Vmax (pu)	Normal Vmin (pu)	Emergency Vmax (pu)	Emergency Vmin (pu)
1	B	11.0	1		1		1		3	1.0000	0.00	1.1000	0.9000	1.1000	0.9000
2	625	11.0	1		1		1		1	1.0000	0.00	1.1000	0.9000	1.1000	0.9000
3	364	11.0	1		1		1		1	1.0000	0.00	1.1000	0.9000	1.1000	0.9000
4	1174	11.0	1		1		1		1	1.0000	0.00	1.1000	0.9000	1.1000	0.9000
5	182	11.0	1		1		1		1	1.0000	0.00	1.1000	0.9000	1.1000	0.9000
6	5	11.0	1		1		1		1	1.0000	0.00	1.1000	0.9000	1.1000	0.9000
7	465	11.0	1		1		1		1	1.0000	0.00	1.1000	0.9000	1.1000	0.9000
8	G625	11.0	1		1		1		2	1.0000	0.00	1.1000	0.9000	1.1000	0.9000
9	G364	11.0	1		1		1		2	1.0000	0.00	1.1000	0.9000	1.1000	0.9000
10	G1174	11.0	1		1		1		2	1.0000	0.00	1.1000	0.9000	1.1000	0.9000
11	G182	11.0	1		1		1		2	1.0000	0.00	1.1000	0.9000	1.1000	0.9000
12	G5	11.0	1		1		1		2	1.0000	0.00	1.1000	0.9000	1.1000	0.9000
13	G465	11.0	1		1		1		2	1.0000	0.00	1.1000	0.9000	1.1000	0.9000

Figure 4.5 Sample network data of buses

4.2.2. Generator data

Figure 4.6 depicts the PSS/E network data of the generators in the network for mode 01 operation of diesel generator. In mode 01, diesel generators in the capacity of 2 MVA were connected to substations B, 1174 and 5 only.

Bus Number	Bus Name	Id	Area Num	Area Name	Zone Num	Zone Name	Code	VSched (pu)	Remote Bus	In Service	PGen (MW)	PMax (MW)	PMin (MW)	QGen (Mvar)	QMax (Mvar)
1	B 11.000	DG	1		1		3	1.0000	0	☑	-4.4141	1.8000	0.0000	2.4206	0.8718
8	G625 11.000	DG	1		1		-2	1.0000	0	☐	0.0000	0.0000	0.0000	0.0000	0.0000
9	G364 11.000	DG	1		1		-2	1.0000	0	☐	0.0000	0.0000	0.0000	0.0000	0.0000
10	G1174 11.00	DG	1		1		-2	1.0000	0	☑	1.8000	1.8000	0.0000	0.8718	0.8718
11	G182 11.000	DG	1		1		-2	1.0000	0	☐	0.0000	0.0000	0.0000	0.0000	0.0000
12	G5 11.000	DG	1		1		-2	1.0000	0	☑	1.8000	1.8000	0.0000	0.8718	0.8718
13	G465 11.000	DG	1		1		-2	1.0000	0	☐	0.0000	0.0000	0.0000	0.0000	0.0000
										☑					

Figure 4.6 Network data of generators

4.2.3. Load data

Loads were introduced to all the substations. Figure 4.7 depicts the PSS/E network data of the loads in the network at 1200h. The solar PV installed capacity is at 100% of maximum demand, which is 5.18 MW. It was lumped to each substation as a negative load equally distributed among all the ring/radial substations.

Bus Number	Bus Name	Id	Code	Area Num	Area Name	Zone Num	Zone Name	Owner	Owner Name	In Service	Scalable	Interruptible	Pload (MW)	Qload (Mvar)
2	625 11.000	L	1	1		1		1		☑	☑ Yes	☐ Yes	0.4839	0.2344
2	625 11.000	PV	1	1		1		1		☑	☑ Yes	☐ Yes	-0.8630	0.0000
3	364 11.000	L	1	1		1		1		☑	☑ Yes	☐ Yes	0.3770	0.1826
3	364 11.000	PV	1	1		1		1		☑	☑ Yes	☐ Yes	-0.8630	0.0000
4	1174 11.000	L	1	1		1		1		☑	☑ Yes	☐ Yes	1.3546	0.6561
4	1174 11.000	PV	1	1		1		1		☑	☑ Yes	☐ Yes	-0.8630	0.0000
5	182 11.000	L	1	1		1		1		☑	☑ Yes	☐ Yes	0.2408	0.1166
5	182 11.000	PV	1	1		1		1		☑	☑ Yes	☐ Yes	-0.8630	0.0000
6	5 11.000	L	1	1		1		1		☑	☑ Yes	☐ Yes	2.2055	1.0681
6	5 11.000	PV	1	1		1		1		☑	☑ Yes	☐ Yes	-0.8630	0.0000
7	465 11.000	L	1	1		1		1		☑	☑ Yes	☐ Yes	0.5143	0.2491
7	465 11.000	PV	1	1		1		1		☑	☑ Yes	☐ Yes	-0.8630	0.0000

Figure 4.7 Network data of loads

Table 4.5 Load data (kVA) corresponding to all the substations

Time	Sub 625	Sub 364	Sub 1174	Sub 182	Sub 5	Sub 465	Total
0:00	343.38	109.96	404.24	235.52	1,179.31	27.09	2,299.49
1:00	314.43	108.36	329.15	226.11	1,144.92	23.50	2,146.48
2:00	301.82	109.96	318.14	217.70	1,153.95	22.88	2,124.46
3:00	292.91	113.06	312.33	211.02	1,074.04	21.52	2,024.89
4:00	292.91	108.11	318.76	205.21	1,051.90	25.73	2,002.62
5:00	316.66	106.63	374.30	241.33	1,095.20	12.74	2,146.85
6:00	297.98	99.33	366.14	237.62	1,071.45	35.38	2,107.89
7:00	293.65	225.37	443.57	220.05	1,039.90	47.62	2,270.17
8:00	351.79	276.46	620.58	230.32	1,268.49	655.46	3,403.10
9:00	456.93	363.17	1,180.79	219.19	1,762.16	544.63	4,526.87
10:00	496.88	411.29	1,441.67	245.29	2,287.00	548.59	5,430.71
11:00	526.07	412.40	1,435.60	256.30	2,374.94	648.66	5,653.97
12:00	537.70	418.83	1,505.12	267.55	2,450.52	571.47	5,751.20
13:00	560.96	432.56	1,517.24	264.46	2,404.01	563.31	5,742.54
14:00	573.82	429.72	1,463.44	269.78	2,400.18	547.60	5,684.53
15:00	569.00	419.20	1,475.06	284.50	2,416.51	530.16	5,694.42
16:00	563.93	419.94	1,473.33	283.88	2,431.97	520.38	5,693.43
17:00	571.47	177.13	1,451.44	268.29	2,379.52	409.43	5,257.28
18:00	487.23	320.37	1,224.09	258.40	2,151.80	73.85	4,515.73
19:00	456.06	275.84	1,207.88	306.39	1,666.91	43.17	3,956.26
20:00	439.24	194.32	831.48	307.13	1,507.84	34.63	3,314.65
21:00	433.43	60.49	680.57	281.78	1,461.21	27.46	2,944.93
22:00	400.65	121.59	545.87	283.63	1,255.38	25.60	2,632.72
23:00	380.73	114.05	503.69	289.45	1,229.16	22.88	2,539.95

Table 4.5 depicts the loads of each substation throughout the day. It can be clearly seen that substation 5 and substation 1174 are the two highest loaded substations and all the loads of substation reaches a peak around 1200 noon. The demand of the selected network peaks to 5.75 MVA at 1200 h.

Appendix A presents the detailed information on loads connected at the satellites.

4.2.4. Time domain analysis of the selected network for power flow

In order to validate the derived PSS/E power flow model, it was compared against a time domain simulation. The network was modeled in Matlab Simulink using the existing models in Simscape Electrical library.

Model for diesel generator and solar PV

Diesel generator and solar PV were modelled using the three-phase voltage source model in Matlab Simulink. Constant PV type generator and constant PQ type generator were used for diesel generator and solar PV respectively.

Model for load

Loads were modelled by properly configuring the three-phase parallel RLC load model. The active and reactive power components were changed as per the substation loads given in Table 4.5. Constant PQ type load was used.

Model of a substation

Time domain model for a substation was obtained by connecting the diesel generator, solar PV and loads in parallel. Figure 4.8 depicts the time domain model of a substation. A distribution transformer was introduced to link the substation to the primary distribution level of the network.

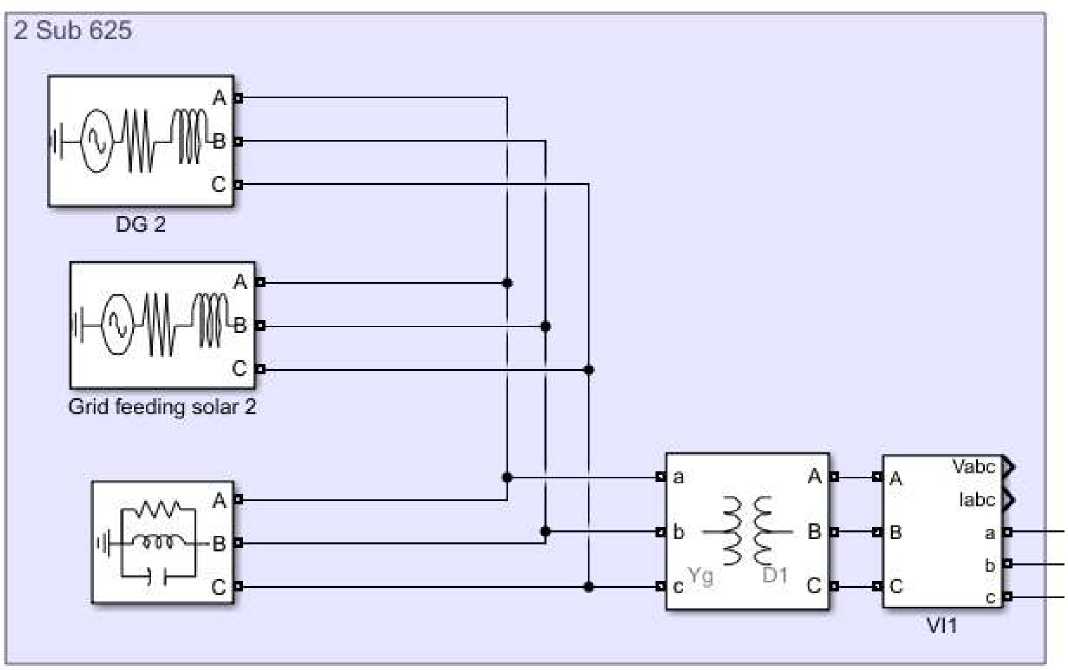

Figure 4.8 Time domain power flow model for a substastion

Model for feeder

Distributed parameters line model was used to represent the 11kV/240sqmm/3 core cables and 11kV/95sqmm/3 core cables. The resistance, inductance and capacitance were changed according to the cable parameters given in Table 4.3.

Complete model

The complete model was obtained by linking the substation models with feeders according to the ring diagram given in Figure 4.1.

4.2.5. Validating the PSS/E power flow model

Steady state phase voltages of all the substations were obtained via powergui module in Matlab Simscape. The line voltages were calculated accordingly. Then the voltages of each substation in the Simulink model were compared with the same of PSS/E model. It was found that the error was below 1%. Table 4.6 depicts the calculation of line bus voltages from the Simulink model and the comparison of the same with the voltages of PSS/E model for the scenario 09, where there are all generators at the all the substations and the solar PV is at 100% of the maximum demand. Thus, the derived model is validated.

Table 4.6 Comparison of bus voltages in Simulink model and PSS/E model

Bus bar	Phase voltages in Simulink model			Line voltages calculated with the Simulink model		Voltage magnitudes in PSS/E model / V	% err. of the magnitude
		Magnitude / V	Angle / degree		Magnitude / V		
B	A	6,390.60	161.27	A-B	11,068.84	11,000.00	0.626%
	B	6,390.60	41.27	B-C	11,068.84	11,000.00	0.626%
	C	6,390.60	-78.73	C-A	11,068.84	11,000.00	0.626%
625	A	6,382.60	161.49	A-B	11,054.99	11,000.00	0.500%
	B	6,382.60	41.49	B-C	11,054.99	11,000.00	0.500%
	C	6,382.60	-78.51	C-A	11,054.99	11,000.00	0.500%
364	A	6,380.20	161.49	A-B	11,050.83	11,004.00	0.426%
	B	6,380.20	41.49	B-C	11,050.83	11,004.00	0.426%
	C	6,380.20	-78.51	C-A	11,050.83	11,004.00	0.426%
1174	A	6,362.10	161.49	A-B	11,019.48	11,003.00	0.150%
	B	6,362.10	41.49	B-C	11,019.48	11,003.00	0.150%
	C	6,362.10	-78.51	C-A	11,019.48	11,003.00	0.150%
182	A	6,365.80	161.48	A-B	11,025.89	10,999.00	0.244%
	B	6,365.80	41.48	B-C	11,025.89	10,999.00	0.244%
	C	6,365.80	-78.52	C-A	11,025.89	10,999.00	0.244%
5	A	6,372.80	161.48	A-B	11,038.01	10,986.00	0.473%
	B	6,372.80	41.48	B-C	11,038.01	10,986.00	0.473%
	C	6,372.80	-78.52	C-A	11,038.01	10,986.00	0.473%
465	A	6,385.20	161.48	A-B	11,059.49	11,001.00	0.532%
	B	6,385.20	41.48	B-C	11,059.49	11,001.00	0.532%
	C	6,385.20	-78.52	C-A	11,059.49	11,001.00	0.532%

4.2.6. Results of power flow analysis on selected network

Power flow analysis were done at 288 operating points selected to conduct small signal analysis. Output data of the power flow analysis was used as the input data for small signal analysis. For the small signal analysis, the voltage and the power input of each bus bar were used as inputs data.

When referring the output data, it was noted that the voltages of buses in N-1 emergency operation has slightly more deviated from the nominal value than that under normal operation. However, the maximum variation at any bus at any given time is less than 0.5% of the nominal value (11 kV), which is a notable improvement of the voltage when compared to the prevailing system. The cause for this improvement is, distributed generators have improved the voltage profile of the system.

Output data of all the scenarios are attached in Appendix B.

CHAPTER 05

SMALL SIGNAL ANALYSIS

5.1. Small Signal Stability Model of the Microgrid

5.1.1. Generator Model

Figure 5.1 depicts the generator model used for developing the small signal model of the microgrid. Steady-state equivalent circuit of the generator was used [13].

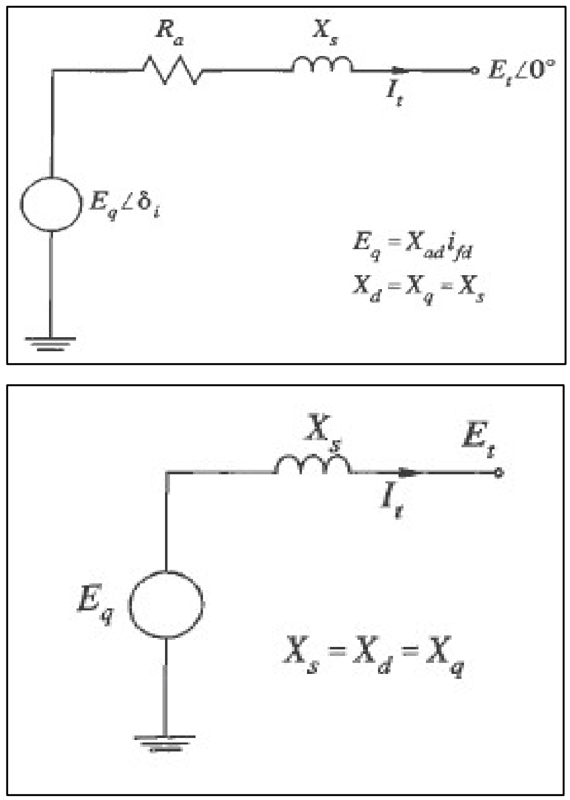

Figure 5.1 Generator model used for small-signal model

The parameteres in Figure 5.1 can be defined as:

E_q - Effective internal voltage

X_s - Synchronous reactance

R_a - Per phase armature resistance but can be neglected as its very small.

5.1.2. Cable Model

The cable was modeled as a π-section [13] as shown in Figure 5.2. Parameters of all the cables are shown in Table 4.3 in Chapter 4.

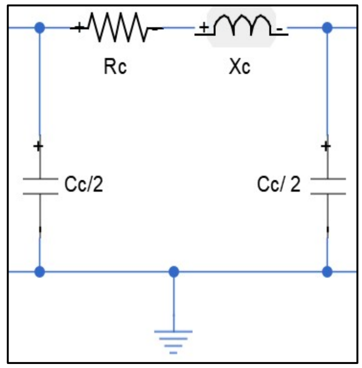

Figure 5.2 Cable model used for small-signal model

The variables in Figure 5.2 can be defined as follows:

Rc - Resistance of the cable

Xc **-** Impedance of the cable

Cc - Capacitance of the cable

The cable parameters ***Rc*****,** ***Xc*** and ***Cc*** change from cable to cable and depends on the type and length of the cable.

5.1.3. Load Model

Loads were modeled as a shunt constant impedance at each substation as illustrated in Figure 5.3.

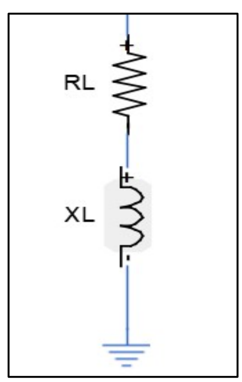

Figure 5.3 Load model used for small-signal model

The variables in Figure 5.3 can be defined as follows:

R_L - Active power component of the load

X_L - Reactive power component of the load.

5.1.4. Transformer Model

Standard simple equivalent circuit was used to model the transformer of each substation. Figure 5.4 depicts the transformer model used in the small signal model, where X_{tr} denotes the internal impedance of the transformer.

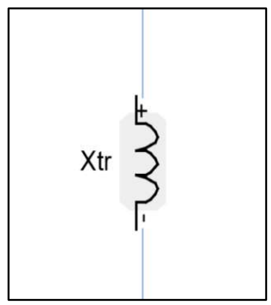

Figure 5.4 Transformer model used for small-signal model

5.1.5. Solar PV Model

Grid feeding mode was considered for all the solar PV inverters. Hence, the solar PV was modeled as a power input, which is varying proportionately with the solar irradiance [9] [10]. Figure.5.5 depicts the solar PV model used in small signal model, and output power, P_{PV} was calculated using the equation (2.3.1) discussed in Chapter 2.

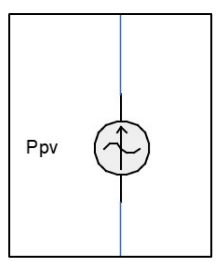

Figure 5.5 Solar PV model used for small-signal model

5.1.6. Complete Small Signal Model

The small signal model for the complete network in Figure 5.6 was formed using the models described in the sections 5.1.1 to 5.1.5 integrating according to the test system discussed in section 1.5.

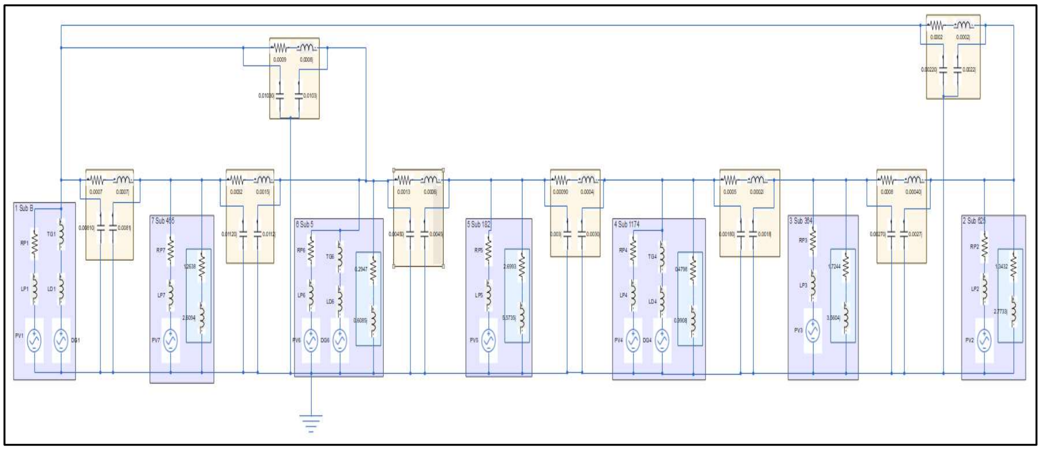

Figure 5.6 Complete model used for small-signal analysis

5.1.7. State space representation of the model

The state space model of the network was obtained initially [17]. Then the analysis was done as per the procedure given in section 2.5.

Bus admittance matrix (Y-bus matrix) was obtained, which can be represented by (5.1.1).

$$Y = G + jB \tag{5.1.1}$$

Based on equation (2.3.2), power generation by solar PV (where, $\emptyset_i$ = irradiance) can be represented by (5.1.2).

$$S_{iPV} = k_{iPV}\emptyset_i \tag{5.1.2}$$

Equation (5.1.3) is written by applying Kirchhoff's Current Law to the i^{th} node and can be expanded as (5.1.4).

$$I_{iDG} + I_{iPV} = Y_{ii} V_i + \sum_{k=1,\, k\neq i}^{n} Y_{ik} V_k \tag{5.1.3}$$

$$I_{iDG} + I_{iPV} = (G_{ii} + j\, B_{ii}).V_i.\ e^{j\delta_i} + \sum_{k=1,\, k\neq i}^{n} (G_{ik} + j\, B_{ik}).V_k.\ e^{j\delta_k} \quad (5.1.4)$$

Consider the power at i[th] node as given by (5.1.5);

$$S_i = V_i\, I_i^* \quad (5.1.5)$$

Equation (5.1.6) can be derived by substituting the expression for the input current in the equation (5.1.4) to the equation (5.1.5);

$$\mathrm{S_{iDG}} + \mathrm{S_{iPV}} = \mathrm{V_i}.\ \mathrm{e^{j\delta_i}}\ .\ \left((\mathrm{G_{ii}} - \mathrm{j\, B_{ii}}).\mathrm{V_i}.\ \mathrm{e^{-j\delta_i}} + \sum_{\mathrm{k=1,\, k\neq i}}^{\mathrm{n}} (\mathrm{G_{ik}} - \mathrm{j\, B_{ik}}).\mathrm{V_k}.\ \mathrm{e^{-j\delta_k}} \right) \quad (5.1.6)$$

Equation (5.1.6) was further solved to obtain equation (5.1.7);

$$\mathrm{S_{iDG}} + \mathrm{S_{iPV}} = (\mathrm{G_{ii}} - \mathrm{j\, B_{ii}}).\mathrm{V_i^2}. + \mathrm{V_i}.\sum_{\mathrm{k=1,k\neq i}}^{\mathrm{n}} (\mathrm{G_{ik}} - \mathrm{j\, B_{ik}}).\mathrm{V_k}.\mathrm{e^{-j\,\delta\,k}} \quad (5.1.7)$$

After separating the real and imaginary components of equation (5.1.7), the expressions for active and reactive components of power can be obtained. Equations (5.1.8) and (5.1.9) give the expressions for active power and reactive power at each node.

$$P_{iDG} + P_{iPV} = G_{ii}.V_i^2. + \sum_{k=1,k\neq i}^{n} V_i.V_k\ [G_{ik}\,.\cos(\delta_i - \delta_k) + B_{ik}\,.\sin(\delta_i - \delta_k)] \quad (5.1.8)$$

$$Q_{iDG} + Q_{iPV} = -B_{ii}.V_i^2. + \sum_{k=1,k\neq i}^{n} V_i.V_k\ [G_{ik}\,.\sin(\delta_i - \delta_k) - B_{ik}\,.\cos(\delta_i - \delta_k)] (5.1.9)$$

Small-signal perturbation for expression of active power

Considering the total power input to the node as P_i, (5.1.8) can be remodeled as (5.1.10):

$$P_i = G_{ii}.V_i^2. + \sum_{k=1,k\neq i}^{n} V_i.V_k\ [G_{ik}\,.\cos(\delta_i - \delta_k) + B_{ik}\,.\sin(\delta_i - \delta_k)] \quad (5.1.10)$$

Small-signal perturbations of ΔV_i and $\Delta\delta_i$ were applied to voltage and rotor angle respectively as shown in (5.1.11).

Assume when $V_i = V_i + \Delta V_i$ and $\delta_i = \delta_i + \Delta\delta_i$, Then $P_i = P_i + \Delta P_i$ (5.1.11)

By applying the perturbed signals in equation (5.1.11) to the equation (5.1.10), the expression shown in (5.1.12) for perturbed power was obtained.

$$P_i + \Delta P_i = G_{ii}.(V_i + \Delta V_i)^2 + \sum_{k=1,k\neq i}^{n}(V_i + \Delta V_i).V_k[G_{ik}.\cos(\delta_i + \Delta\delta_i - \delta_k) + B_{ik}.\sin(\delta_i + \Delta\delta_i - \delta_k)] \quad (5.1.12)$$

Equation (5.1.12) was expanded to (5.1.13).

$$P_i + \Delta P_i = G_{ii}.(V_i^2 + \Delta V_i^2 + 2.V_i.\Delta V_i) + \sum_{k=1,k\neq i}^{n}(V_i + \Delta V_i).V_k[G_{ik}.[cos(\delta_i - \delta_k) - sin(\delta_i - \delta_k).\Delta\delta_i] + B_{ik}.[sin(\delta_i - \delta_k) + cos(\delta_i - \delta_k).\Delta\delta_i]] \quad (5.1.13)$$

Equation (5.1.13) was further expanded to (5.1.14).

$$P_i + \Delta P_i = G_{ii}.(V_i^2 + \Delta V_i^2 + 2.V_i.\Delta V_i) + \sum_{k=1,k\neq i}^{n}(V_i).V_k[G_{ik}.[\cos(\delta_i - \delta_k) - \sin(\delta_i - \delta_k).\Delta\delta_i] + B_{ik}.[\sin(\delta_i - \delta_k) + \cos(\delta_i - \delta_k).\Delta\delta_i]] + \sum_{k=1,k\neq i}^{n}\Delta V_i.V_k[G_{ik}.[\cos(\delta_i - \delta_k) - \sin(\delta_i - \delta_k).\Delta\delta_i] + B_{ik}.[\sin(\delta_i - \delta_k) + \cos(\delta_i - \delta_k).\Delta\delta_i]] \quad (5.1.14)$$

As ΔV_i is a small perturbation, ΔV_i^2 was considered as negligible. Equation (5.1.14) was modified accordingly and the equation (5.1.15) was obtained.

$$P_i + \Delta P_i = G_{ii}.(V_i^2 + 2.V_i.\Delta V_i) + \sum_{k=1,k\neq i}^{n}[V_i.V_k.G_{ik}.cos(\delta_i - \delta_k) - V_i.V_k.G_{ik}.sin(\delta_i - \delta_k).\Delta\delta_i + V_i.V_k.B_{ik}sin(\delta_i - \delta_k) + V_i.V_k.B_{ik}.cos(\delta_i - \delta_k).\Delta\delta_i] + \sum_{k=1,k\neq i}^{n}[\Delta V_i.V_k.G_{ik}.cos(\delta_i - \delta_k) + \Delta V_i.V_k.B_{ik}sin(\delta_i - \delta_k)] \quad (5.1.15)$$

Equation (5.1.16) was obtained by subtracting equations (5.1.15) and (5.1.10).

$$\Delta P_i = 2.V_i.\Delta V_i.G_{ii}. + \sum_{k=1,k\neq i}^{n}V_i.V_k.[-G_{ik}.sin(\delta_i - \delta_k) + B_{ik}.cos(\delta_i - \delta_k)].\Delta\delta_i + \sum_{k=1,k\neq i}^{n}V_k.[G_{ik}.cos(\delta_i - \delta_k) + B_{ik}sin(\delta_i - \delta_k)].\Delta V_i \quad (5.1.16)$$

Equation (5.1.16) was further modified as equation (5.1.17).

$$\Delta P_i = \sum_{k=1,k\neq i}^{n}V_i.V_k.[-G_{ik}.\sin(\delta_i - \delta_k) + B_{ik}.\cos(\delta_i - \delta_k)].\Delta\delta_i + \left[2.V_i.G_{ii} + \sum_{k=1,k\neq i}^{n}V_k.[G_{ik}.\cos(\delta_i - \delta_k) + B_{ik}\sin(\delta_i - \delta_k)]\right].\Delta V_i \quad (5.1.17)$$

Equation (5.1.17) gives the expression for perturbed signal for active power.

Small-signal perturbation for expression of reactive power

Considering the total reactive power input to the node as Q_i, equation (5.1.9) can be remodeled as equation (5.1.18):

$$Q_i = -B_{ii}.V_i^2.+ \sum_{k=1,k\neq i}^{n} V_i.V_k\,[G_{ik}\,.\sin(\delta_i - \delta_k) - B_{ik}\,.\cos(\delta_i - \delta_k)] \qquad (5.1.18)$$

Small-signal perturbations of ΔV_i and $\Delta\delta_i$ were applied to voltage and rotor angle respectively as shown in (5.1.19).

Assume when $V_i = V_i + \Delta V_i$ and $\delta_i = \delta_i + \Delta\delta_i$, Then $Q_i = Q_i + \Delta Q_i$ (5.1.19)

By applying the perturbed signals in equation (5.1.19) to the equation (5.1.18), the expression shown in (5.1.20) for perturbed power was obtained.

$$Q_i + \Delta Q_i = -B_{ii}.(V_i + \Delta V_i)^2 + \sum_{k=1,k\neq i}^{n} (V_i + \Delta V_i).V_k[G_{ik}\,.\sin(\delta_i + \Delta\delta_i - \delta_k) - B_{ik}.\cos(\delta_i + \Delta\delta_i - \delta_k)] \qquad (5.1.20)$$

Equation (5.1.20) was expanded to (5.1.21).

$$\Delta Q_i = -B_{ii}.(V_i^2 + \Delta V_i^2 + 2.V_i.\Delta V_i) + \sum_{k=1,k\neq i}^{n} (V_i + \Delta V_i).V_k\,[G_{ik}.[\sin(\delta_i - \delta_k) + \cos(\delta_i - \delta_k).\Delta\delta_i] - B_{ik}\,.[\cos(\delta_i - \delta_k) - \sin(\delta_i - \delta_k)\,.\Delta\delta_i]] \qquad (5.1.21)$$

Equation (5.1.21) was further expanded to (5.1.22).

$$Q_i + \Delta Q_i = -B_{ii}.\left(V_i^2 + \Delta V_i^2 + 2.V_i.\Delta V_i\right) + \sum_{k=1,k\neq i}^{n}[\,V_i.V_k.G_{ik}.\sin(\delta_i - \delta_k) + V_i.V_k.G_{ik}.\cos(\delta_i - \delta_k).\Delta\delta_i] - V_i.V_k.B_{ik}\cos(\delta_i - \delta_k) + V_i.V_k.B_{ik}.\sin(\delta_i - \delta_k)\,.\Delta\delta_i] + \sum_{k=1,k\neq i}^{n}[\,\Delta V_i.V_k.G_{ik}.\sin(\delta_i - \delta_k) + \Delta V_i.V_k.G_{ik}.\cos(\delta_i - \delta_k).\Delta\delta_i] - \Delta V_i.V_k.B_{ik}\cos(\delta_i - \delta_k) + \Delta V_i.V_k.B_{ik}.\sin(\delta_i - \delta_k)\,.\Delta\delta_i] \qquad (5.1.22)$$

As ΔV_i is a small perturbation, ΔV_i^2 was considered as negligible. Equation (5.1.22) was modified accordingly and the equation (5.1.23) was obtained.

$$Q_i + \Delta Q_i = -B_{ii}.\left(V_i^2 + 2.V_i.\Delta V_i\right) + \sum_{k=1,k\neq i}^{n}[\,V_i.V_k.G_{ik}.\sin(\delta_i - \delta_k) + V_i.V_k.G_{ik}.\cos(\delta_i - \delta_k).\Delta\delta_i] - V_i.V_k.B_{ik}\cos(\delta_i - \delta_k) + V_i.V_k.B_{ik}.\sin(\delta_i - \delta_k)\,.\Delta\delta_i] + \sum_{k=1,k\neq i}^{n}[\,\Delta V_i.V_k.G_{ik}.\sin(\delta_i - \delta_k)] - \Delta V_i.V_k.B_{ik}\cos(\delta_i - \delta_k)] \qquad (5.1.23)$$

Equation (5.1.24) was obtained by subtracting equations (5.1.23) and (5.1.18).

$$\Delta Q_i = \sum_{k=1,k\neq i}^{n}[\ V_i.V_k.G_{ik}.\cos(\delta_i - \delta_k).\Delta\delta_i] + V_i.V_k.B_{ik}.\sin(\delta_i - \delta_k).\Delta\delta_i] + \sum_{k=1,k\neq i}^{n}[\ \Delta V_i.V_k.G_{ik}.\sin(\delta_i - \delta_k)] - \Delta V_i.V_k.B_{ik}\cos(\delta_i - \delta_k)] \qquad (5.1.24)$$

Equation (5.1.24) was further modified as equation (5.1.25).

$$\Delta Q_i = \sum_{k=1,k\neq i}^{n}[\ V_i.V_k.G_{ik}.\cos(\delta_i - \delta_k).\Delta\delta_i + V_i.V_k.B_{ik}.\sin(\delta_i - \delta_k).\Delta\delta_i + \Delta V_i.V_k.G_{ik}.\sin(\delta_i - \delta_k) - \Delta V_i.V_k.B_{ik}\cos(\delta_i - \delta_k)\ ] \qquad (5.1.25)$$

Equation (5.1.25) gives the expression for perturbed signal for reactive power.

Using (5.1.17) and (5.1.25) the expressions for perturbed signals of active and reactive power can be derived as in (5.1.26) and (5.1.27) respectively;

$$\Delta P_i = \sum_{k=1}^{n} V_i.V_k.[-G_{ik}.\sin(\delta_i - \delta_k) + B_{ik}.\cos(\delta_i - \delta_k)].\ \Delta\delta_i + [\ V_i.G_{ii} + \sum_{k=1}^{n} V_k.[\ G_{ik}.\cos(\delta_i - \delta_k) + B_{ik}\sin(\delta_i - \delta_k)]].\Delta V_i \qquad (5.1.26)$$

$$\Delta Q_i = \sum_{k=1}^{n} V_i.V_k.[\ G_{ik}.\cos(\delta_i - \delta_k) + B_{ik}.\sin(\delta_i - \delta_k)].\ \Delta\delta_i + [-V_i.B_{ii} + \sum_{k=1}^{n} V_k.[\ G_{ik}.\sin(\delta_i - \delta_k) - B_{ik}\cos(\delta_i - \delta_k)]].\Delta V_i \qquad (5.1.27)$$

Equations (5.1.26) and (5.1.27) can be written in matrix format as shown in (5.1.28).

$$\left.\begin{array}{l}
\begin{bmatrix}\Delta P_i\\ \Delta Q_i\end{bmatrix} = \begin{bmatrix}a & b\\ c & d\end{bmatrix}\begin{bmatrix}\Delta\delta_i\\ \Delta V_i\end{bmatrix}\\
\\
a = \sum_{k=1}^{n} V_i.V_k.[-G_{ik}.\sin(\delta_i - \delta_k) + B_{ik}.\cos(\delta_i - \delta_k)]\\
b = V_i.G_{ii} + \sum_{k=1}^{n} V_k.[\ G_{ik}.\cos(\delta_i - \delta_k) + B_{ik}\sin(\delta_i - \delta_k)]\\
c = \sum_{k=1}^{n} V_i.V_k.[\ G_{ik}.\cos(\delta_i - \delta_k) + B_{ik}.\sin(\delta_i - \delta_k)]\\
d = -V_i.B_{ii} + \sum_{k=1}^{n} V_k.[\ G_{ik}.\sin(\delta_i - \delta_k) - B_{ik}\cos(\delta_i - \delta_k)]
\end{array}\right\} \qquad (5.1.28)$$

From (5.1.28), an expression was obtained for ΔP_i, which is given in (5.1.29).

$$\Delta P_i = a\ \Delta\delta_i + b\ \Delta V_i \qquad (5.1.29)$$

If generators are considered as current sources, since the loads are incorporated inside the Y-bus matrix, then the voltages are constant and;

$$\Delta V_i = 0 \qquad (5.1.30)$$

By applying (5.1.30) to equation (5.1.29) and separating the power input by solar PV (P_{iPV}) and the diesel generator (P_{iDG}), an expression for ΔP_{iDG} was obtained as (5.1.31).

$$\Delta P_{iDG} = a\,\Delta\delta_i - \Delta P_{iPV} \tag{5.1.31}$$

Consider the swing equation given in (5.1.32) for the generator.

$$\left.\begin{array}{l} \Delta P_{mi} - \Delta P_{ei} = M_i.\frac{d\Delta\omega_i}{dt} + D_i\,.\,\Delta\omega_i \\ \\ \Delta P_{mi} - \text{change in mechanical power} \\ \Delta P_{ei} - \text{change in electrical power} \\ M_i - \text{ angular momentum} \\ D_i - \text{damping constant} \\ \delta_i - \text{rotor angle} \end{array}\right\} \tag{5.1.32}$$

As the governor response is slower than the power angle response;

$$\Delta P_{mi} \approx 0 \tag{5.1.33}$$

By applying (5.1.33) to (5.1.32), it was modified in to (5.1.34).

$$-\,\Delta P_{iDG} = M_i.\frac{d\Delta\omega_i}{dt} + D_i\,.\,\Delta\omega_i \tag{5.1.34}$$

Equation (5.1.34) was remodeled to (5.1.35).

$$\frac{d\Delta\omega_i}{dt} = -\frac{1}{M_i}\Delta P_{iDG} - \frac{D_i}{M_i}\Delta\omega_i \tag{5.1.35}$$

When the solar PV inverter is operated at grid feeding mode, the output apparent power is equal to the output active power.

$$S_{iPV} = P_{iPV} \tag{5.1.36}$$

Equation (5.1.36) can be further evaluated by comparing it with (2.3.2).

$$S_{iPV} = P_{iPV} = k_{iPV}\emptyset_i \tag{5.1.37}$$

By applying (5.1.37) to (5.1.31);

$$\Delta P_{iDG} = a\,\Delta\delta_i - k_{iPV}\Delta\emptyset_i \tag{5.1.38}$$

Equation (5.1.39) was obtained by applying (5.1.38) to (5.1.35).

$$\frac{d\Delta\omega_i}{dt} = -\frac{a}{M_i}\Delta\delta_i + \frac{k_{iPV}}{M_i}\Delta\emptyset_i - \frac{D_i}{M_i}\Delta\omega_i \tag{5.1.39}$$

Rate of change in rotor angle was considered as the change in angular velocity as shown in (5.1.40).

$$\frac{d\Delta\delta_i}{dt} = \Delta\omega_i \tag{5.1.40}$$

Equations (5.1.40) and (5.1.39) were written to all ***n*** number of nodes as shown in (5.1.41).

$$\left.\begin{aligned} \Delta\dot{\delta}_1 &= \Delta\omega_1 \\ \Delta\dot{\delta}_i &= \Delta\omega_i \\ \Delta\dot{\delta}_n &= \Delta\omega_n \\ \Delta\dot{\omega}_1 &= -\frac{a}{M_1}\Delta\delta_1 - \frac{D_1}{M_1}\Delta\omega_1 + \frac{k_{1PV}}{M_1}\Delta\emptyset_1 \\ \Delta\dot{\omega}_i &= -\frac{a}{M_i}\Delta\delta_i - \frac{D_i}{M_i}\Delta\omega_i + \frac{k_{iPV}}{M_i}\Delta\emptyset_i \\ \Delta\dot{\omega}_n &= -\frac{a}{M_n}\Delta\delta_n - \frac{D_n}{M_n}\Delta\omega_n + \frac{k_{nPV}}{M_n}\Delta\emptyset_n \end{aligned}\right\} \tag{5.1.41}$$

Equation (5.1.38) was written to all ***n*** number of nodes as shown in (5.1.42)

$$\left.\begin{aligned} \Delta P_{1DG} &= a\,\Delta\delta_1 - k_{1PV}\Delta\emptyset_1 \\ \Delta P_{iDG} &= a\,\Delta\delta_i - k_{iPV}\Delta\emptyset_i \\ \Delta P_{nDG} &= a\,\Delta\delta_n - k_{iPV}\Delta n \end{aligned}\right\} \tag{5.1.42}$$

Considering the change of rotor angle (***δ***) and change of speed of the generator (***ω***) as the state variables of the system and the change in irradiance ($\emptyset$) as the input of the system, the expressions in (5.1.41) and (5.1.42) were modeled in matrix format as shown in (5.1.43) and (5.1.44).

$$\begin{bmatrix} \Delta\dot{\delta}_1 \\ \Delta\dot{\delta}_2 \\ \dots \\ \Delta\dot{\delta}_n \\ \Delta\dot{\omega}_1 \\ \Delta\dot{\omega}_2 \\ \dots \\ \Delta\dot{\omega}_n \end{bmatrix} = \begin{bmatrix} 0 & 0 & \dots & 0 & 1 & 0 & \dots & 0 \\ 0 & 0 & \dots & 0 & 0 & 1 & \dots & 0 \\ \vdots & \vdots & \vdots & \vdots & \vdots & \vdots & \vdots & \vdots \\ 0 & 0 & \dots & 0 & 0 & 0 & \dots & 1 \\ \frac{-a_1}{M_1} & 0 & \dots & 0 & \frac{-D_1}{M_1} & 0 & \dots & 0 \\ 0 & \frac{-a_2}{M_2} & \dots & 0 & 0 & \frac{-D_2}{M_2} & \dots & 0 \\ \vdots & \vdots & \vdots & \vdots & \vdots & \vdots & \vdots & \vdots \\ 0 & 0 & \dots & \frac{-a_n}{M_n} & 0 & 0 & \dots. & \frac{-D_n}{M_n} \end{bmatrix} \begin{bmatrix} \Delta\delta_1 \\ \Delta\delta_2 \\ \dots \\ \Delta\delta_n \\ \Delta\omega_1 \\ \Delta\omega_2 \\ \dots \\ \Delta\omega_3 \end{bmatrix} + \begin{bmatrix} 0 \\ 0 \\ \vdots \\ 0 \\ \frac{k_{1PV}}{M_1} \\ \frac{k_{2PV}}{M_2} \\ \vdots \\ \frac{k_{nPV}}{M_n} \end{bmatrix} \Delta\emptyset \quad (5.1.43)$$

$$\begin{bmatrix} \Delta P_{1D} \\ \Delta P_{2D} \\ \vdots \\ \Delta P_{nDG} \end{bmatrix} = [a_1 \quad a_2 \quad \dots \quad a_n \quad 0 \quad 0 \quad \dots \quad 0] \begin{bmatrix} \Delta\delta_1 \\ \Delta\delta_2 \\ \dots \\ \Delta\delta_n \\ \Delta\omega_1 \\ \Delta\omega_2 \\ \dots \\ \Delta\omega_3 \end{bmatrix} + \begin{bmatrix} -k_{1PV} \\ -k_{2PV} \\ \vdots \\ -k_{nPV} \\ 0 \\ 0 \\ \vdots \\ 0 \end{bmatrix} \Delta\emptyset \quad (5.1.44)$$

With the (5.1.43) and (5.1.44), the state space model of the system was obtained as shown in (5.1.45).

$$\left.\begin{array}{l}
[\Delta\dot{x}] = [A][\Delta x] + [B]\Delta u \\
[\Delta y] = [C][\Delta x] + [D]\Delta u \\
A = \begin{bmatrix} 0 & 0 & \dots & 0 & 1 & 0 & \dots & 0 \\ 0 & 0 & \dots & 0 & 0 & 1 & \dots & 0 \\ \vdots & \vdots & \vdots & \vdots & \vdots & \vdots & \vdots & \vdots \\ 0 & 0 & \dots & 0 & 0 & 0 & \dots & 1 \\ \frac{-a_1}{M_1} & 0 & \dots & 0 & \frac{-D_1}{M_1} & 0 & \dots & 0 \\ 0 & \frac{-a_2}{M_2} & \dots & 0 & 0 & \frac{-D_2}{M_2} & \dots & 0 \\ \vdots & \vdots & \vdots & \vdots & \vdots & \vdots & \vdots & \vdots \\ 0 & 0 & \dots & \frac{-a_n}{M_n} & 0 & 0 & \dots. & \frac{-D_n}{M_n} \end{bmatrix} \\
B = \begin{bmatrix} 0 \\ 0 \\ \vdots \\ 0 \\ \frac{k_{1PV}}{M_1} \\ \frac{k_{2PV}}{M_2} \\ \vdots \\ \frac{k_{nPV}}{M_n} \end{bmatrix} \\
C = [a_1 \quad a_2 \quad \dots \quad a_n \quad 0 \quad 0 \quad \dots \quad 0] \\
D = \begin{bmatrix} -k_{1PV} \\ -k_{2PV} \\ \vdots \\ -k_{nPV} \\ 0 \\ 0 \\ \vdots \\ 0 \end{bmatrix}
\end{array}\right\} \qquad (5.1.45)$$

The $\boldsymbol{A}$ matrix in (5.1.45) is called as the state transition matrix of the system. It is a $(\mathbf{2n} \times \mathbf{2n})$ matrix where, $\boldsymbol{n}$ is the number of generators in the network, because each generator has two state variables.

The $\boldsymbol{B}$ matrix in (5.1.45) is the input matrix of the system. It is a $(\mathbf{2n} \times \mathbf{1})$ matrix where $\boldsymbol{n}$ is the number of generators in the network.

The $\boldsymbol{C}$ matrix in (5.1.45) is the output matrix of the system. It is a $(\mathbf{1} \times \mathbf{2n})$ matrix where $\boldsymbol{n}$ is the number of generators the network has.

The $\boldsymbol{D}$ matrix in (5.1.45) shows the proportions of input in output. It is a $(\mathbf{2n} \times \mathbf{1})$ matrix where $\boldsymbol{n}$ is the number of generators in the network.

5.1.8. Time domain analysis of the selected network for a small perturbation

To validate the derived small signal model, it was required to test the model against the results of a time domain analysis. The method used to validate the power flow model in 4.2.4 is used to validate the small signal model as well.

The models used for diesel generator, solar PV, load and feeders in power flow model were used in small signal model.

Model of a substation

Substation model was modified by introducing the measuring devices to the power flow model to measure the power and frequency. Figure 5.7 depicts the time domain model of a substation. A distribution transformer was introduced to link the substation to the primary distribution level of the network.

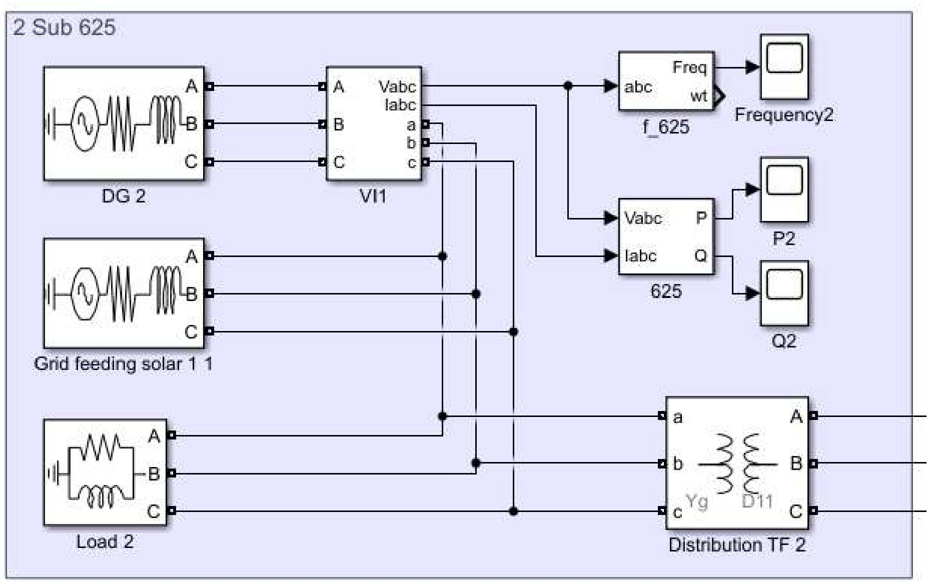

Figure 5.7 Time domain model for a substastion

Model of a small-signal perturbation

Small signal disturbance was introduced by connecting a constant PQ load to the system through a timed breaker operation. The active and reactive power components were changed according to the summation of substation loads given in Table 4.5 at the given time.

Complete model

The complete model was obtained by linking the substation models with feeders according to the ring diagram given in Figure 4.1. Then the disturbance was also connected. To model the N-1 emergency operation a circuit breaker model was connected to the feeder between primary substation B and radial substation 5. The complete model is attached in Appendix C.

Results of the time domain model

The frequency and the power output of each generator were evaluated. The 1% perturbation was switched at 1 s.

- Stable scenarios

  For stable scenarios, the generators were able to maintain the frequency within the acceptable limits of $\pm$ 10 %. The maximum observed frequency deviation at the small-signal perturbation is 0.0004 Hz. The inrush of the power output for 1% small-signal perturbation was 2% of the instantaneous power output and the generator came back to steady-state after a decaying oscillation within 600 ms. Figure 5.8 depicts the behavior of the frequency and the output power of the generator at substation B for a stable scenario.

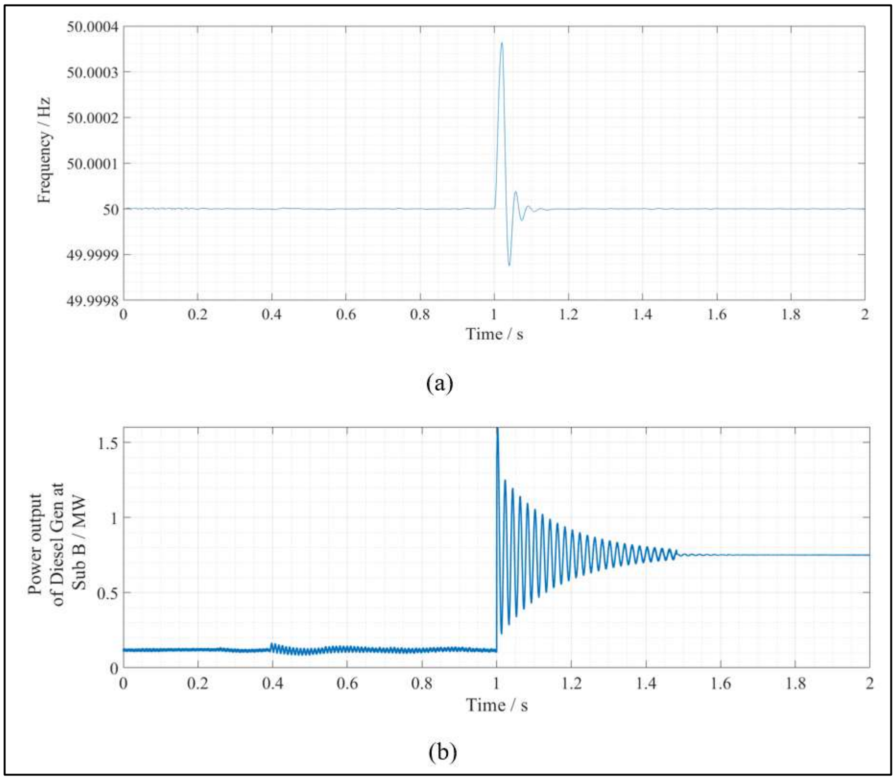

Figure 5.8 Results of the generator at substation B of time domain model for a small-signal perturbation – a stable scenario (a) Frequency response for perturbation (b) Output power response for perturbation

- Unstable scenarios

  For unstable scenarios, the generators were unable to maintain either the frequency or the power output. As there were no protection schemes modeled in the time domain model, the simulation could not stop when the generators exceeded their limits. Hence both the frequency and the power output of all the generators reached into decreasing or increasing trends. Figure 5.9 depicts the behavior of the frequency and the output power of the generator at substation B for an unstable scenario.

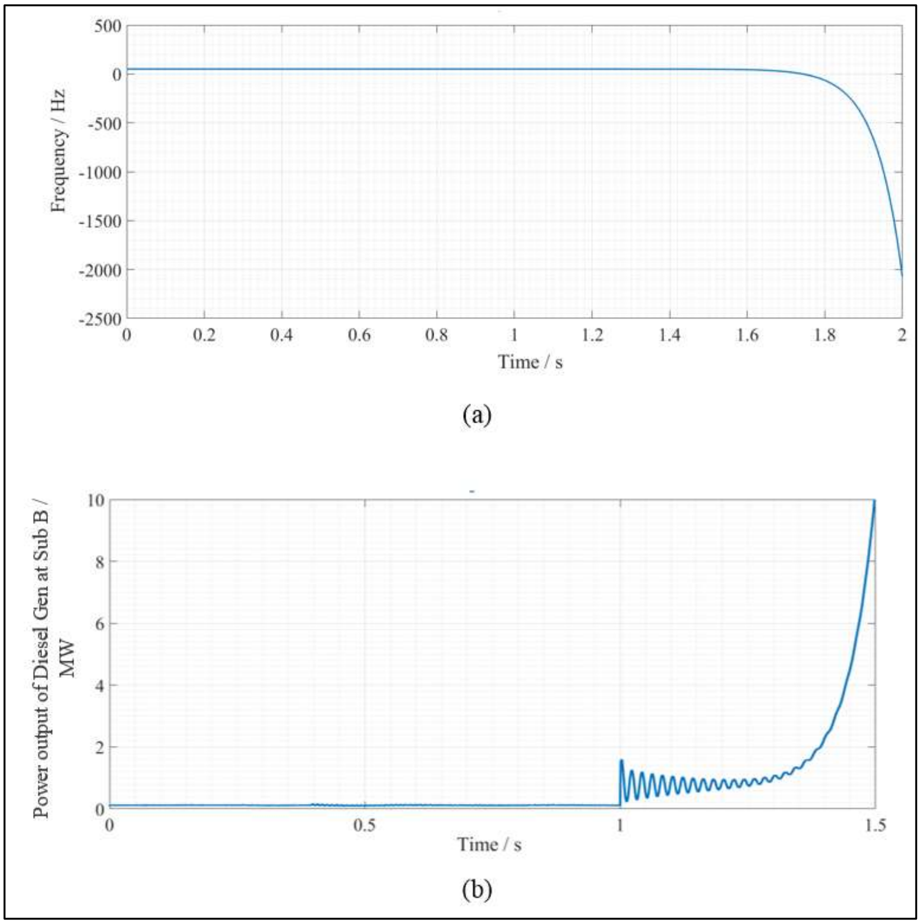

Figure 5.9 Results of the generator at substation B of time domain model for a small-signal perturbation – an unstable scenario (a) Frequency response for perturbation (b) Output power response for perturbation

The responses of all generator output and frequencies are attached in Appendix C.

5.1.9. Validating the small-signal model against the results of the time domain model

To validate the derived small signal model, the results were compared against the time domain simulation results of the same network.

Initially, the small signal model was transformed to the continuous time domain model and step responses for each scenario were obtained. A step of 0.01 of the magnitude was given to model the small-signal perturbation. Then the responses from the simulink model for the small-signal perturbation were compared against the step responses of the small-signal model.

Comparisons of the output of primary substation B generator for stable scenario is given in Figure 5.10. The step response of the derived model for a stable scenario shows a decaying oscillation in the output at a magnitude of twice the size of the step response. The response of a 1% perturbation for the time domain model in the stable scenario also shows the same decaying oscillation in the output in the magnitude of twice the size of the perturbation.

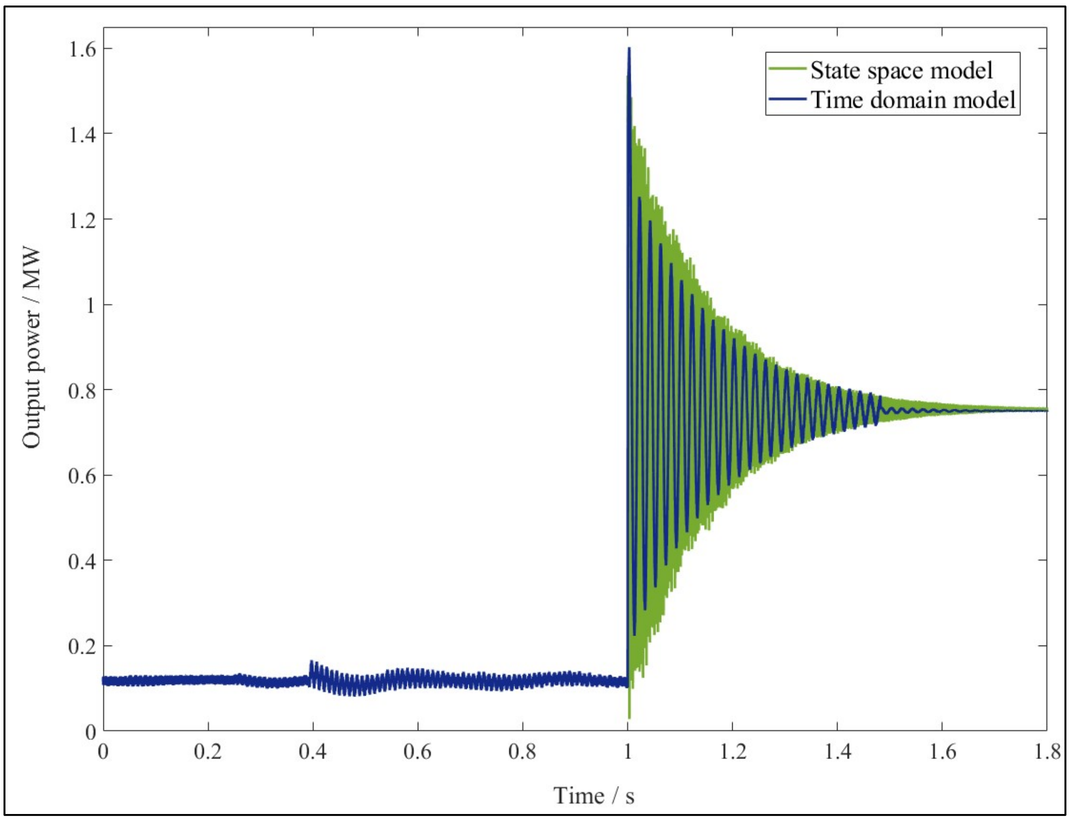

Figure 5.10 Responses of the generator at substation B for a small perturbation for a stable scenario

Comparisons of the output of primary substation B generator for an unstable scenario is given in Figure 5.11. The step response of the derived model for an unstable scenario shows an increasing trend in the generator output. The response of a 1% perturbation of the time domain model for the same scenario also shows the same increasing trend in the output.

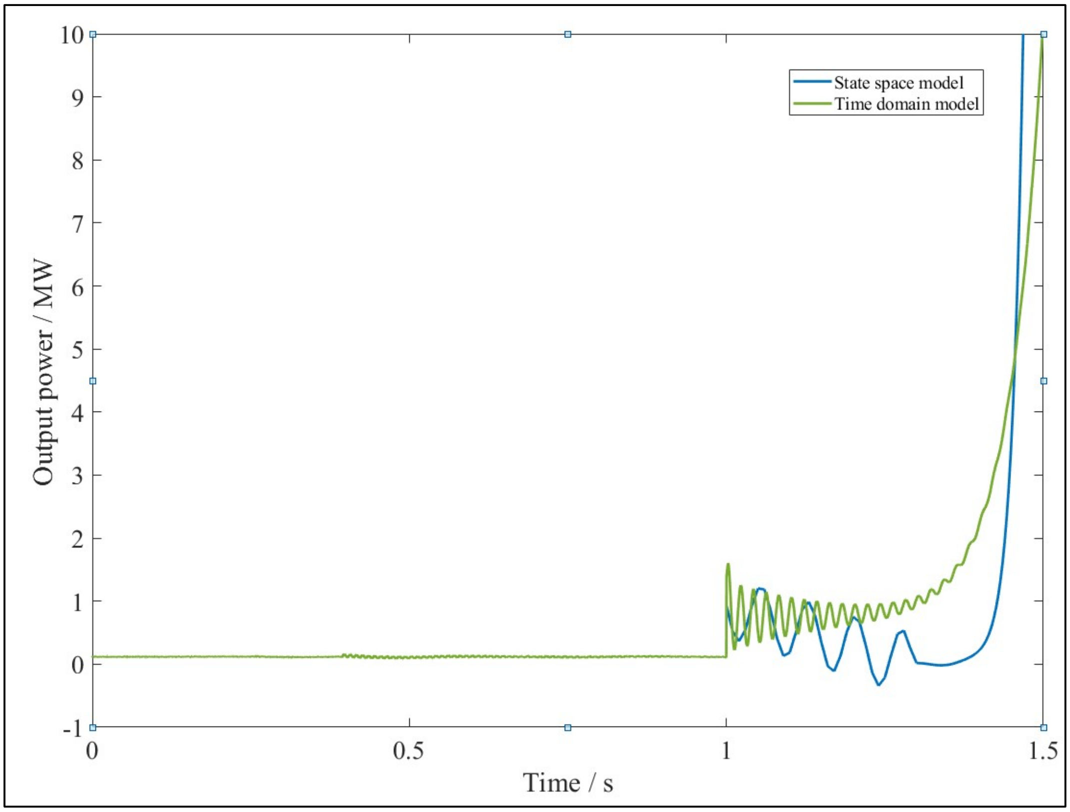

Figure 5.11 Responses of the generator at substation B for a small perturbation for an unstable scenario

Further, by evaluating the behavior of frequency of the system, it found that the frequency became unstable under a small-signal perturbation in unstable scenarios as shown in Figure 5.9 (a).

Hence, by comparing the step response results obtained by the developed small-signal model with the time domain responses shown in Figures 5.8 and 5.9, and by analyzing the behaviors of frequency, the derived small signal model was validated.

5.2. Analysis

The A, B, C and D matrices described in 5.1.7 were derived using Matlab M-scripts to obtain the Eigenvalues, left Eigen matrix, right Eigen matrix and participation matrix to evaluate the 288 operating points, which was described in section 3.4.3.

If all the Eigenvalues corresponding to all 24 operating points corresponding to a particular scenario are stable, then that scenario is considered as a stable case. Out of all the stable scenarios the dominant Eigenvalues and their critical times of day were obtained. Then by finding the participation matrices of all the critical operating points, the effective states were found.

5.2.1. Parameters used

Values used for parameters in the small signal analysis are given in the Table 5.1.

Table 5.1 Parameters used

Parameter	Used values
D	0.01
H	1.2 s
S_{DG}	1 MVA
	2 MVA
S_{base}	10 MVA
V_{base}	11 kV

5.2.2. State transition matrix

One generator has two state variables. Hence the state transition matrices of scenarios corresponding to mode 01 operation of diesel generators are (6 × 6) matrices and the state transition matrices of scenarios corresponding to mode 02 operation of diesel generators are (14 ×14) matrices. Equation 5.2.1 depicts the State transition matrix for Scenario 09 at 1200 h. The full state space system is attached in Appendix D.

$$A = \begin{bmatrix} 0 & 0 & 0 & 0 & 0 & 0 & 0 & 1 & 0 & 0 & 0 & 0 & 0 & 0 \\ 0 & 0 & 0 & 0 & 0 & 0 & 0 & 0 & 1 & 0 & 0 & 0 & 0 & 0 \\ 0 & 0 & 0 & 0 & 0 & 0 & 0 & 0 & 0 & 1 & 0 & 0 & 0 & 0 \\ 0 & 0 & 0 & 0 & 0 & 0 & 0 & 0 & 0 & 0 & 1 & 0 & 0 & 0 \\ 0 & 0 & 0 & 0 & 0 & 0 & 0 & 0 & 0 & 0 & 0 & 1 & 0 & 0 \\ 0 & 0 & 0 & 0 & 0 & 0 & 0 & 0 & 0 & 0 & 0 & 0 & 1 & 0 \\ 0 & 0 & 0 & 0 & 0 & 0 & 0 & 0 & 0 & 0 & 0 & 0 & 0 & 1 \\ -7.02\,e+05 & 1.13\,e+05 & 8.74\,e+04 & 0 & 0 & 0 & 3.96\,e+05 & -1.309 & 0 & 0 & 0 & 0 & 0 & 0 \\ 1.13\,e+05 & -1.66\,e+05 & 1.9\,e+04 & 0 & 0 & 0 & 0 & 0 & -1.309 & 0 & 0 & 0 & 0 & 0 \\ 8.74\,e+04 & 1.90\,e+04 & -2.19\,e+05 & 3.61\,e+04 & 0 & 0 & 0 & 0 & 0 & -1.309 & 0 & 0 & 0 & 0 \\ 0 & 0 & 5.61\,e+04 & -1.64\,e+05 & 7.96\,e+04 & 0 & 0 & 0 & 0 & 0 & -1.309 & 0 & 0 & 0 \\ 0 & 0 & 0 & 5.02\,e+04 & -3.18\,e+05 & 8.12\,e+04 & 0 & 0 & 0 & 0 & 0 & -1.309 & 0 & 0 \\ 0 & 0 & 0 & 0 & 1.36\,e+05 & -3.31\,e+05 & 9.44\,e+04 & 0 & 0 & 0 & 0 & 0 & -1.309 & 0 \\ 3.96\,e+05 & 0 & 0 & 0 & 0 & 6.29\,e+04 & -6.07\,e+05 & 0 & 0 & 0 & 0 & 0 & 0 & -1.309 \end{bmatrix} \quad (5.2.1)$$

5.2.3. Eigen matrix

The Eigen matrices of scenarios corresponding to mode 01 operation of diesel generators are (6×6) matrices with six Eigenvalues and the Eigen matrices of scenarios corresponding to mode 02 operation of diesel generators are (14×14) matrices with 14 Eigenvalues.

Initially the stable scenarios were found.

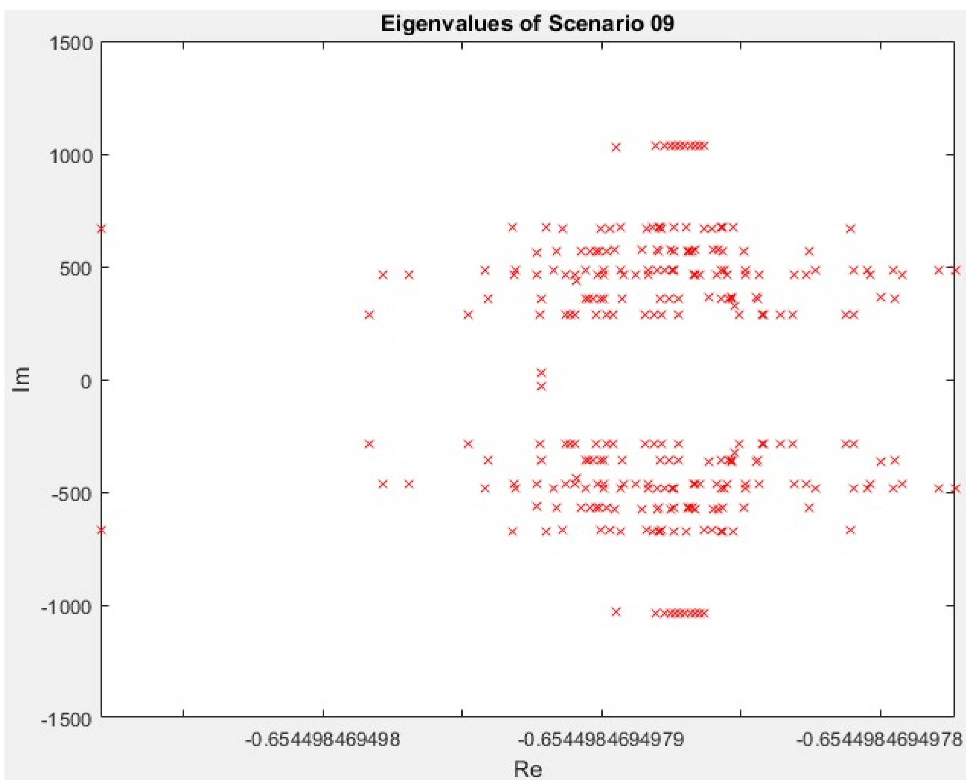

Figure 5.12 Eigen value plot for scenario 09

Figure 5.12 depicts the Eigen value plot for scenario 09. Scenario 09 has seven 1 MVA diesel generators connected to all seven substations. The network configuration is at normal closed ring topology and the installed solar PV capacity is at 50% of the maximum demand. Since there are seven diesel generators in the network, an operating point has 14 Eigenvalues and the 24-hour Eigen value plot has 336 Eigenvalues. All the 336 eigen values are laying on the negative half of the real axis, which means that all the eigen values have negative real parts. Hence, the scenario 09 is stable for all the evaluated 24-hour operating points. Above analysis was conducted for all the 12 scenarios.

Figure 5.13 depicts the summary of stability analysis of all the scenarios. It was noted that during N-1 emergency operation in mode 02 operation of diesel generators, the system can go unstable under a small perturbation irrespective of the amount of solar PV connected. Hence, scenarios 08, 10 and 12 cannot be evaluated further. When observing the stable scenarios, it is evident that solar integration at any level, even up to 100% of the maximum demand is possible for mode 01 operation of diesel generators. Even though, the solar integration up to 100% of the maximum demand is possible, under the normal operation for mode 02 operation of diesel generators, under N-1 emergency operation the system becomes unstable. Hence the mode 02 operation of diesel generators cannot be considered.

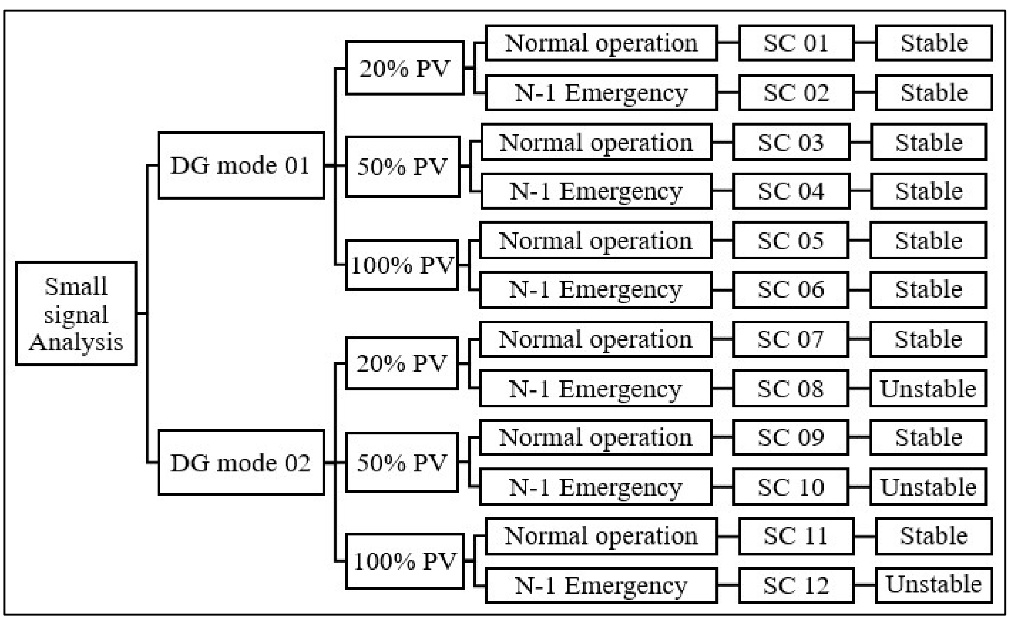

Figure 5.13 Summary of stability of all the scenarios

In stable scenarios, it is possible to identify the dominant Eigenvalues by evaluating the damping ratios of each conjugate pairs of Eigenvalues[13]. It was noted that the maximum damping ratio of any conjugate Eigen value pair at any given operating point is less than 0.32% and the amplitude of the oscillation decays within 0.05sec (less than 3 cycles). Damping ratios and the time to decay the oscillations for all the Eigenvalues of the stable scenarios are attached in Appendix E. Hence there are no dominant Eigenvalues in any stable scenario.

However, when observing the Eigen value plots of stable scenarios throughout the 24-hour analysis, it was noted that the travel of some Eigenvalues along the real axis are higher than the others. These Eigenvalues can be considered as "critical Eigenvalues," which poses threat to the stability of the system. We can further analyze the behavior of each of those Eigenvalues and identify the time where the Eigen value travels closer to the imaginary axis. These can be considered as the "critical times of day" of those critical Eigenvalues.

Table 5.2 depicts the critical Eigenvalues and their critical times of day for all the scenarios. Critical Eigenvalues were found in scenarios 07, 09 and 11. In scenario 07, the Eigenvalues 11 and 12 were found as critical Eigenvalues and both the Eigenvalues reaches their critical times at 1600h and 1700 h. In scenario 09 also, the Eigenvalues 11 and 12 were found as critical Eigenvalues and both the Eigenvalues reach their critical times at 1300h and 1400 h. In scenario 11, the Eigenvalues 7 and 8 were found as critical Eigenvalues and both the Eigenvalues reaches their critical time at 1600h.

Table 5.2 Critical Eigenvalues and their critical time

Scenario	Critical Eigen values	Critical Time
7	$\lambda 11$, $\lambda 12$	1600 h
	$\lambda 11$, $\lambda 12$	1700 h
9	$\lambda 11$, $\lambda 12$	1300 h
	$\lambda 11$, $\lambda 12$	1400 h
11	$\lambda 7$, $\lambda 8$	1600 h

5.2.4. Participation matrix

In order to determine the contribution of each state variable to the instability of the system, further evaluation of critical Eigenvalues at critical times was done. By evaluating the participation matrix, the contribution of each state to each Eigen value was found. State variables with highest contributions are the effective states. Participation matrices of all critical times for scenarios 07, 09 and 11 are attached in Appendix F.

Table 5.3 depicts the contribution of states to λ11 and λ12 at 1300h for scenario 07. Figure 5.14 depicts the graphical representation of contribution of states to λ12 at 1600h for scenario 07.

Table 5.3 Contribution of all the states to eigenvalues 11 and 12 at 1600 h

State variable	Participation for λ11	Participation for λ12
$\Delta\delta_1$	2.5621	2.5621
$\Delta\delta_2$	14.6865	14.6865
$\Delta\delta_3$	17.5857	17.5857
$\Delta\delta_4$	7.9629	7.9629
$\Delta\delta_5$	0.0013	0.0013
$\Delta\delta_6$	2.9487	2.9487
$\Delta\delta_7$	4.2528	4.2528
$\Delta\omega_1$	2.5621	2.5621
$\Delta\omega_2$	14.6865	14.6865
$\Delta\omega_3$	17.5857	17.5857
$\Delta\omega_4$	7.9629	7.9629
$\Delta\omega_5$	0.0013	0.0013
$\Delta\omega_6$	2.9487	2.9487
$\Delta\omega_7$	4.2528	4.2528

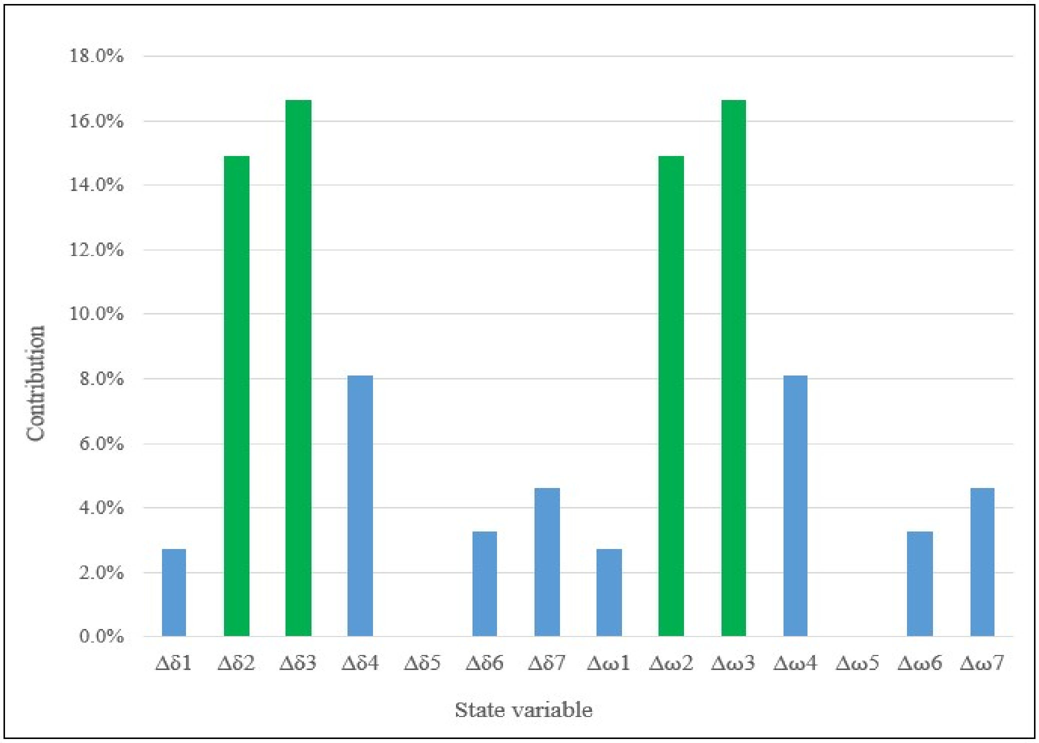

Figure 5.14 Contribution of all the states to Eigen value 12 of scenario 7 at 1600 h

Hence, with the participation matrix it can be predicted that small perturbations to rotor angle and speed of the diesel generators at substation 625 and substation 364 can make the system become unstable when the network is operated in scenario 07 (mode 02 operation of diesel generators, installed solar PV capacity of 20% of the maximum demand of the system and the system is operated under normal closed ring topology) at 1600 h.

Similarly, the effective states of all the said critical Eigenvalues at critical times were identified. Table 5.4 depicts the effective states of all the critical Eigenvalues at critical times.

Table 5.4 Effective states of all the critical Eigenvalues at critical times

Scenario	Critical Eigen values	Critical Time	Effective states
7	$\lambda 11$	1600 h	$\Delta\delta 2$ - rotor angle of sub-625 $\Delta\delta 3$ - rotor angle of sub-364 $\Delta\omega 2$ - frequency of sub-625 $\Delta\omega 3$ - frequency of sub-364
	$\lambda 12$	1600 h	
	$\lambda 11$	1700 h	
	$\lambda 12$	1700 h	
9	$\lambda 11$	1300 h	
	$\lambda 12$	1300 h	
	$\lambda 11$	1400 h	
	$\lambda 12$	1400 h	
11	$\lambda 7$	1600 h	
	$\lambda 8$	1600 h	

Hence, it can be predicted that small perturbations to the system can make the diesel generators at substation 625 and substation 364 unstable causing instabilities in the system in any scenario under mode 02 operation of diesel generators. These two substations are connected at the end of the ring and the distance to the second radial feeder is longer compared to other substations.

CHAPTER 06

CONCLUSION

The main objective of the research was to evaluate the steady state stability of an islanded, ring connected microgrid with the distributed generation of solar PV and diesel generators by devising a comprehensive technique. Further, the amount of possible solar penetration to a system with an elephant shaped daily load pattern was also evaluated.

The devised method has three main stages.

At stage one, the network and the operating modes have to be identified. This identification includes the substations, feeders, interconnectors, loads, proposed distributed generation (diesel generator and solar PV) and the operating scenarios.

Stage two comprises the power flow analysis. The two main objectives of this stage are to determine the operating point for the small-signal analysis and providing the input data for the small-signal analysis. From the power flow analysis, the voltages and the power output of each generator bus have to be taken to the next stage. Several power flow analyses have to be done depending on the predetermined operating scenarios.

The final stage is the steady state stability analysis. Small-signal analysis is used to evaluate the stability of the selected network. Initially the small-signal model has to be obtained. M scripts were developed to obtain the bus admittance matrix, to import the voltages, power output and generator parameters to the model. Then M scripts were developed to run the small-signal analysis, to identify the Eigenvalues with positive real parts, to identify the critical Eigenvalues and the effective states corresponding to critical Eigenvalues for all the predetermined scenarios

A portion of the ring network formed around primary substations B of Colombo city, Sri Lanka was used for the case study, considering its specific features: (1) the existing network of Colombo city is developed in a ring topology and, (2) the load patterns of all the substations in Colombo city follows a pattern similar to solar generation curve.

Two modes of operations for diesel generators were proposed in the research to develop the selected ring portion of primary substation B as a microgrid as shown in Table 6.1. After evaluating both the modes, it was found only mode 01 of diesel generator connection is possible for any given scenario. During mode 02 of diesel generator connection, the system gets unstable during N-1 emergency operation irrespective of the capacity of solar PV. When considering the cost involved with the both modes, even though a 2 MVA generator is expensive than a 1 MVA generator, when compared with the number of generators, space restrictions and as there are no major infrastructure changes like ring main units or MV switchgear, mode 01 is economically feasible as well.

Table 6.1 Summary of operating modes

Mode 01	**Mode 02**
Closed Ring	Closed Ring
DG connected to substations B, 1174 & 5	DG connected to all the subs
DG capacity – 2 MVA	DG capacity – 1 MVA
Stable	Unstable under N-1 Emergency operation mode Network can go unstable if the radial cable B-5 is removed.

Under normal operation of the mode 02 of diesel generator connection, the states of the diesel generators at sub 625 and 364 have highest contribution towards the stability of the system when compared with the other states. When the system enters to N-1 emergency criteria, with the disconnection of the radial feeder, the aforesaid states change and push the respective Eigenvalues with highest contribution to the positive region of the real axis making the system unstable.

Amount of solar PV integration was also evaluated with the same method. Three scenarios based on the installed solar PV capacity and the maximum demand were considered. Installed solar PV capacities were 20%, 50% and 100% of the maximum demand.

The results of the analysis based on capacities of installed solar PV concluded that solar PV capacity up to 100% of the maximum demand of the system is possible in both modes of diesel generator connection. However, as the system gets unstable under N-1 emergency criteria in mode 02 of diesel generator, it cannot be considered.

The power flow results revealed that the distributed generation has aided in improving the voltage profile of the selected network. The voltage variation is limited to ±0.5% of the nominal value resulting high power quality. However, the prevailing limits in Colombo city MV network is around ±2%, which is well within the accepted limit of ±6% given in the distribution code.

As recommendations for the continuation of this project, solar integration above 100% can be considered. With the excess solar PV generation, an energy storage(s) can be introduced to the network and offset the diesel generators. This would enable more renewable energy integration into the grid and eliminate the use of fossil fuels. As per the Figure 1.8 the total land area is around 0.5 km^2. If we consider 1 MW of solar PV generation by 70,000 ft^2 of roof top area considering the roof top area to be around 10% of the land area, the selected area has a roof top solar PV capacity of 7.5 MW, which is around 134% of the maximum demand. A techno economic analysis including the requirement of infrastructure development is recommended to evaluate the feasibility of transferring the present network into a ring and radial connected microgrid with increased penetration of solar PV. Study can be extended to evaluate the connection of multiple energy storages with each solar rooftop installation against connecting a single energy storage for the microgrid.

REFERENCES

[1] P. &. D. Unit, *132kV, 33kV & 11kV NETWORK of CEB -Colombo City,* unpublished: CEB, 2017.

[2] C. C. C. C. SCADA, "Daily Load Report of Colombo City," unpublished, Colombo City, 2020.

[3] L. N. W. Arachchige, *EE 5102 - Power Distribution System Characteristics,* Moratuwa: unpublished, 2018.

[4] M. Wadi, M. Baysal and A. Shobole, "Comparison between open-ring and closed-ring grids reliability," in *2017 4th International Conference on Electrical and Electronic Engineering (ICEEE)*, Ankara, 2017.

[5] O. Ayan, N. Jafarzadeh and B. Turkay, "An Examination of the Effects of Distributed Generation on Distribution Systems by Load Flow Analysis," in *2018 20th International Symposium on Electrical Apparatus and Technologies (SIELA)*, Bourgas, 2018.

[6] A. Zhang, Y. Li, Y. Huang, F. Huang and Z. Liu, "Research on Wide-Area Protection and Control Scheme for Closed-Loop Distribution Network," in *2018 International Conference on Power System Technology (POWERCON)*, Guangzhou, 2018.

[7] A. Keyhani, Keyhani, A.. "Design of Smart Power Grid Renewable Energy Systems." (2011)., Hoboken, New Jersey: A John Wiley & Sons, Inc., Publications, 2011.

[8] E. Aprilia, K. Meng, M. Al Hosani, H. Zeineldin and Z. Dong, "Unified Power Flow Algorithm for Standalone AC/DC Hybrid Microgrids," *IEEE Transactions on Smart Grid,* vol. 10, no. 1, pp. 639-649, 2019.

[9] A. Adib, F. Fateh and B. Mirafzal, "A Stabilizer for Inverters Operating in Grid-Feeding, Grid-Supporting and Grid-Forming Modes," in *Adib, A., Fateh, F., & Mirafzal, B. (2019). A Stabilizer for Inverters Operating in Grid-Feeding, Grid-Supporti2019 IEEE Energy Conversion Congress and Exposition (ECCE)*, Baltimore, MD, USA, 2019.

[10] S. Reichert, B. Stickan and G. Griepentrog, "Comparison between grid-feeding and grid-supporting inverters regarding power quality," in *IEEE 8th International Symposium on Power Electronics for Distributed Generation Systems (PEDG)*, Florianopolis, Brazil, 2017.

[11] D.-J. Lee and L. Wang, "Small-Signal Stability Analysis of an Autonomous Hybrid Renewable Energy Power Generation/Energy Storage System Part I: Time-Domain Simulations," in *IEEE TRANSACTIONS ON ENERGY CONVERSION*, 2008.

[12] L. Ren and P. Zhang, "Generalized Microgrid Power Flow," in *IEEE Transactions on Smart Grid*, 2018.

[13] P. Kundur, Power System Stability and Control, New York: McGraw-Hill, Inc., 1994.

[14] N. de Silva, *EE 5094 - Power System Stability and Control,* Moratuwa: unpublished, 2019.

[15] L. Y. H. W. G. L. a. W. W. H. Liu, "Small signal modeling and stability analysis on parallel photovoltaic inverters in microgrid," in *IEEE Energy Conversion Congress and Exposition (ECCE)*, Montreal, QC, 2015.

[16] H. L. P. S. a. L. W. Y. Zhang, "Small-signal Stability Analysis of Multiple Grid-connected Virtual Synchronous Generators," in *2018 China International Conference on Electricity Distribution (CICED)*, Tianjin, 2018.

[17] J. Machowski, J. W. Bialek and J. R. Bumby, POWER SYSTEM DYNAMICS Stability and Control, West Sussex: John Wiley & Sons, Ltd., 2008.

[18] M. B. a. A. M. Wadi, "Comparison between open-ring and closed-ring grid reliability," in *2017 4th International Conference on Electrical and Electronic Engineering (ICEEE)*, Ankara, 2017.

[19] D. D. F. G.-E. a. N. C. C. V. Valdivia, "Systematic small signal modeling and stability analysis of a microgrid," in *IEEE 5th International Symposium on Power Electronics for Distributed Generation Systems (PEDG)*, Galway, 2014.

APPENDIX A: LOAD DATA OF PROJECT

Table A1 - Loads and satellite loads connected to all the ring and radial substations

Time	625				364		1174				182		5						465			Total
	625-319	625-7	625-B	625-364	364-L1	364-L2	1174-1370	1174-182	1174-364	1174-L1	182-1174	182-L1	5-B	5-621	5-443	5-L1	5-L2	5-L3	465-B	465-BS1	465-BS2	
0:00	171.07	172.31	668.32	658.80	52.20	57.77	356.86	226.11	633.19	47.38	234.65	235.52	1,811.09	249.37	803.15	71.74	55.04	-	-	15.59	11.50	2,299.49
1:00	157.96	156.47	623.67	620.70	55.29	53.07	329.15	226.11	585.94	-	227.35	226.11	1,753.04	246.77	778.54	70.26	49.35	-	-	13.61	9.90	2,146.48
2:00	150.29	151.53	613.65	606.23	53.56	56.40	318.14	221.54	569.62	-	222.65	217.70	1,695.19	277.20	759.73	67.66	49.35	-	-	12.86	10.02	2,124.46
3:00	148.31	144.60	588.91	582.60	54.55	58.51	312.33	205.21	562.69	-	213.37	211.02	1,610.32	224.38	735.00	65.31	49.35	-	-	12.12	9.40	2,024.89
4:00	145.22	147.69	582.73	578.52	52.82	55.29	318.76	206.45	555.76	-	205.83	205.21	1,581.39	234.77	703.21	64.57	49.35	-	-	15.59	10.14	2,002.62
5:00	159.07	157.59	594.35	598.19	52.57	54.05	325.69	213.37	575.43	48.61	216.84	241.33	1,668.36	237.00	746.62	62.22	49.35	-	-	12.74	-	2,146.85
6:00	149.55	148.43	642.84	643.34	56.65	42.67	366.14	209.91	603.26	-	214.49	237.62	1,668.36	232.05	727.82	62.22	49.35	-	-	21.52	13.85	2,107.89
7:00	148.31	145.34	750.09	746.13	83.99	141.38	443.57	215.72	683.04	-	224.38	220.05	1,581.39	234.77	703.21	65.68	36.24	-	-	28.33	19.30	2,270.17
8:00	182.94	168.84	935.01	935.13	119.74	156.72	565.04	208.80	803.03	55.54	212.26	230.32	1,898.05	402.50	710.38	68.40	43.54	43.66	620.95	332.86	322.60	3,403.10
9:00	232.30	224.63	1,603.21	1,589.48	194.08	169.09	1,084.31	208.80	1,373.88	96.48	219.81	219.19	2,703.21	547.85	990.18	100.32	43.54	80.28	532.01	270.03	274.60	4,526.87
10:00	253.08	243.80	1,910.84	1,917.77	228.46	182.82	1,288.41	247.02	1,618.92	153.26	244.55	245.29	3,479.45	648.90	1,332.32	146.21	55.04	104.52	543.64	268.42	280.17	5,430.71
11:00	265.33	260.75	1,965.64	1,945.97	234.65	177.75	1,254.14	252.46	1,674.21	181.46	258.40	256.30	3,651.29	656.20	1,370.05	168.60	60.86	119.24	594.35	322.72	325.94	5,653.97
12:00	272.75	264.95	2,030.33	2,012.02	238.98	179.85	1,291.13	261.74	1,731.11	213.99	268.79	267.55	3,738.25	695.17	1,413.59	172.43	60.86	108.48	557.49	282.15	289.32	5,751.20
13:00	285.49	275.47	2,056.43	2,047.15	243.18	189.38	1,302.14	261.74	1,772.55	215.11	266.44	264.46	3,680.21	670.80	1,407.77	160.06	60.86	104.52	551.68	274.97	288.33	5,742.54
14:00	290.44	283.39	1,982.46	1,979.12	239.60	190.12	1,264.53	264.09	1,725.30	198.90	260.75	269.78	3,651.29	673.15	1,388.85	164.27	68.16	105.76	530.78	267.43	280.17	5,684.53
15:00	286.97	282.02	1,990.13	1,986.67	240.71	178.49	1,270.35	269.90	1,703.28	204.72	277.45	284.50	3,709.14	692.94	1,383.03	165.87	68.16	106.50	519.27	262.36	267.80	5,694.42
16:00	283.14	280.79	1,998.66	1,999.28	238.48	181.46	1,254.14	262.98	1,719.48	219.19	275.10	283.88	3,709.14	684.40	1,407.77	168.97	60.86	109.96	499.48	251.35	269.04	5,693.43
17:00	288.83	282.64	2,273.89	2,243.21	-	177.13	1,258.35	261.74	1,507.59	193.09	275.10	268.29	3,680.21	654.72	1,401.96	162.41	60.86	99.57	407.08	199.27	210.16	5,257.28
18:00	244.92	242.32	1,688.81	1,692.39	209.66	110.71	1,107.94	250.23	1,462.94	116.15	243.93	258.40	3,307.79	611.92	1,264.16	132.72	55.04	87.95	-	38.10	35.75	4,515.73
19:00	226.49	229.58	1,594.68	1,608.53	191.36	84.48	1,114.86	273.37	1,486.07	93.02	283.88	306.39	2,529.28	545.49	914.85	98.34	55.04	53.19	-	22.88	20.29	3,956.26
20:00	221.54	217.70	1,169.29	1,167.43	138.91	55.42	766.79	275.72	1,092.10	64.69	282.02	307.13	2,299.59	455.69	903.22	88.07	60.86	-	-	16.33	18.31	3,314.65
21:00	216.84	216.59	995.13	990.05	-	60.49	617.11	272.25	922.15	63.46	276.33	281.78	2,127.74	451.49	865.49	83.37	60.86	-	-	15.09	12.37	2,944.93
22:00	200.76	199.89	851.76	853.62	60.49	61.11	494.41	279.18	808.84	51.46	284.37	283.63	1,927.17	264.83	852.51	77.19	60.86	-	-	15.83	9.77	2,632.72
23:00	191.11	189.62	799.44	784.97	56.03	58.01	451.12	267.55	749.96	52.57	269.90	289.45	1,898.05	269.53	835.06	69.52	55.04	-	-	12.74	10.14	2,539.95

APPENDIX B: OUTPUT DATA OF SCENARIO 09

Table A2 - Bus voltages taken from power flow data of scenario 09

Time	1			2			3			4			5			6		
Sub no.	V /pu	V / kV	Angle	V /pu	V / kV	Angle	V /pu	V / kV	Angle	V /pu	V / kV	Angle	V /pu	V / kV	Angle	V /pu	V / kV	Angle
B	1.0000	11.0000	-	1.0000	11.0000	-	1.0000	11.0000	-	1.0000	11.0000	-	1.0000	11.0000	-	1.0000	11.0000	-
625	1.0003	11.0030	-	1.0030	11.0030	-	1.0030	11.0030	-	1.0003	11.0030	-	1.0003	11.0030	-	1.0003	11.0030	-
364	1.0011	11.0120	0.1000	1.0011	11.0120	0.1000	1.0011	11.0120	0.1000	1.0011	11.0130	0.1000	1.0011	11.0120	0.1000	1.0011	11.0120	0.1000
1174	1.0013	11.0140	0.1000	1.0013	11.0140	0.1000	1.0013	11.0140	0.1000	1.0013	11.0150	0.1000	1.0012	11.0140	0.1000	1.0013	11.0140	0.1000
182	1.0012	11.0130	0.1000	1.0012	11.0130	0.1000	1.0012	11.0130	0.1000	1.0013	11.0140	0.1000	1.0011	11.0130	0.1000	1.0012	11.0130	0.1000
5	1.0002	11.0030	-	1.0002	11.0030	-	1.0003	11.0030	-	1.0003	11.0040	-	1.0003	11.0030	-	1.0003	11.0030	-
465	1.0005	11.0060	-	1.0005	11.0060	-	1.0005	11.0060	-	1.0005	11.0060	-	1.0005	11.0060	-	1.0005	11.0060	-

Time	7			8			9			10			11			12		
Sub no.	V /pu	V / kV	Angle	V /pu	V / kV	Angle	V /pu	V / kV	Angle	V /pu	V / kV	Angle	V /pu	V / kV	Angle	V /pu	V / kV	Angle
B	1.0000	11.0000	-	1.0000	11.0000	-	1.0000	11.0000	-	1.0000	11.0000	-	1.0000	11.0000	-	1.0000	11.0000	-
625	1.0003	11.0030	-	1.0002	11.0030	-	1.0001	11.0020	-	1.0001	11.0010	-	1.0002	11.0020	-	1.0002	11.0020	-
364	1.0010	11.0110	0.1000	1.0008	11.0090	0.1000	1.0004	11.0040	0.1000	1.0002	11.0020	0.1000	1.0003	11.0030	0.1000	1.0003	11.0030	0.1000
1174	1.0012	11.0130	0.1000	1.0010	11.0110	0.1000	1.0005	11.0060	0.1000	1.0004	11.0040	0.1000	1.0005	11.0060	0.1000	1.0005	11.0060	0.1000
182	1.0012	11.0130	0.1000	1.0011	11.0120	0.1000	1.0008	11.0090	0.1000	1.0007	11.0080	0.1000	1.0010	11.0110	0.1000	1.0010	11.0110	0.1000
5	1.0003	11.0030	0.1000	1.0002	11.0020	0.1000	0.9999	10.9990	0.1000	0.9998	10.9980	-	0.9999	10.9990	-	0.9999	10.9990	0.1000
465	1.0005	11.0060	-	1.0001	11.0010	-	1.0003	11.0030	-	1.0004	11.0040	-	1.0004	11.0050	-	1.0005	11.0060	0.1000

Time	13			14			15			16			17			18		
Sub no.	V /pu	V / kV	Angle	V /pu	V / kV	Angle	V /pu	V / kV	Angle	V /pu	V / kV	Angle	V /pu	V / kV	Angle	V /pu	V / kV	Angle
B	1.0000	11.0000	-	1.0000	11.0000	-	1.0000	11.0000	-	1.0000	11.0000	-	1.0000	11.0000	-	1.0000	11.0000	-
625	1.0001	11.0010	-	1.0001	11.0010	-	1.0001	11.0010	-	1.0000	11.0010	-	1.0000	11.0010	-	1.0000	11.0000	-
364	1.0002	11.0020	0.1000	1.0002	11.0020	0.1000	1.0001	11.0010	0.1000	1.0000	11.0000	0.1000	1.0001	11.0020	0.1000	1.0001	11.0010	-
1174	1.0005	11.0050	0.1000	1.0004	11.0050	0.1000	1.0003	11.0030	0.1000	1.0001	11.0010	0.1000	1.0000	11.0000	0.1000	0.9999	10.9990	0.1000
182	1.0009	11.0100	0.1000	1.0008	11.0090	0.1000	1.0006	11.0070	0.1000	1.0004	11.0040	0.1000	1.0002	11.0020	0.1000	1.0000	11.0000	-
5	0.9999	10.6660	0.1000	0.9999	10.9990	0.1000	0.9997	10.9970	-	0.9995	10.9950	-	0.9994	10.9940	-	0.9994	10.9930	-
465	1.0005	11.0050	0.1000	1.0005	11.0050	-	1.0004	11.0040	-	1.0003	11.0030	-	1.0002	11.0020	-	1.0003	11.0030	-

Time	19			20			21			22			23			24		
Sub no.	V /pu	V / kV	Angle	V /pu	V / kV	Angle	V /pu	V / kV	Angle	V /pu	V / kV	Angle	V /pu	V / kV	Angle	V /pu	V / kV	Angle
B	1.0000	11.0000	-	1.0000	11.0000	-	1.0000	11.0000	-	1.0000	11.0000	-	1.0000	11.0000	-	1.0000	11.0000	-
625	1.0000	11.0010	-	1.0001	11.0010	-	1.0002	11.0020	-	1.0002	11.0020	-	1.0002	11.0020	-	1.0003	11.0030	-
364	1.0002	11.0020	-	1.0006	11.0060	0.1000	0.0008	11.0090	0.1000	1.0009	11.0100	0.1000	1.0009	11.0100	0.1000	1.0010	11.0110	0.1000
1174	1.0000	11.0010	0.1000	1.0005	11.0060	0.1000	1.0008	11.0090	0.1000	1.0009	11.0100	0.1000	1.0010	11.0110	0.1000	1.0012	11.0130	0.1000
182	1.0002	11.0020	0.1000	1.0006	11.0060	0.1000	1.0007	11.0080	0.1000	1.0009	11.0090	0.1000	1.0009	11.0090	0.1000	1.0011	11.0120	0.1000
5	0.9997	10.9970	-	0.9999	10.9990	-	0.9999	10.9990	-	1.0000	11.0010	-	1.0001	11.0010	-	1.0002	11.0020	-
465	1.0004	11.0050	-	1.0004	11.0050	-	1.0004	11.0050	-	1.0005	11.0050	-	1.0005	11.0050	-	1.0005	11.0050	-

Table A3 – Power generation data taken from power flow of scenario 09

Time	1		2		3		4		5		6		7		8	
Sub no.	MW	MVAR	MW	MVAR	MW	MVAR	MW	MVAR	MW	MVAR	MW	MVAR	MW	MVAR	MW	MVAR
B	-3.2	0.8	-3.2	0.8	-3.3	0.8	-3.3	0.8	-3.2	0.8	-3.2	0.8	-3.2	0.9	-2.8	1.4
625	0.9	0	0.9	0	0.9	0	0.9	0	0.9	0	0.9	0	0.9	0	0.9	0
364	0.9	0	0.9	0	0.9	0	0.9	0	0.9	0	0.9	0	0.9	0	0.9	0
1174	0.9	0	0.9	0	0.9	0	0.9	0	0.9	0	0.9	0	0.9	0	0.9	0
182	0.9	0	0.9	0	0.9	0	0.9	0	0.9	0	0.9	0	0.9	0	0.9	0
5	0.9	0	0.9	0	0.9	0	0.9	0	0.9	0	0.9	0	0.9	0	0.9	0
465	0.9	0	0.9	0	0.9	0	0.9	0	0.9	0	0.9	0	0.9	0	0.9	0

Time	9		10		11		12		13		14		15		16	
Sub no.	MW	MVAR	MW	MVAR	MW	MVAR	MW	MVAR	MW	MVAR	MW	MVAR	MW	MVAR	MW	MVAR
B	-2.7	1.8	-2.6	1.8	-3.1	2	-3.4	2.1	-3.1	2	-2.8	1.9	-2.4	1.9	-1.8	1.9
625	0.9	0	0.9	0	0.9	0	0.9	0	0.9	0	0.9	0	0.9	0	0.9	0
364	0.9	0	0.9	0	0.9	0	0.9	0	0.9	0	0.9	0	0.9	0	0.9	0
1174	0.9	0	0.9	0	0.9	0	0.9	0	0.9	0	0.9	0	0.9	0	0.9	0
182	0.9	0	0.9	0	0.9	0	0.9	0	0.9	0	0.9	0	0.9	0	0.9	0
5	0.9	0	0.9	0.5	0.9	0.4	0.9	0.3	0.9	0.4	0.9	0.5	0.9	0.5	0.9	0.5
465	0.9	0	0.9	0	0.9	0	0.9	0	0.9	0	0.9	0	0.9	0	0.9	0

Time	17		18		19		20		21		22		23		24	
Sub no.	MW	MVAR	MW	MVAR	MW	MVAR	MW	MVAR	MW	MVAR	MW	MVAR	MW	MVAR	MW	MVAR
B	-1.5	1.7	-1	1.3	-1.5	1.1	-2.1	1	-2.4	1.1	-2.7	1.1	-2.8	1	-3	0.9
625	0.9	0	0.9	0	0.9	0	0.9	0	0.9	0	0.9	0	0.9	0	0.9	0
364	0.9	0	0.9	0	0.9	0	0.9	0	0.9	0	0.9	0	0.9	0	0.9	0
1174	0.9	0	0.9	0	0.9	0	0.9	0	0.9	0	0.9	0	0.9	0	0.9	0
182	0.9	0	0.9	0	0.9	0	0.9	0	0.9	0	0.9	0	0.9	0	0.9	0
5	0.9	0.5	0.9	0.5	0.9	0.5	0.9	0.4	0.9	0.1	0.9	0	0.9	0	0.9	0
465	0.9	0	0.9	0	0.9	0	0.9	0	0.9	0	0.9	0	0.9	0	0.9	0

APPENDIX C: SIMULINK MODEL FOR VALIDATION AND RESULTS

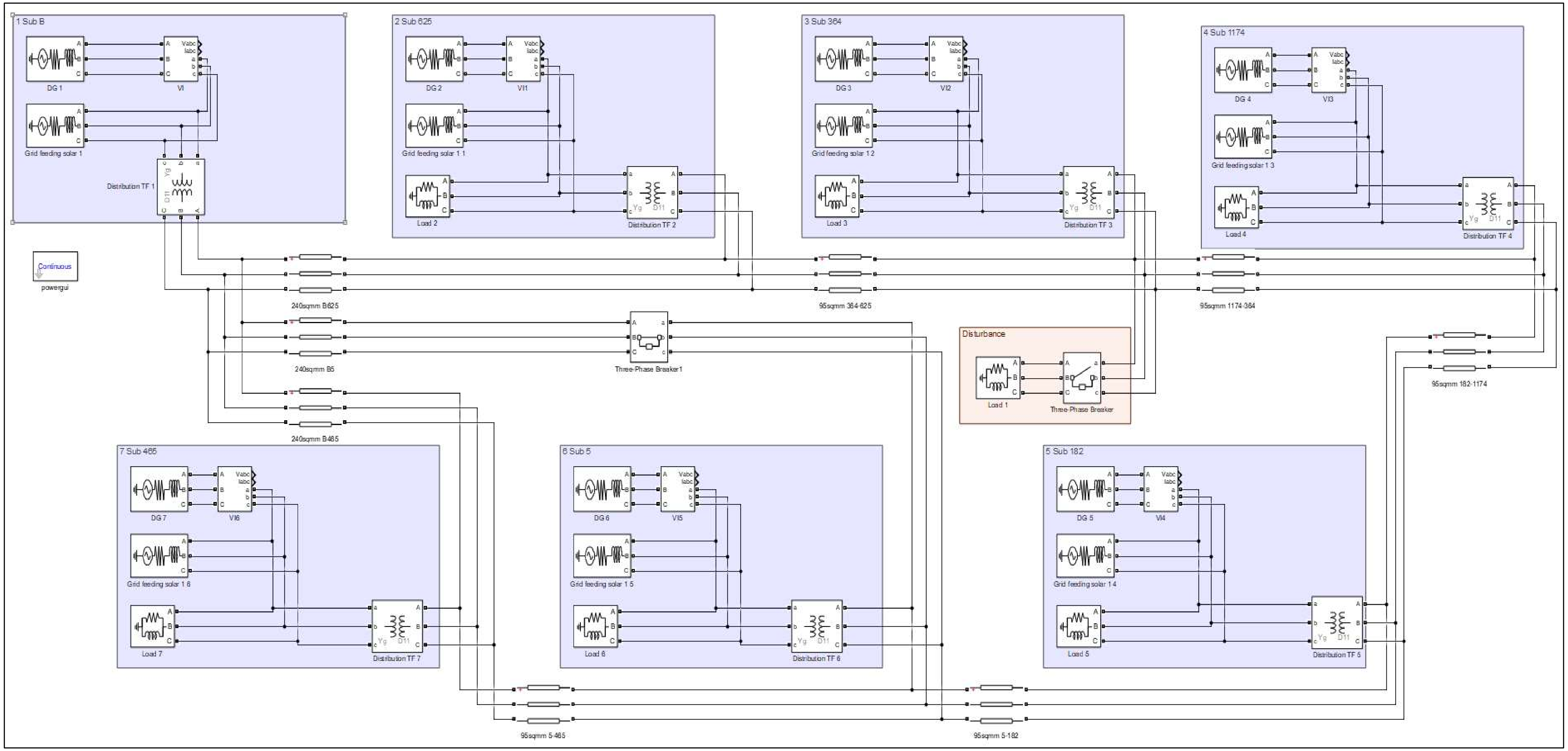

Figure A1 - Simulink model to validate the small-signal model

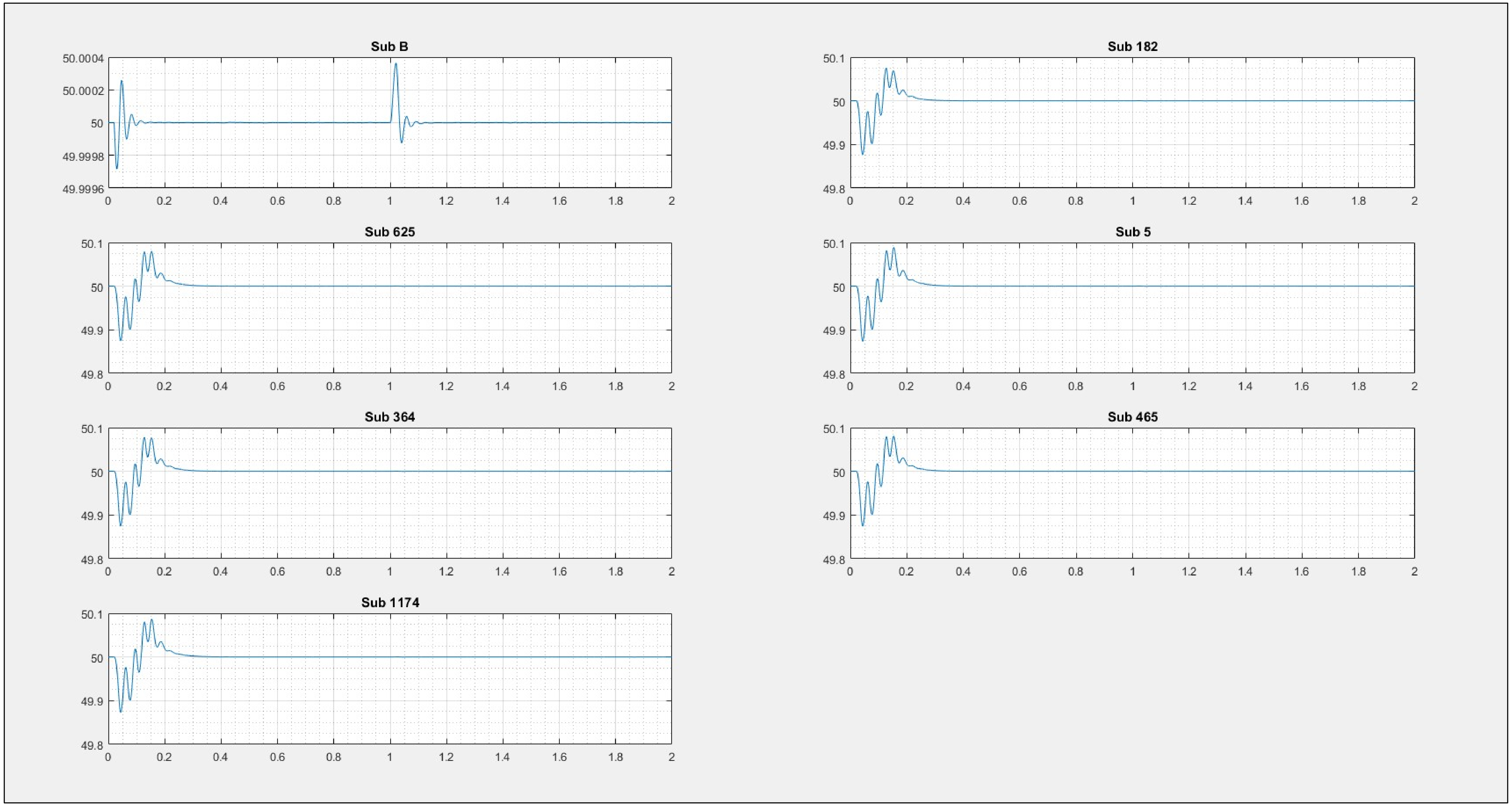

Figure A2 - Responses of the frequencies of each generator for a small perturbation (stable scenario)

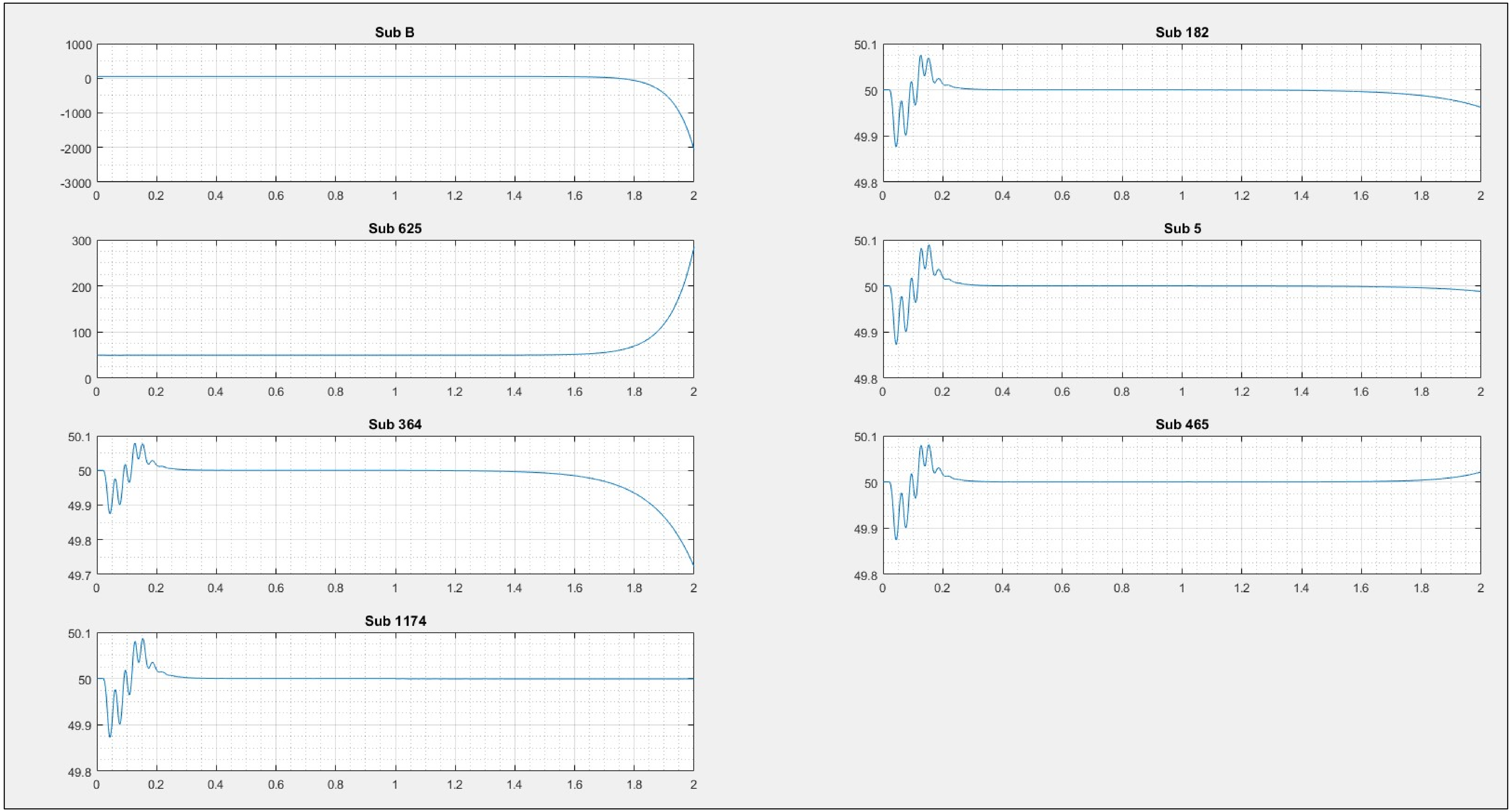

Figure A3 - Responses of the frequencies of each generator for a small perturbation (unstable scenario)

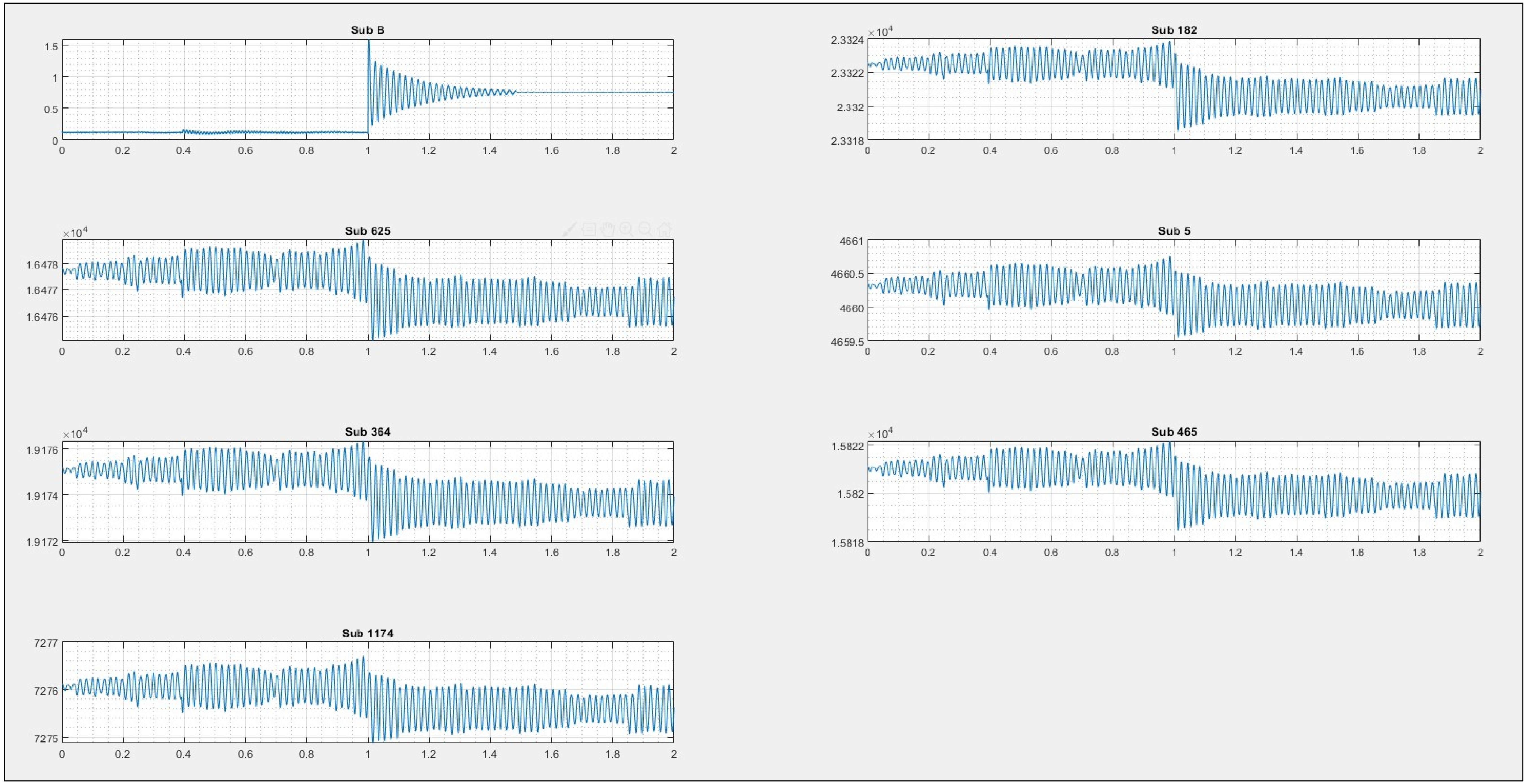

Figure A4 - Responses of the generator outputs for a small perturbation (stable scenario)

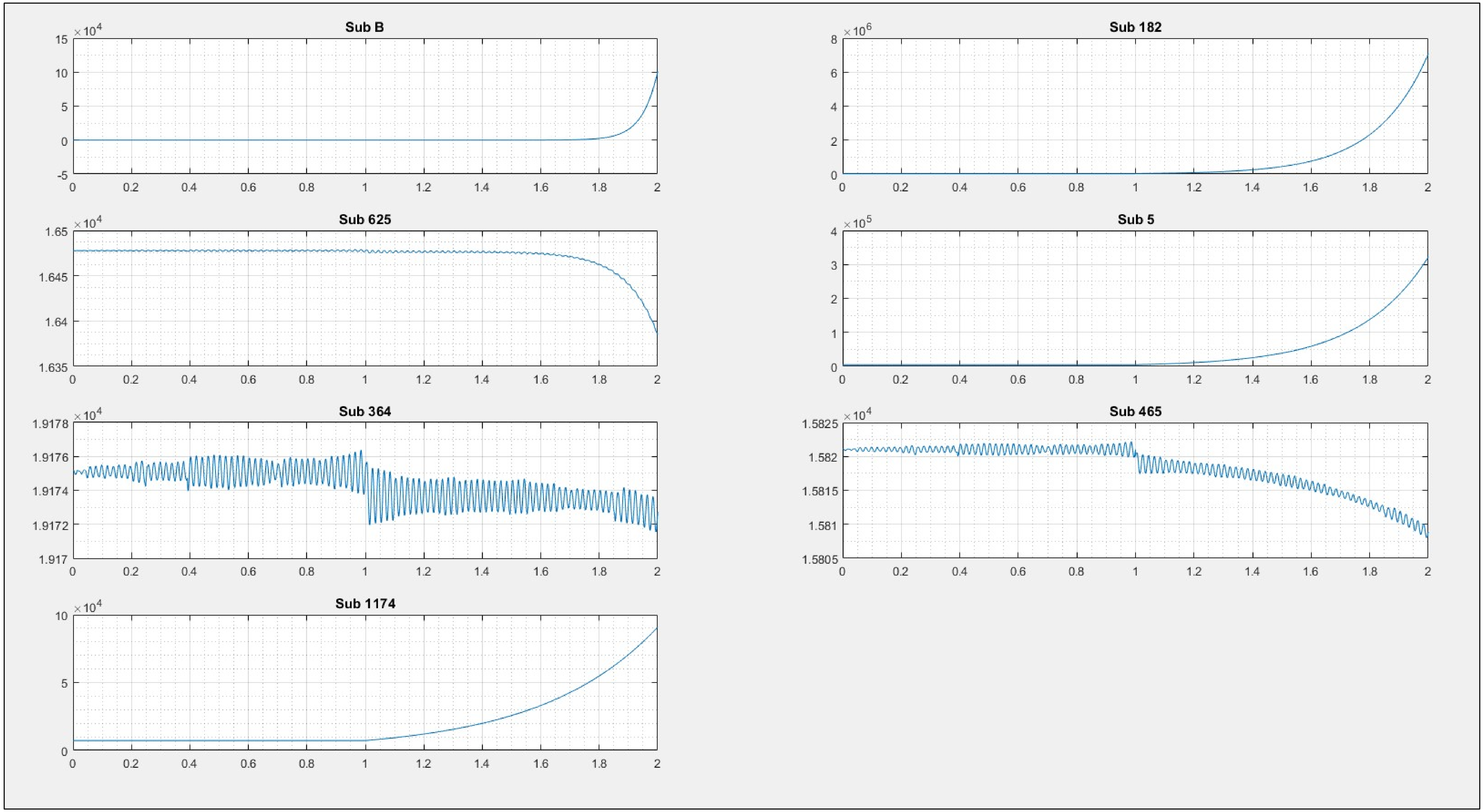

Figure A5- Responses of the generator outputs for a small perturbation (unstable scenario)

APPENDIX D: STATE SPACE REPRESENTAION OF THE SYSTEM

A =

	x1	x2	x3	x4	x5	x6	x7	x8	x9	x10	x11	x12	x13	x14
x1	0	0	0	0	0	0	0	1	0	0	0	0	0	0
x2	0	0	0	0	0	0	0	0	1	0	0	0	0	0
x3	0	0	0	0	0	0	0	0	0	1	0	0	0	0
x4	0	0	0	0	0	0	0	0	0	0	1	0	0	0
x5	0	0	0	0	0	0	0	0	0	0	0	1	0	0
x6	0	0	0	0	0	0	0	0	0	0	0	0	1	0
x7	0	0	0	0	0	0	0	0	0	0	0	0	0	1
x8	-7.021e+05	1.131e+05	8.738e+04	0	0	0	3.959e+05	-1.309	0	0	0	0	0	0
x9	1.131e+05	-1.659e+05	1.902e+04	0	0	0	0	0	-1.309	0	0	0	0	0
x10	8.738e+04	1.902e+04	-2.187e+05	3.607e+04	0	0	0	0	0	-1.309	0	0	0	0
x11	0	0	5.611e+04	-1.643e+05	7.959e+04	0	0	0	0	0	-1.309	0	0	0
x12	0	0	0	5.028e+04	-3.184e+05	8.124e+04	0	0	0	0	0	-1.309	0	0
x13	0	0	0	0	1.356e+05	-3.31e+05	9.44e+04	0	0	0	0	0	-1.309	0
x14	3.959e+05	0	0	0	0	6.285e+04	-6.07e+05	0	0	0	0	0	0	-1.309

B =

	u1
x1	0
x2	0
x3	0
x4	0
x5	0
x6	0
x7	0
x8	237.3
x9	237.3
x10	237.3
x11	237.3
x12	237.3
x13	237.3
x14	237.3

C =

	x1	x2	x3	x4	x5	x6	x7	x8	x9	x10	x11	x12	x13	x14
y1	-807	0	0	0	0	0	0	0	0	0	0	0	0	0
y2	0	-257.5	0	0	0	0	0	0	0	0	0	0	0	0
y3	0	0	-429.4	0	0	0	0	0	0	0	0	0	0	0
y4	0	0	0	-595.2	0	0	0	0	0	0	0	0	0	0
y5	0	0	0	0	-788.3	0	0	0	0	0	0	0	0	0
y6	0	0	0	0	0	-1428	0	0	0	0	0	0	0	0
y7	0	0	0	0	0	0	-891.6	0	0	0	0	0	0	0

D =

	u1
y1	1.813
y2	1.813
y3	1.813
y4	1.813
y5	1.813
y6	1.813
y7	1.813

Figure A6- A,B,C and D matrices related to the network of scenario 09 at 1200 h

Table A4 - Damping ratios of conjugate Eigenvalues of stable scenarios

		0100h	0200h	0300h	0400h	0500h	0600h	0700h	0800h	0900h	1000h	1100h	1200h	1300h	1400h	1500h	1600h	1700h	1800h	1900h	2000h	2100h	2200h	2300h	0000h
	Eig1	0.002012	0.002012	0.002012	0.002012	0.002012	0.002012	0.002012	0.002007	0.001916	0.001916	0.001914	0.001914	0.001914	0.001914	0.001915	0.001914	0.001915	0.001917	0.001918	0.002010	0.002010	0.002011	0.002012	0.002012
	Eig2	0.002012	0.002012	0.002012	0.002012	0.002012	0.002012	0.002012	0.002007	0.001916	0.001916	0.001914	0.001914	0.001914	0.001914	0.001915	0.001914	0.001915	0.001917	0.001918	0.002010	0.002010	0.002011	0.002012	0.002012
SC01	**Eig3**	0.001728	0.002849	0.002849	0.001727	0.001727	0.002850	0.001727	0.001582	0.001831	0.001834	0.001834	0.001834	0.001834	0.001834	0.001834	0.001835	0.001834	0.001834	0.002858	0.001583	0.002519	0.001728	0.001728	0.001728
	Eig4	0.001728	0.002849	0.002849	0.001727	0.001727	0.002850	0.001727	0.001582	0.001831	0.001834	0.001834	0.001834	0.001834	0.001834	0.001834	0.001835	0.001834	0.001834	0.002858	0.001583	0.002519	0.001728	0.001728	0.001728
	Eig5	0.002850	0.001728	0.001727	0.002849	0.002850	0.001727	0.002851	0.003161	0.002858	0.002861	0.002861	0.002861	0.002861	0.002861	0.002862	0.002862	0.002862	0.002859	0.001584	0.001584	0.001583	0.002852	0.002851	0.002850
	Eig6	0.002850	0.001728	0.001727	0.002849	0.002850	0.001727	0.002851	0.003161	0.002858	0.002861	0.002861	0.002861	0.002861	0.002861	0.002862	0.002862	0.002862	0.002859	0.001584	0.001584	0.001583	0.002852	0.002851	0.002850
	Eig1	0.000844	0.000844	0.000844	0.000844	0.000844	0.000844	0.000844	0.000845	0.000845	0.000845	0.000845	0.000845	0.000845	0.000845	0.000845	0.000845	0.000845	0.000844	0.000844	0.000844	0.001334	0.000844	0.000844	0.000844
	Eig2	0.000844	0.000844	0.000844	0.000844	0.000844	0.000844	0.000844	0.000845	0.000845	0.000845	0.000845	0.000845	0.000845	0.000845	0.000845	0.000845	0.000845	0.000844	0.000844	0.000844	0.001334	0.000844	0.000844	0.000844
SC02	**Eig3**	0.001899	0.001899	0.001899	0.001899	0.001899	0.001899	0.001899	0.001900	0.001933	0.002026	0.002024	0.002026	0.002026	0.001856	0.001856	0.001856	0.001856	0.001856	0.001933	0.001932	0.001165	0.001899	0.001899	0.001899
	Eig4	0.001899	0.001899	0.001899	0.001899	0.001899	0.001899	0.001899	0.001900	0.001933	0.002026	0.002024	0.002026	0.002026	0.001856	0.001856	0.001856	0.001856	0.001856	0.001933	0.001932	0.001165	0.001899	0.001899	0.001899
	Eig5	0.001165	0.001165	0.001165	0.001165	0.001165	0.001165	0.001165	0.001165	0.001166	0.001195	0.001195	0.001195	0.001254	0.001166	0.001166	0.001166	0.001166	0.001140	0.001166	0.001166	0.001900	0.001165	0.001165	0.001165
	Eig6	0.001165	0.001165	0.001165	0.001165	0.001165	0.001165	0.001165	0.001165	0.001166	0.001195	0.001195	0.001195	0.001254	0.001166	0.001166	0.001166	0.001166	0.001140	0.001166	0.001166	0.001900	0.001165	0.001165	0.001165
	Eig1	0.002012	0.002012	0.002012	0.002012	0.002012	0.002012	0.002012	0.002008	0.001916	0.001916	0.001915	0.001916	0.001917	0.001916	0.001915	0.001915	0.001915	0.001917	0.001918	0.002010	0.002010	0.002011	0.002012	0.002012
	Eig2	0.002012	0.002012	0.002012	0.002012	0.002012	0.002012	0.002012	0.002008	0.001916	0.001916	0.001915	0.001916	0.001917	0.001916	0.001915	0.001915	0.001915	0.001917	0.001918	0.002010	0.002010	0.002011	0.002012	0.002012
SC03	**Eig3**	0.001728	0.002849	0.002849	0.001727	0.001727	0.002850	0.001727	0.003160	0.002857	0.002858	0.002859	0.001834	0.001834	0.001834	0.001834	0.001834	0.001834	0.001834	0.002858	0.001583	0.002519	0.001728	0.001728	0.001728
	Eig4	0.001728	0.002849	0.002849	0.001727	0.001727	0.002850	0.001727	0.003160	0.002857	0.002858	0.002859	0.001834	0.001834	0.001834	0.001834	0.001834	0.001834	0.001834	0.002858	0.001583	0.002519	0.001728	0.001728	0.001728
	Eig5	0.002850	0.001728	0.001727	0.002849	0.002850	0.001727	0.002851	0.001582	0.001584	0.001709	0.001833	0.002859	0.002859	0.002859	0.002859	0.002861	0.002861	0.002859	0.001584	0.001584	0.001583	0.002852	0.002851	0.002850
	Eig6	0.002850	0.001728	0.001727	0.002849	0.002850	0.001727	0.002851	0.001582	0.001584	0.001709	0.001833	0.002859	0.002859	0.002859	0.002859	0.002861	0.002861	0.002859	0.001584	0.001584	0.001583	0.002852	0.002851	0.002850
	Eig1	0.002012	0.002012	0.002012	0.002012	0.002012	0.002012	0.002012	0.002008	0.001916	0.001916	0.001915	0.001916	0.001917	0.001916	0.001915	0.001915	0.001915	0.001917	0.001918	0.002010	0.002010	0.002011	0.002012	0.002012
	Eig2	0.002012	0.002012	0.002012	0.002012	0.002012	0.002012	0.002012	0.002008	0.001916	0.001916	0.001915	0.001916	0.001917	0.001916	0.001915	0.001915	0.001915	0.001917	0.001918	0.002010	0.002010	0.002011	0.002012	0.002012
SC04	**Eig3**	0.001728	0.002849	0.002849	0.001727	0.001727	0.002850	0.001727	0.003160	0.002857	0.002858	0.002859	0.001834	0.001834	0.001834	0.001834	0.001834	0.001834	0.001834	0.002858	0.001583	0.002519	0.001728	0.001728	0.001728
	Eig4	0.001728	0.002849	0.002849	0.001727	0.001727	0.002850	0.001727	0.003160	0.002857	0.002858	0.002859	0.001834	0.001834	0.001834	0.001834	0.001834	0.001834	0.001834	0.002858	0.001583	0.002519	0.001728	0.001728	0.001728
	Eig5	0.002850	0.001728	0.001727	0.002849	0.002850	0.001727	0.002851	0.001582	0.001584	0.001709	0.001833	0.002859	0.002859	0.002859	0.002859	0.002861	0.002861	0.002859	0.001584	0.001584	0.001583	0.002852	0.002851	0.002850
	Eig6	0.002850	0.001728	0.001727	0.002849	0.002850	0.001727	0.002851	0.001582	0.001584	0.001709	0.001833	0.002859	0.002859	0.002859	0.002859	0.002861	0.002861	0.002859	0.001584	0.001584	0.001583	0.002852	0.002851	0.002850
	Eig1	0.002012	0.002012	0.002012	0.002012	0.002012	0.002012	0.002012	0.002008	0.001918	0.002014	0.001647	0.001647	0.001647	0.001647	0.001917	0.001916	0.001916	0.001917	0.001918	0.002010	0.002010	0.002011	0.002012	0.002012
	Eig2	0.002012	0.002012	0.002012	0.002012	0.002012	0.002012	0.002012	0.002008	0.001918	0.002014	0.001647	0.001647	0.001647	0.001647	0.001917	0.001916	0.001916	0.001917	0.001918	0.002010	0.002010	0.002011	0.002012	0.002012
SC05	**Eig3**	0.001728	0.002849	0.002849	0.001727	0.001727	0.002850	0.001727	0.001828	0.001830	0.001725	0.001584	0.001831	0.001831	0.001584	0.001661	0.001662	0.002860	0.001834	0.002858	0.001583	0.002519	0.001728	0.001728	0.001728
	Eig4	0.001728	0.002849	0.002849	0.001727	0.001727	0.002850	0.001727	0.001828	0.001830	0.001725	0.001584	0.001831	0.001831	0.001584	0.001661	0.001662	0.002860	0.001834	0.002858	0.001583	0.002519	0.001728	0.001728	0.001728
	Eig5	0.002850	0.001728	0.001727	0.002849	0.002850	0.001727	0.002851	0.003159	0.002855	0.002848	0.003164	0.003163	0.003164	0.003165	0.003165	0.002522	0.001833	0.002859	0.001584	0.001584	0.001583	0.002852	0.002851	0.002850
	Eig6	0.002850	0.001728	0.001727	0.002849	0.002850	0.001727	0.002851	0.003159	0.002855	0.002848	0.003164	0.003163	0.003164	0.003165	0.003165	0.002522	0.001833	0.002859	0.001584	0.001584	0.001583	0.002852	0.002851	0.002850
	Eig1	0.002012	0.002012	0.002012	0.002012	0.002012	0.002012	0.002012	0.002008	0.001918	0.002014	0.001647	0.001647	0.001647	0.001647	0.001917	0.001916	0.001916	0.001917	0.001918	0.002010	0.002010	0.002011	0.002012	0.002012
	Eig2	0.002012	0.002012	0.002012	0.002012	0.002012	0.002012	0.002012	0.002008	0.001918	0.002014	0.001647	0.001647	0.001647	0.001647	0.001917	0.001916	0.001916	0.001917	0.001918	0.002010	0.002010	0.002011	0.002012	0.002012
SC06	**Eig3**	0.001728	0.002849	0.002849	0.001727	0.001727	0.002850	0.001727	0.001828	0.001830	0.001725	0.001584	0.001831	0.001831	0.001584	0.001661	0.001662	0.002860	0.001834	0.002858	0.001583	0.002519	0.001728	0.001728	0.001728
	Eig4	0.001728	0.002849	0.002849	0.001727	0.001727	0.002850	0.001727	0.001828	0.001830	0.001725	0.001584	0.001831	0.001831	0.001584	0.001661	0.001662	0.002860	0.001834	0.002858	0.001583	0.002519	0.001728	0.001728	0.001728
	Eig5	0.002850	0.001728	0.001727	0.002849	0.002850	0.001727	0.002851	0.003159	0.002855	0.002848	0.003164	0.003163	0.001831	0.001584	0.001661	0.002522	0.001833	0.002859	0.001584	0.001584	0.001583	0.002852	0.002851	0.002850
	Eig6	0.002850	0.001728	0.001727	0.002849	0.002850	0.001727	0.002851	0.003159	0.002855	0.002848	0.003164	0.003163	0.001831	0.001584	0.001661	0.002522	0.001833	0.002859	0.001584	0.001584	0.001583	0.002852	0.002851	0.002850
	Eig1	0.000633	0.000633	0.000633	0.000633	0.000633	0.000633	0.000633	0.000633	0.000633	0.000633	0.000633	0.000633	0.000633	0.000633	0.000633	0.000633	0.000633	0.000633	0.000633	0.000633	0.000635	0.000633	0.000633	0.000633
	Eig2	0.000633	0.000633	0.000633	0.000633	0.000633	0.000633	0.000633	0.000633	0.000633	0.000633	0.000633	0.000633	0.000633	0.000633	0.000633	0.000633	0.000633	0.000633	0.000633	0.000633	0.000635	0.000633	0.000633	0.000633
	Eig3	0.000975	0.000975	0.000975	0.000975	0.000975	0.000975	0.000975	0.000975	0.000975	0.000980	0.000979	0.000980	0.000980	0.000979	0.000979	0.000979	0.000979	0.000980	0.000975	0.000975	0.000977	0.000975	0.000975	0.000975
	Eig4	0.000975	0.000975	0.000975	0.000975	0.000975	0.000975	0.000975	0.000975	0.000975	0.000980	0.000979	0.000980	0.000980	0.000979	0.000979	0.000979	0.000979	0.000980	0.000975	0.000975	0.000977	0.000975	0.000975	0.000975
	Eig5	0.001144	0.001144	0.001144	0.001144	0.001144	0.001144	0.001144	0.001144	0.001143	0.001143	0.001144	0.001143	0.001144	0.001143	0.001143	0.001143	0.001143	0.001143	0.001143	0.001143	0.001161	0.001144	0.001144	0.001144
	Eig6	0.001144	0.001144	0.001144	0.001144	0.001144	0.001144	0.001144	0.001144	0.001143	0.001143	0.001144	0.001143	0.001144	0.001143	0.001143	0.001143	0.001143	0.001143	0.001143	0.001143	0.001161	0.001144	0.001144	0.001144
SC07	**Eig7**	0.002279	0.002279	0.002278	0.002278	0.002279	0.002279	0.002279	0.002279	0.002290	0.002282	0.002283	0.002282	0.002268	0.002279	0.002279	0.002279	0.002279	0.002282	0.002290	0.002290	0.002284	0.002279	0.002279	0.002279
	Eig8	0.002279	0.002279	0.002278	0.002278	0.002279	0.002279	0.002279	0.002279	0.002290	0.002282	0.002283	0.002282	0.002268	0.002279	0.002279	0.002279	0.002279	0.002282	0.002290	0.002290	0.002284	0.002279	0.002279	0.002279
	Eig9	0.001816	0.001816	0.001816	0.001816	0.001816	0.001816	0.001816	0.001817	0.001816	0.001808	0.001808	0.001808	0.001807	0.001814	0.001814	0.001815	0.001815	0.001807	0.001816	0.001816	0.002009	0.001816	0.001816	0.001816
	Eig10	0.001816	0.001816	0.001816	0.001816	0.001816	0.001816	0.001816	0.001817	0.001816	0.001808	0.001808	0.001808	0.001807	0.001814	0.001814	0.001815	0.001815	0.001807	0.001816	0.001816	0.002009	0.001816	0.001816	0.001816
	Eig11	0.001352	0.001352	0.001352	0.001352	0.001352	0.001352	0.001352	0.001353	0.001353	0.001353	0.001353	0.001353	0.001356	0.001354	0.001354	0.003166	0.003166	0.001353	0.001353	0.001353	0.001486	0.001352	0.001352	0.001352
	Eig12	0.001352	0.001352	0.001352	0.001352	0.001352	0.001352	0.001352	0.001353	0.001353	0.001353	0.001353	0.001353	0.001356	0.001354	0.001354	0.003166	0.003166	0.001353	0.001353	0.001353	0.001486	0.001352	0.001352	0.001352
	Eig13	0.001412	0.001412	0.001412	0.001412	0.001412	0.001412	0.001412	0.001412	0.001414	0.001408	0.001407	0.001408	0.001406	0.001406	0.001406	0.001406	0.001406	0.001407	0.001414	0.001414	0.001413	0.001412	0.001412	0.001412
	Eig14	0.001412	0.001412	0.001412	0.001412	0.001412	0.001412	0.001412	0.001412	0.001414	0.001408	0.001407	0.001408	0.001406	0.001406	0.001406	0.001406	0.001406	0.001407	0.001414	0.001414	0.001413	0.001412	0.001412	0.001412
	Eig1	0.000633	0.000633	0.000633	0.000633	0.000633	0.000633	0.000633	0.000633	0.000633	0.000633	0.000633	0.000633	0.000633	0.000633	0.000633	0.000633	0.000633	0.000633	0.000633	0.000633	0.000635	0.000633	0.000633	0.000633
	Eig2	0.000633	0.000633	0.000633	0.000633	0.000633	0.000633	0.000633	0.000633	0.000633	0.000633	0.000633	0.000633	0.000633	0.000633	0.000633	0.000633	0.000633	0.000633	0.000633	0.000633	0.000635	0.000633	0.000633	0.000633
	Eig3	0.000975	0.000975	0.000975	0.000975	0.000975	0.000975	0.000975	0.000975	0.000975	0.000975	0.000980	0.000980	0.000975	0.000975	0.000975	0.000980	0.000979	0.000979	0.000975	0.000975	0.000977	0.000975	0.000975	0.000975
	Eig4	0.000975	0.000975	0.000975	0.000975	0.000975	0.000975	0.000975	0.000975	0.000975	0.000975	0.000980	0.000980	0.000975	0.000975	0.000975	0.000980	0.000979	0.000979	0.000975	0.000975	0.000977	0.000975	0.000975	0.000975
	Eig5	0.001144	0.001144	0.001144	0.001144	0.001144	0.001144	0.001144	0.001144	0.001144	0.001143	0.001143	0.001144	0.001143	0.001143	0.001143	0.001143	0.001143	0.001144	0.001143	0.001143	0.001161	0.001144	0.001144	0.001144
	Eig6	0.001144	0.001144	0.001144	0.001144	0.001144	0.001144	0.001144	0.001144	0.001144	0.001143	0.001143	0.001144	0.001143	0.001143	0.001143	0.001143	0.001143	0.001144	0.001143	0.001143	0.001161	0.001144	0.001144	0.001144
SC09	**Eig7**	0.002279	0.002279	0.002278	0.002278	0.002279	0.002279	0.002279	0.002279	0.002279	0.002290	0.002284	0.002273	0.002290	0.002290	0.002290	0.002282	0.002279	0.002283	0.002290	0.002290	0.002284	0.002279	0.002279	0.002279
	Eig8	0.002279	0.002279	0.002278	0.002278	0.002279	0.002279	0.002279	0.002279	0.002279	0.002290	0.002284	0.002273	0.002290	0.002290	0.002290	0.002282	0.002279	0.002283	0.002290	0.002290	0.002284	0.002279	0.002279	0.002279
	Eig9	0.001816	0.001816	0.001816	0.001816	0.001816	0.001816	0.001816	0.001816	0.001808	0.001816	0.001814	0.001806	0.001816	0.001816	0.001816	0.001808	0.001814	0.001807	0.001816	0.001816	0.002009	0.001816	0.001816	0.001816
	Eig10	0.001816	0.001816	0.001816	0.001816	0.001816	0.001816	0.001816	0.001816	0.001808	0.001816	0.001814	0.001806	0.001816	0.001816	0.001816	0.001808	0.001814	0.001807	0.001816	0.001816	0.002009	0.001816	0.001816	0.001816
	Eig11	0.001352	0.001352	0.001352	0.001352	0.001352	0.001352	0.001352	0.001353	0.001355	0.001353	0.001352	0.001354	0.003168	0.003167	0.001353	0.001353	0.001354	0.001353	0.001353	0.001353	0.001486	0.001352	0.001352	0.001352
	Eig12	0.001352	0.001352	0.001352	0.001352	0.001352	0.001352	0.001352	0.001353	0.001355	0.001353	0.001352	0.001354	0.003168	0.003167	0.001353	0.001353	0.001354	0.001353	0.001353	0.001353	0.001486	0.001352	0.001352	0.001352
	Eig13	0.001412	0.001412	0.001412	0.001412	0.001412	0.001412	0.001412	0.001412	0.001415	0.001415	0.001405	0.001405	0.001415	0.001415	0.001415	0.001408	0.001406	0.001407	0.001414	0.001414	0.001413	0.001412	0.001412	0.001412
	Eig14	0.001412	0.001412	0.001412	0.001412	0.001412	0.001412	0.001412	0.001412	0.001415	0.001415	0.001405	0.001405	0.001415	0.001415	0.001415	0.001408	0.001406	0.001407	0.001414	0.001414	0.001413	0.001412	0.001412	0.001412
	Eig1	0.000633	0.000633	0.000633	0.000633	0.000633	0.000633	0.000633	0.000633	0.000633	0.000634	0.000634	0.000634	0.000634	0.000634	0.000634	0.000633	0.000633	0.000633	0.000633	0.000633	0.000635	0.000633	0.000633	0.000633
	Eig2	0.000633	0.000633	0.000633	0.000633	0.000633	0.000633	0.000633	0.000633	0.000633	0.000634	0.000634	0.000634	0.000634	0.000634	0.000634	0.000633	0.000633	0.000633	0.000633	0.000633	0.000635	0.000633	0.000633	0.000633
	Eig3	0.000975	0.000975	0.000975	0.000975	0.000975	0.000975	0.000975	0.000975	0.000975	0.000975	0.000975	0.000975	0.000975	0.000979	0.000975	0.000980	0.000975	0.000980	0.000975	0.000975	0.000977	0.000975	0.000975	0.000975
	Eig4	0.000975	0.000975	0.000975	0.000975	0.000975	0.000975	0.000975	0.000975	0.000975	0.000975	0.000975	0.000975	0.000975	0.000979	0.000975	0.000980	0.000975	0.000980	0.000975	0.000975	0.000977	0.000975	0.000975	0.000975
	Eig5	0.001144	0.001144	0.001144	0.001144	0.001144	0.001144	0.001144	0.001144	0.001144	0.001140	0.001141	0.001141	0.001141	0.001140	0.001140	0.001144	0.001143	0.001143	0.001143	0.001143	0.001161	0.001144	0.001144	0.001144
	Eig6	0.001144	0.001144	0.001144	0.001144	0.001144	0.001144	0.001144	0.001144	0.001144	0.001140	0.001141	0.001141	0.001141	0.001140	0.001140	0.001144	0.001143	0.001143	0.001143	0.001143	0.001161	0.001144	0.001144	0.001144
SC11	**Eig7**	0.002279	0.002279	0.002278	0.002278	0.002279	0.002279	0.002279	0.002279	0.002279	0.002271	0.002261	0.002261	0.002261	0.002263	0.002271	0.003166	0.002290	0.002282	0.002290	0.002290	0.002284	0.002279	0.002279	0.002279
	Eig8	0.002279	0.002279	0.002278	0.002278	0.002279	0.002279	0.002279	0.002279	0.002279	0.002271	0.002261	0.002261	0.002261	0.002263	0.002271	0.003166	0.002290	0.002282	0.002290	0.002290	0.002284	0.002279	0.002279	0.002279
	Eig9	0.001816	0.001816	0.001816	0.001816	0.001816	0.001816	0.001816	0.001816	0.001817	0.001815	0.001814	0.001814	0.001814	0.001806	0.001815	0.001806	0.001816	0.001807	0.001816	0.001816	0.002009	0.001816	0.001816	0.001816
	Eig10	0.001816	0.001816	0.001816	0.001816	0.001816	0.001816	0.001816	0.001816	0.001817	0.001815	0.001814	0.001814	0.001814	0.001806	0.001815	0.001806	0.001816	0.001807	0.001816	0.001816	0.002009	0.001816	0.001816	0.001816
	Eig11	0.001352	0.001352	0.001352	0.001352	0.001352	0.001352	0.001352	0.001353	0.001353	0.001352	0.001353	0.001353	0.001353	0.001352	0.001352	0.001354	0.001353	0.001353	0.001353	0.001353	0.001486	0.001352	0.001352	0.001352
	Eig12	0.001352	0.001352	0.001352	0.001352	0.001352	0.001352	0.001352	0.001353	0.001353	0.001352	0.001353	0.001353	0.001353	0.001352	0.001352	0.001354	0.001353	0.001353	0.001353	0.001353	0.001486	0.001352	0.001352	0.001352
	Eig13	0.001412	0.001412	0.001412	0.001412	0.001412	0.001412	0.001412	0.001412	0.001413	0.001414	0.001412	0.001412	0.001412	0.001407	0.001414	0.001405	0.001415	0.001407	0.001414	0.001414	0.001413	0.001412	0.001412	0.001412
	Eig14	0.001412	0.001412	0.001412	0.001412	0.001412	0.001412	0.001412	0.001412	0.001413	0.001414	0.001412	0.001412	0.001412	0.001407	0.001414	0.001405	0.001415	0.001407	0.001414	0.001414	0.001413	0.001412	0.001412	0.001412

Table A5 - Decay times of conjugate Eigenvalues of stable scenarios

		0100h	0200h	0300h	0400h	0500h	0600h	0700h	0800h	0900h	1000h	1100h	1200h	1300h	1400h	1500h	1600h	1700h	1800h	1900h	2000h	2100h	2200h	2300h	0000h
SC01	**Eig1**	0.003074	0.003075	0.003075	0.003075	0.003074	0.003074	0.003074	0.003067	0.002927	0.002927	0.002925	0.002925	0.002925	0.002925	0.002925	0.002925	0.002926	0.002930	0.002931	0.003071	0.003072	0.003073	0.003073	0.003074
	Eig2	0.003074	0.003075	0.003075	0.003075	0.003074	0.003074	0.003074	0.003067	0.002927	0.002927	0.002925	0.002925	0.002925	0.002925	0.002925	0.002925	0.002926	0.002930	0.002931	0.003071	0.003072	0.003073	0.003073	0.003074
	Eig3	0.002640	0.004353	0.004353	0.002639	0.002639	0.004354	0.002639	0.002418	0.002798	0.002802	0.002803	0.002803	0.002803	0.002802	0.002803	0.002803	0.002803	0.002802	0.004367	0.002419	0.003848	0.002640	0.002640	0.002640
	Eig4	0.002640	0.004353	0.004353	0.002639	0.002639	0.004354	0.002639	0.002418	0.002798	0.002802	0.002803	0.002803	0.002803	0.002802	0.002803	0.002803	0.002803	0.002802	0.004367	0.002419	0.003848	0.002640	0.002640	0.002640
	Eig5	0.004354	0.002640	0.002639	0.004353	0.004355	0.002639	0.004356	0.004829	0.004367	0.004371	0.004371	0.004372	0.004372	0.004372	0.004372	0.004373	0.004373	0.004369	0.002420	0.004834	0.002419	0.004357	0.004356	0.004355
	Eig6	0.004354	0.002640	0.002639	0.004353	0.004355	0.002639	0.004356	0.004829	0.004367	0.004371	0.004371	0.004372	0.004372	0.004372	0.004372	0.004373	0.004373	0.004369	0.002420	0.004834	0.002419	0.004357	0.004356	0.004355
SC02	**Eig1**	0.001290	0.001290	0.001290	0.001290	0.001290	0.001290	0.001290	0.001290	0.001290	0.001290	0.001291	0.001290	0.001290	0.001290	0.001290	0.001290	0.001290	0.001290	0.001290	0.001290	0.002038	0.001290	0.001290	0.001290
	Eig2	0.001290	0.001290	0.001290	0.001290	0.001290	0.001290	0.001290	0.001290	0.001290	0.001290	0.001291	0.001290	0.001290	0.001290	0.001290	0.001290	0.001290	0.001290	0.001290	0.001290	0.002038	0.001290	0.001290	0.001290
	Eig3	0.002902	0.002902	0.002901	0.002901	0.002902	0.002901	0.002901	0.002903	0.002953	0.003095	0.003092	0.003096	0.003096	0.002836	0.002836	0.002836	0.002836	0.002835	0.002953	0.002952	0.001781	0.002902	0.002902	0.002902
	Eig4	0.002902	0.002902	0.002901	0.002901	0.002902	0.002901	0.002901	0.002903	0.002953	0.003095	0.003092	0.003096	0.003096	0.002836	0.002836	0.002836	0.002836	0.002835	0.002953	0.002952	0.001781	0.002902	0.002902	0.002902
	Eig5	0.001780	0.001780	0.001780	0.001780	0.001780	0.001780	0.001780	0.001781	0.001781	0.001825	0.001825	0.001825	0.001916	0.001781	0.001781	0.001782	0.001782	0.001742	0.001781	0.001781	0.002903	0.001780	0.001780	0.001780
	Eig6	0.001780	0.001780	0.001780	0.001780	0.001780	0.001780	0.001780	0.001781	0.001781	0.001825	0.001825	0.001825	0.001916	0.001781	0.001781	0.001782	0.001782	0.001742	0.001781	0.001781	0.002903	0.001780	0.001780	0.001780
SC03	**Eig1**	0.003074	0.003075	0.003075	0.003075	0.003074	0.003074	0.003074	0.003067	0.002928	0.032210	0.002926	0.002928	0.002929	0.002927	0.002926	0.002926	0.002926	0.002930	0.002931	0.003071	0.003072	0.003073	0.003073	0.003074
	Eig2	0.003074	0.003075	0.003075	0.003075	0.003074	0.003074	0.003074	0.003067	0.002928	0.032210	0.002926	0.002928	0.002929	0.002927	0.002926	0.002926	0.002926	0.002930	0.002931	0.003071	0.003072	0.003073	0.003073	0.003074
	Eig3	0.002640	0.004353	0.004353	0.002639	0.002639	0.004354	0.002639	0.004828	0.004365	0.026656	0.004368	0.002802	0.002802	0.002802	0.002802	0.002802	0.002803	0.002802	0.004367	0.002419	0.003848	0.002640	0.002640	0.002640
	Eig4	0.002640	0.004353	0.004353	0.002639	0.002639	0.004354	0.002639	0.004828	0.004365	0.026656	0.004368	0.002802	0.002802	0.002802	0.002802	0.002802	0.002803	0.002802	0.004367	0.002419	0.003848	0.002640	0.002640	0.002640
	Eig5	0.004354	0.002640	0.002639	0.004353	0.004355	0.002639	0.004355	0.002417	0.002420	0.048105	0.002801	0.004368	0.004369	0.004368	0.004369	0.004371	0.004371	0.004369	0.002420	0.004834	0.002419	0.004357	0.004356	0.004355
	Eig6	0.004354	0.002640	0.002639	0.004353	0.004355	0.002639	0.004355	0.002417	0.002420	0.048105	0.002801	0.004368	0.004369	0.004368	0.004369	0.004371	0.004371	0.004369	0.002420	0.004834	0.002419	0.004357	0.004356	0.004355
SC04	**Eig1**	0.003074	0.003075	0.003075	0.003075	0.003074	0.003074	0.003074	0.003067	0.002928	0.032210	0.002926	0.002928	0.002929	0.002927	0.002926	0.002926	0.002926	0.002930	0.002931	0.003071	0.003072	0.003073	0.003073	0.003074
	Eig2	0.003074	0.003075	0.003075	0.003075	0.003074	0.003074	0.003074	0.003067	0.002928	0.032210	0.002926	0.002928	0.002929	0.002927	0.002926	0.002926	0.002926	0.002930	0.002931	0.003071	0.003072	0.003073	0.003073	0.003074
	Eig3	0.002640	0.004353	0.004353	0.002639	0.002639	0.004354	0.002639	0.004828	0.004365	0.026656	0.004368	0.002802	0.002802	0.002802	0.002802	0.002802	0.002803	0.002802	0.004367	0.002419	0.003848	0.002640	0.002640	0.002640
	Eig4	0.002640	0.004353	0.004353	0.002639	0.002639	0.004354	0.002639	0.004828	0.004365	0.026656	0.004368	0.002802	0.002802	0.002802	0.002802	0.002802	0.002803	0.002802	0.004367	0.002419	0.003848	0.002640	0.002640	0.002640
	Eig5	0.004354	0.002640	0.002639	0.004353	0.004355	0.002639	0.004355	0.002417	0.002420	0.048105	0.002801	0.004368	0.004369	0.004368	0.004369	0.004371	0.004371	0.004369	0.002420	0.004834	0.002419	0.004357	0.004356	0.004355
	Eig6	0.004354	0.002640	0.002639	0.004353	0.004355	0.002639	0.004355	0.002417	0.002420	0.048105	0.002801	0.004368	0.004369	0.004368	0.004369	0.004371	0.004371	0.004369	0.002420	0.004834	0.002419	0.004357	0.004356	0.004355
SC05	**Eig1**	0.003074	0.003075	0.003075	0.003075	0.003074	0.003074	0.003074	0.003068	0.002930	0.003077	0.002516	0.002517	0.002516	0.002516	0.002929	0.002928	0.002927	0.002930	0.002931	0.003071	0.003072	0.003073	0.003073	0.003074
	Eig2	0.003074	0.003075	0.003075	0.003075	0.003074	0.003074	0.003074	0.003068	0.002930	0.003077	0.002516	0.002517	0.002516	0.002516	0.002929	0.002928	0.002927	0.002930	0.002931	0.003071	0.003072	0.003073	0.003073	0.003074
	Eig3	0.002640	0.004353	0.004353	0.002639	0.002639	0.004354	0.002639	0.002793	0.002796	0.002635	0.002420	0.002798	0.002798	0.002420	0.002538	0.002539	0.004370	0.002802	0.004367	0.002419	0.003848	0.002640	0.002640	0.002640
	Eig4	0.002640	0.004353	0.004353	0.002639	0.002639	0.004354	0.002639	0.002793	0.002796	0.002635	0.002420	0.002798	0.002798	0.002420	0.002538	0.002539	0.004370	0.002802	0.004367	0.002419	0.003848	0.002640	0.002640	0.002640
	Eig5	0.004354	0.002640	0.002639	0.004353	0.004355	0.002639	0.004356	0.004827	0.004362	0.004352	0.004834	0.004833	0.004834	0.004835	0.004837	0.003853	0.002801	0.004369	0.002420	0.004834	0.002419	0.004357	0.004356	0.004355
	Eig6	0.004354	0.002640	0.002639	0.004353	0.004355	0.002639	0.004356	0.004827	0.004362	0.004352	0.004834	0.004833	0.004834	0.004835	0.004837	0.003853	0.002801	0.004369	0.002420	0.004834	0.002419	0.004357	0.004356	0.004355
SC06	**Eig1**	0.003074	0.003075	0.003075	0.003075	0.003074	0.003074	0.003074	0.003068	0.002930	0.003077	0.002516	0.002517	0.002516	0.002516	0.002929	0.002928	0.002927	0.002930	0.002931	0.003071	0.003072	0.003073	0.003073	0.003074
	Eig2	0.003074	0.003075	0.003075	0.003075	0.003074	0.003074	0.003074	0.003068	0.002930	0.003077	0.002516	0.002517	0.002516	0.002516	0.002929	0.002928	0.002927	0.002930	0.002931	0.003071	0.003072	0.003073	0.003073	0.003074
	Eig3	0.002640	0.004353	0.004353	0.002639	0.002639	0.004354	0.002639	0.002793	0.002796	0.002635	0.002420	0.002798	0.002798	0.002420	0.002538	0.002539	0.004370	0.002802	0.004367	0.002419	0.003848	0.002640	0.002640	0.002640
	Eig4	0.002640	0.004353	0.004353	0.002639	0.002639	0.004354	0.002639	0.002793	0.002796	0.002635	0.002420	0.002798	0.002798	0.002420	0.002538	0.002539	0.004370	0.002802	0.004367	0.002419	0.003848	0.002640	0.002640	0.002640
	Eig5	0.004354	0.002640	0.002639	0.004353	0.004355	0.002639	0.004356	0.004827	0.004362	0.004352	0.004834	0.004833	0.004834	0.004835	0.004837	0.003853	0.002801	0.004369	0.002420	0.004834	0.002419	0.004357	0.004356	0.004355
	Eig6	0.004354	0.002640	0.002639	0.004353	0.004355	0.002639	0.004356	0.004827	0.004362	0.004352	0.004834	0.004833	0.004834	0.004835	0.004837	0.003853	0.002801	0.004369	0.002420	0.004834	0.002419	0.004357	0.004356	0.004355
SC07	**Eig1**	0.000967	0.000967	0.000967	0.000967	0.000967	0.000967	0.000967	0.000967	0.000967	0.000967	0.000968	0.000967	0.000967	0.000967	0.000967	0.000967	0.000967	0.000967	0.000967	0.000967	0.000970	0.000967	0.000967	0.000967
	Eig2	0.000967	0.000967	0.000967	0.000967	0.000967	0.000967	0.000967	0.000967	0.000967	0.000967	0.000968	0.000967	0.000967	0.000967	0.000967	0.000967	0.000967	0.000967	0.000967	0.000967	0.000970	0.000967	0.000967	0.000967
	Eig3	0.001490	0.001490	0.001490	0.001490	0.001490	0.001490	0.001490	0.001490	0.001490	0.001497	0.001496	0.001497	0.001497	0.001496	0.001496	0.001496	0.001496	0.001497	0.001490	0.001490	0.001493	0.001490	0.001490	0.001490
	Eig4	0.001490	0.001490	0.001490	0.001490	0.001490	0.001490	0.001490	0.001490	0.001490	0.001497	0.001496	0.001497	0.001497	0.001496	0.001496	0.001496	0.001496	0.001497	0.001490	0.001490	0.001493	0.001490	0.001490	0.001490
	Eig5	0.001747	0.001747	0.001747	0.001747	0.001747	0.001747	0.001748	0.001748	0.001747	0.001747	0.001748	0.001747	0.001748	0.001746	0.001746	0.001746	0.001746	0.001747	0.001746	0.001746	0.001774	0.001748	0.001748	0.001748
	Eig6	0.001747	0.001747	0.001747	0.001747	0.001747	0.001747	0.001748	0.001748	0.001747	0.001747	0.001748	0.001747	0.001748	0.001746	0.001746	0.001746	0.001746	0.001747	0.001746	0.001746	0.001774	0.001748	0.001748	0.001748
	Eig7	0.003481	0.003481	0.003481	0.003481	0.003482	0.003482	0.003482	0.003482	0.003499	0.003487	0.003488	0.003487	0.003466	0.003482	0.003482	0.003482	0.003482	0.003487	0.003499	0.003499	0.030872	0.003482	0.003482	0.003482
	Eig8	0.003481	0.003481	0.003481	0.003481	0.003482	0.003482	0.003482	0.003482	0.003499	0.003487	0.003488	0.003487	0.003466	0.003482	0.003482	0.003482	0.003482	0.003487	0.003499	0.003499	0.030872	0.003482	0.003482	0.003482
	Eig9	0.002775	0.002775	0.002774	0.002774	0.002775	0.002775	0.002775	0.002775	0.002775	0.002762	0.002762	0.002762	0.002760	0.002772	0.002772	0.002772	0.002772	0.002762	0.002775	0.002774	0.003070	0.002775	0.002775	0.002775
	Eig10	0.002775	0.002775	0.002774	0.002774	0.002775	0.002775	0.002775	0.002775	0.002775	0.002762	0.002762	0.002762	0.002760	0.002772	0.002772	0.002772	0.002772	0.002762	0.002775	0.002774	0.003070	0.002775	0.002775	0.002775
	Eig11	0.002066	0.002066	0.002066	0.002066	0.002066	0.002066	0.002066	0.002067	0.002067	0.002068	0.002068	0.002068	0.002072	0.002069	0.002069	0.002069	0.002069	0.002068	0.002067	0.002067	0.002271	0.002066	0.002066	0.002066
	Eig12	0.002066	0.002066	0.002066	0.002066	0.002066	0.002066	0.002066	0.002067	0.002067	0.002068	0.002068	0.002068	0.002072	0.002069	0.002069	0.002069	0.002069	0.002068	0.002067	0.002067	0.002271	0.002066	0.002066	0.002066
	Eig13	0.002157	0.002157	0.002157	0.002157	0.002157	0.002157	0.002157	0.002158	0.002161	0.002151	0.002149	0.002151	0.002149	0.002148	0.002148	0.002148	0.002148	0.002150	0.002161	0.002161	0.002159	0.002158	0.002158	0.002158
	Eig14	0.002157	0.002157	0.002157	0.002157	0.002157	0.002157	0.002157	0.002158	0.002161	0.002151	0.002149	0.002151	0.002149	0.002148	0.002148	0.002148	0.002148	0.002150	0.002161	0.002161	0.002159	0.002158	0.002158	0.002158
SC09	**Eig1**	0.000967	0.000967	0.000967	0.000967	0.000967	0.000967	0.000967	0.000967	0.000967	0.000967	0.000967	0.000967	0.000967	0.000967	0.000967	0.000967	0.000967	0.000967	0.000967	0.000967	0.000970	0.000967	0.000967	0.000967
	Eig2	0.000967	0.000967	0.000967	0.000967	0.000967	0.000967	0.000967	0.000967	0.000967	0.000967	0.000967	0.000967	0.000967	0.000967	0.000967	0.000967	0.000967	0.000967	0.000967	0.000967	0.000970	0.000967	0.000967	0.000967
	Eig3	0.001490	0.001490	0.001490	0.001490	0.001490	0.001490	0.001490	0.001490	0.001490	0.001490	0.001497	0.001498	0.001490	0.001490	0.001490	0.001497	0.001496	0.001496	0.001490	0.001490	0.001493	0.001490	0.001490	0.001490
	Eig4	0.001490	0.001490	0.001490	0.001490	0.001490	0.001490	0.001490	0.001490	0.001490	0.001490	0.001497	0.001498	0.001490	0.001490	0.001490	0.001497	0.001496	0.001496	0.001490	0.001490	0.001493	0.001490	0.001490	0.001490
	Eig5	0.001747	0.001747	0.001747	0.001747	0.001747	0.001747	0.001748	0.001748	0.001749	0.001747	0.001746	0.001748	0.001747	0.001747	0.001747	0.001747	0.001746	0.001748	0.001746	0.001746	0.001774	0.001748	0.001748	0.001748
	Eig6	0.001747	0.001747	0.001747	0.001747	0.001747	0.001747	0.001748	0.001748	0.001749	0.001747	0.001746	0.001748	0.001747	0.001747	0.001747	0.001747	0.001746	0.001748	0.001746	0.001746	0.001774	0.001748	0.001748	0.001748
	Eig7	0.003481	0.003481	0.003481	0.003481	0.003482	0.003482	0.003482	0.003482	0.003482	0.003499	0.003489	0.003473	0.003499	0.003499	0.003499	0.003487	0.003482	0.003487	0.003499	0.003499	0.030865	0.003482	0.003482	0.003482
	Eig8	0.003481	0.003481	0.003481	0.003481	0.003482	0.003482	0.003482	0.003482	0.003482	0.003499	0.003489	0.003473	0.003499	0.003499	0.003499	0.003487	0.003482	0.003487	0.003499	0.003499	0.030865	0.003482	0.003482	0.003482
	Eig9	0.002775	0.002775	0.002774	0.002774	0.002775	0.002775	0.002775	0.002775	0.002762	0.002775	0.002772	0.002760	0.002775	0.002775	0.002775	0.002762	0.002772	0.002762	0.002775	0.002774	0.003070	0.002775	0.002775	0.002775
	Eig10	0.002775	0.002775	0.002774	0.002774	0.002775	0.002775	0.002775	0.002775	0.002762	0.002775	0.002772	0.002760	0.002775	0.002775	0.002775	0.002762	0.002772	0.002762	0.002775	0.002774	0.003070	0.002775	0.002775	0.002775
	Eig11	0.002066	0.002066	0.002066	0.002066	0.002066	0.002066	0.002066	0.002067	0.002070	0.002068	0.002066	0.002069	0.002068	0.002068	0.002068	0.002068	0.002069	0.002068	0.002067	0.002067	0.002271	0.002066	0.002066	0.002066
	Eig12	0.002066	0.002066	0.002066	0.002066	0.002066	0.002066	0.002066	0.002067	0.002070	0.002068	0.002066	0.002069	0.002068	0.002068	0.002068	0.002068	0.002069	0.002068	0.002067	0.002067	0.002271	0.002066	0.002066	0.002066
	Eig13	0.002157	0.002157	0.002157	0.002157	0.002157	0.002157	0.002157	0.002158	0.002162	0.002161	0.002146	0.002147	0.002162	0.002162	0.002162	0.002151	0.002148	0.002149	0.002161	0.002161	0.002159	0.002158	0.002158	0.002158
	Eig14	0.002157	0.002157	0.002157	0.002157	0.002157	0.002157	0.002157	0.002158	0.002162	0.002161	0.002146	0.002147	0.002162	0.002162	0.002162	0.002151	0.002148	0.002149	0.002161	0.002161	0.002159	0.002158	0.002158	0.002158
SC11	**Eig1**	0.000967	0.000967	0.000967	0.000967	0.000967	0.000967	0.000967	0.000967	0.000967	0.000969	0.000969	0.000969	0.000969	0.000969	0.000969	0.000967	0.000967	0.000967	0.000967	0.000967	0.000970	0.000967	0.000967	0.000967
	Eig2	0.000967	0.000967	0.000967	0.000967	0.000967	0.000967	0.000967	0.000967	0.000967	0.000969	0.000969	0.000969	0.000969	0.000969	0.000969	0.000967	0.000967	0.000967	0.000967	0.000967	0.000970	0.000967	0.000967	0.000967
	Eig3	0.001490	0.001490	0.001490	0.001490	0.001490	0.001490	0.001490	0.001490	0.001490	0.001489	0.001490	0.001490	0.001490	0.001496	0.001490	0.001498	0.001490	0.001497	0.001490	0.001490	0.001493	0.001490	0.001490	0.001490
	Eig4	0.001490	0.001490	0.001490	0.001490	0.001490	0.001490	0.001490	0.001490	0.001490	0.001489	0.001490	0.001490	0.001490	0.001496	0.001490	0.001498	0.001490	0.001497	0.001490	0.001490	0.001493	0.001490	0.001490	0.001490
	Eig5	0.001747	0.001747	0.001747	0.001747	0.001747	0.001747	0.001748	0.001748	0.001748	0.001742	0.001744	0.001744	0.001744	0.001742	0.001742	0.001748	0.001747	0.001747	0.001746	0.001746	0.001774	0.001748	0.001748	0.001748
	Eig6	0.001747	0.001747	0.001747	0.001747	0.001747	0.001747	0.001748	0.001748	0.001748	0.001742	0.001744	0.001744	0.001744	0.001742	0.001742	0.001748	0.001747	0.001747	0.001746	0.001746	0.001774	0.001748	0.001748	0.001748
	Eig7	0.003481	0.003481	0.003481	0.003481	0.003482	0.003482	0.003482	0.003482	0.003482	0.003469	0.003455	0.003455	0.003455	0.003457	0.003469	0.003473	0.003499	0.003487	0.003499	0.003499	0.030865	0.003482	0.003482	0.003482
	Eig8	0.003481	0.003481	0.003481	0.003481	0.003482	0.003482	0.003482	0.003482	0.003482	0.003469	0.003455	0.003455	0.003455	0.003457	0.003469	0.003473	0.003499	0.003487	0.003499	0.003499	0.030865	0.003482	0.003482	0.003482
	Eig9	0.002775	0.002775	0.002774	0.002774	0.002775	0.002775	0.002775	0.002775	0.002776	0.002773	0.002772	0.002772	0.002772	0.002760	0.002773	0.002760	0.002775	0.002762	0.002775	0.002774	0.003070	0.002775	0.002775	0.002775
	Eig10	0.002775	0.002775	0.002774	0.002774	0.002775	0.002775	0.002775	0.002775	0.002776	0.002773	0.002772	0.002772	0.002772	0.002760	0.002773	0.002760	0.002775	0.002762	0.002775	0.002774	0.003070	0.002775	0.002775	0.002775
	Eig11	0.002066	0.002066	0.002066	0.002066	0.002066	0.002066	0.002066	0.002067	0.002067	0.002065	0.002067	0.002067	0.002067	0.002065	0.002065	0.002069	0.002068	0.002068	0.002067	0.002067	0.002271	0.002066	0.002066	0.002066
	Eig12	0.002066	0.002066	0.002066	0.002066	0.002066	0.002066	0.002066	0.002067	0.002067	0.002065	0.002067	0.002067	0.002067	0.002065	0.002065	0.002069	0.002068	0.002068	0.002067	0.002067	0.002271	0.002066	0.002066	0.002066
	Eig13	0.002157	0.002157	0.002157	0.002157	0.002157	0.002157	0.002157	0.002158	0.002158	0.002161	0.002157	0.002157	0.002157	0.002150	0.002161	0.002147	0.002162	0.002150	0.002161	0.002161	0.002159	0.002158	0.002158	0.002158
	Eig14	0.002157	0.002157	0.002157	0.002157	0.002157	0.002157	0.002157	0.002158	0.002158	0.002161	0.002157	0.002157	0.002157	0.002150	0.002161	0.002147	0.002162	0.002150	0.002161	0.002161	0.002159	0.002158	0.002158	0.002158

APPENDIX F: PARTICIPATION MATRIX

P_1400

14x14 complex double

	1	2	3	4	5	6	7
1	0.2786 - 0.0002i	0.2786 + 0.0002i	0.0206 - 0.0000i	0.0206 + 0.0000i	0.0899 - 0.0001i	0.0899 + 0.0001i	0.0652 - 0.0001i
2	0.0042 - 0.0000i	0.0042 + 0.0000i	0.0030 - 0.0000i	0.0030 + 0.0000i	0.0306 - 0.0000i	0.0306 + 0.0000i	0.1721 - 0.0004i
3	0.0028 - 0.0000i	0.0028 + 0.0000i	8.8240e-04 - 8.6068e-07i	8.8240e-04 + 8.6068e-07i	0.0868 - 0.0001i	0.0868 + 0.0001i	0.1007 - 0.0002i
4	1.0583e-05 - 6.6963e-09i	1.0583e-05 + 6.6963e-09i	0.0099 - 0.0000i	0.0099 + 0.0000i	0.0399 - 0.0000i	0.0399 + 0.0000i	0.0822 - 0.0002i
5	5.7513e-05 - 3.6392e-08i	5.7513e-05 + 3.6392e-08i	0.2091 - 0.0002i	0.2091 + 0.0002i	0.0851 - 0.0001i	0.0851 + 0.0001i	0.0189 - 0.0000i
6	0.0025 - 0.0000i	0.0025 + 0.0000i	0.2436 - 0.0002i	0.2436 + 0.0002i	0.0089 - 0.0000i	0.0089 + 0.0000i	0.0162 - 0.0000i
7	0.2117 - 0.0001i	0.2117 + 0.0001i	0.0129 - 0.0000i	0.0129 + 0.0000i	0.1588 - 0.0002i	0.1588 + 0.0002i	0.0448 - 0.0001i
8	0.2786 + 0.0002i	0.2786 - 0.0002i	0.0206 + 0.0000i	0.0206 - 0.0000i	0.0899 + 0.0001i	0.0899 - 0.0001i	0.0652 + 0.0001i
9	0.0042 + 0.0000i	0.0042 - 0.0000i	0.0030 + 0.0000i	0.0030 - 0.0000i	0.0306 + 0.0000i	0.0306 - 0.0000i	0.1721 + 0.0004i
10	0.0028 + 0.0000i	0.0028 - 0.0000i	8.8240e-04 + 8.6068e-07i	8.8240e-04 - 8.6068e-07i	0.0868 + 0.0001i	0.0868 - 0.0001i	0.1007 + 0.0002i
11	1.0583e-05 + 6.6963e-09i	1.0583e-05 - 6.6963e-09i	0.0099 + 0.0000i	0.0099 - 0.0000i	0.0399 + 0.0000i	0.0399 - 0.0000i	0.0822 + 0.0002i
12	5.7513e-05 + 3.6392e-08i	5.7513e-05 - 3.6392e-08i	0.2091 + 0.0002i	0.2091 - 0.0002i	0.0851 + 0.0001i	0.0851 - 0.0001i	0.0189 + 0.0000i
13	0.0025 + 0.0000i	0.0025 - 0.0000i	0.2436 + 0.0002i	0.2436 - 0.0002i	0.0089 + 0.0000i	0.0089 - 0.0000i	0.0162 + 0.0000i
14	0.2117 + 0.0001i	0.2117 - 0.0001i	0.0129 + 0.0000i	0.0129 - 0.0000i	0.1588 + 0.0002i	0.1588 - 0.0002i	0.0448 + 0.0001i

	8	9	10	11	12	13	14
1	0.0652 + 0.0001i	0.0170 - 0.0000i	0.0170 + 0.0000i	0.0256 - 0.0000i	0.0256 + 0.0000i	0.0030 - 0.0000i	0.0030 + 0.0000i
2	0.1721 + 0.0004i	0.1430 - 0.0003i	0.1430 + 0.0003i	0.1469 - 0.0002i	0.1469 + 0.0002i	1.7020e-04 - 2.4079e-07i	1.7020e-04 + 2.4079e-07i
3	0.1007 + 0.0002i	0.0036 - 0.0000i	0.0036 + 0.0000i	0.1759 - 0.0002i	0.1759 + 0.0002i	0.1294 - 0.0002i	0.1294 + 0.0002i
4	0.0822 + 0.0002i	0.2672 - 0.0005i	0.2672 + 0.0005i	0.0796 - 0.0001i	0.0796 + 0.0001i	0.0211 - 0.0000i	0.0211 + 0.0000i
5	0.0189 + 0.0000i	0.0527 - 0.0001i	0.0527 + 0.0001i	1.2646e-05 - 1.7113e-08i	1.2646e-05 + 1.7113e-08i	0.1341 - 0.0002i	0.1341 + 0.0002i
6	0.0162 + 0.0000i	0.0077 - 0.0000i	0.0077 + 0.0000i	0.0295 - 0.0000i	0.0295 + 0.0000i	0.1916 - 0.0003i	0.1916 + 0.0003i
7	0.0448 + 0.0001i	0.0088 - 0.0000i	0.0088 + 0.0000i	0.0425 - 0.0001i	0.0425 + 0.0001i	0.0206 - 0.0000i	0.0206 + 0.0000i
8	0.0652 - 0.0001i	0.0170 + 0.0000i	0.0170 - 0.0000i	0.0256 + 0.0000i	0.0256 - 0.0000i	0.0030 + 0.0000i	0.0030 - 0.0000i
9	0.1721 - 0.0004i	0.1430 + 0.0003i	0.1430 - 0.0003i	0.1469 + 0.0002i	0.1469 - 0.0002i	1.7020e-04 + 2.4079e-07i	1.7020e-04 - 2.4079e-07i
10	0.1007 - 0.0002i	0.0036 + 0.0000i	0.0036 - 0.0000i	0.1759 + 0.0002i	0.1759 - 0.0002i	0.1294 + 0.0002i	0.1294 - 0.0002i
11	0.0822 - 0.0002i	0.2672 + 0.0005i	0.2672 - 0.0005i	0.0796 + 0.0001i	0.0796 - 0.0001i	0.0211 + 0.0000i	0.0211 - 0.0000i
12	0.0189 - 0.0000i	0.0527 + 0.0001i	0.0527 - 0.0001i	1.2646e-05 + 1.7113e-08i	1.2646e-05 - 1.7113e-08i	0.1341 + 0.0002i	0.1341 - 0.0002i
13	0.0162 - 0.0000i	0.0077 + 0.0000i	0.0077 - 0.0000i	0.0295 + 0.0000i	0.0295 - 0.0000i	0.1916 + 0.0003i	0.1916 - 0.0003i
14	0.0448 - 0.0001i	0.0088 + 0.0000i	0.0088 - 0.0000i	0.0425 + 0.0001i	0.0425 - 0.0001i	0.0206 + 0.0000i	0.0206 - 0.0000i

Figure A7- Participation matrix of eigenvalue 11 of scenario 09 at 1400 h